NOAA Technical Report ERL 388-APCL 41

DEPARTMENT OF COMMERCE · UNITED STATES OF AMERICA

Meteorological Aspects of the Big Thompson Flash Flood of 31 July 1976

Robert A. Maddox, Fernando Caracena,
Lee R. Hoxit, and Charles F. Chappell

July 1977

U.S. DEPARTMENT OF COMMERCE
National Oceanic and Atmospheric Administration
Environmental Research Laboratories

NOAA Technical Report ERL 388-APCL 41

Meteorological Aspects of the Big Thompson Flash Flood of 31 July 1976

Robert A. Maddox, Fernando Caracena,
Lee R. Hoxit, and Charles F. Chappell

July 1977

Boulder, Colorado

U.S. DEPARTMENT OF COMMERCE
Juanita M. Kreps, Secretary

National Oceanic and Atmospheric Administration
Richard A. Frank, Administrator

Environmental Research Laboratories
Wilmot Hess, Director

For sale by the Superintendent of Documents, U.S. Government Printing Office, Washington, D.C. 20402


1


2

3

Photographs taken by John Asztalos from Mitchell Lake (near the Continental Divide 20 miles west-northwest of Boulder, Colorado). The sequence (1–4) captures the development of a large thunderstorm just southwest of Lyons, Colorado, during the period from about 0010 to 0045 GMT (6:10 to 6:45 p.m. MDT). This was one of the initial storms in the northeastern Colorado foothills on the evening of the Big Thompson flood.

4

Contents

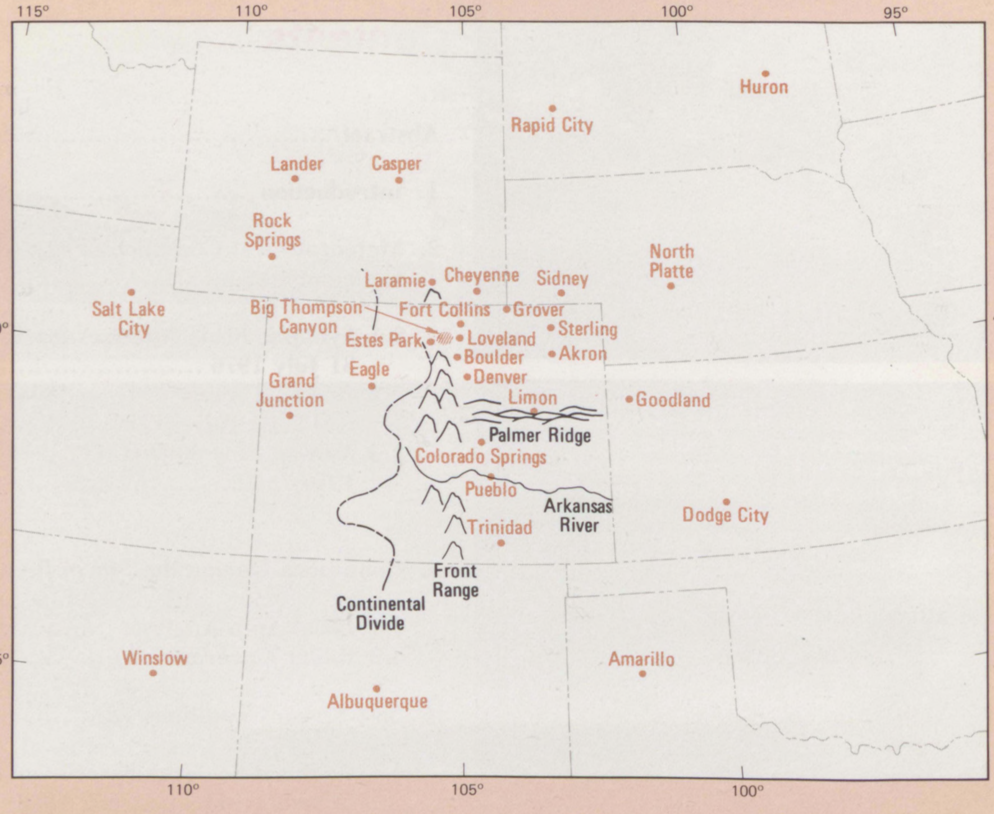

Figure 1. Locations and topographical features in Colorado and surrounding states.

METEOROLOGICAL ASPECTS OF THE BIG THOMPSON FLASH FLOOD OF 31 JULY 1976

Robert A. Maddox, Fernando Caracena, Lee R. Hoxit, and Charles F. Chappell

Abstract. Analyses and descriptions of meteorological conditions that produced the devastating flash flood in the Big Thompson Canyon on 31 July 1976 are presented. The storm developed when strong low-level easterly winds to the rear of a polar front pushed a moist, conditionally unstable air mass upslope into the Front Range of the Rocky Mountains. Orographic uplift released the convective instability, and light south-southeasterly winds at steering levels allowed the storm complex to remain nearly stationary over the foothills. Minimal entrainment of relatively moist air at middle and upper levels, very low cloud bases, and a slightly tilted updraft structure contributed to a high precipitation efficiency. Meteorological conditions that produced the Big Thompson and Rapid City flash floods are compared and shown to have been very similar. A set of meteorological conditions is defined for the purpose of identifying the potential for flash floods in Front Range canyons.

1. Introduction

During the evening hours of 31 July 1976, a destructive flash flood rushed through the Big Thompson Canyon west of Loveland, Colorado. U.S. Highway 34—the primary route into Estes Park and Rocky Mountain National Park—parallels the river; the canyon had been extensively developed with businesses, motels, and campgrounds located along the scenic river bank. Larimer County officials estimated that between 2,500 and 3,500 people were in the canyon when the flood occurred (NOAA, 1976), and the toll was heavy: at least 139 people were killed, and property damage of about $35.5 million occurred.

The storm produced very heavy rains in a narrow band along the Front Range from the Big Thompson drainage northward into Wyoming. Maximum amounts exceeded 12 in (305 mm) with much of the precipitation in the Big Thompson drainage falling during the 4 h from 0030 to 0430 Greenwich Mean Time (GMT). (GMT is converted to Mountain Daylight Time by subtracting 6 h.) Significant flooding and damage occurred in Colorado on the Big Thompson and the North Fork of the Big Thompson River, within Rist Canyon west of Ft. Collins, on the lower portion of the Cache la Poudre River (Poudre Park to Ft. Collins), and on the North Fork of the Cache la Poudre River. Flash flooding was also reported over areas south and west of Wheatland, Wyoming.

Fig. 1 shows Colorado and surrounding states and identifies landmarks and towns that are referred to in the report. The Big Thompson drainage, areas affected

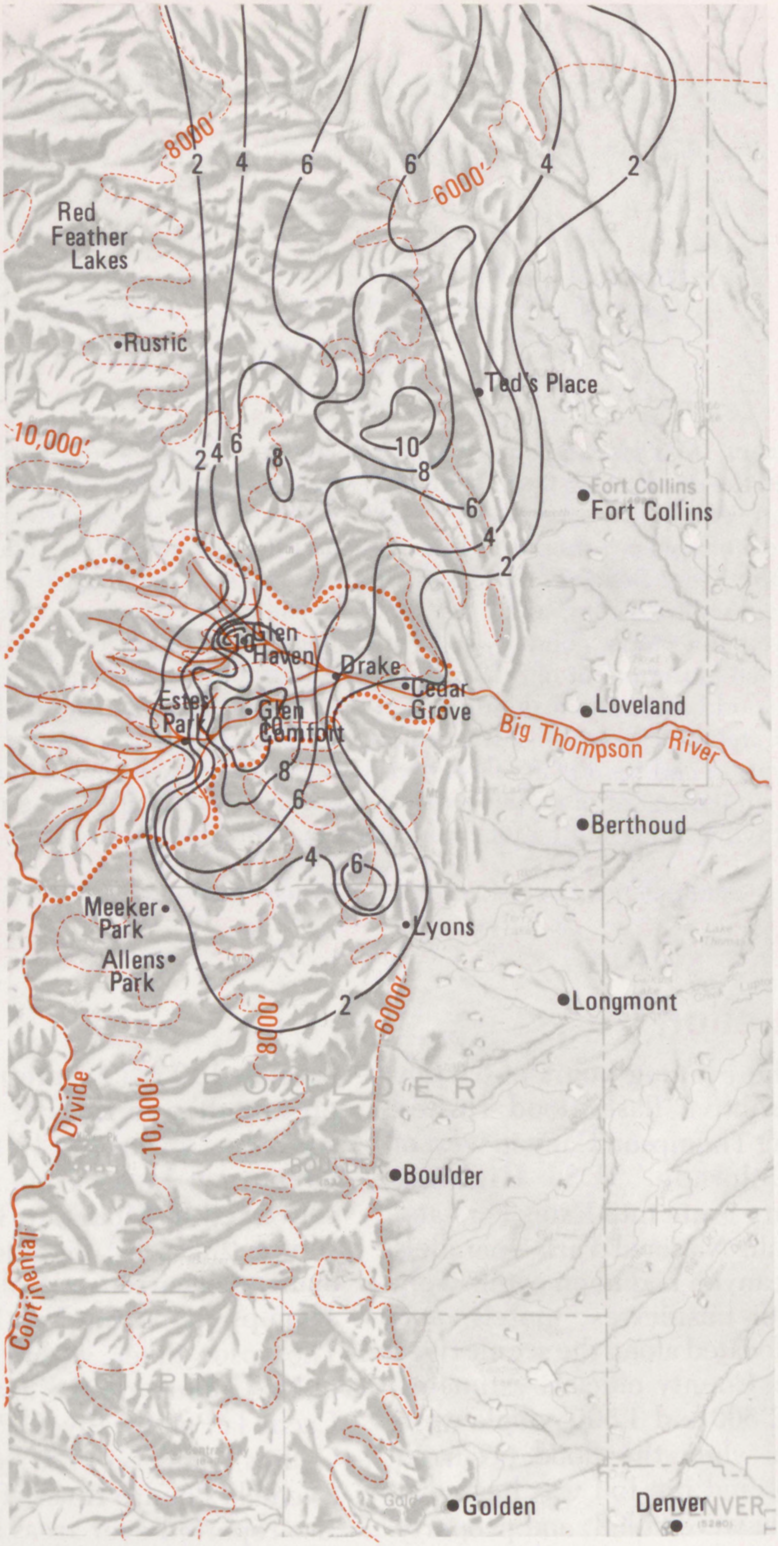

Figure 2. Big Thompson and North Fork of the Big Thompson drainages. Towns within and near the flash flood area are identified. Cumulative rainfall isohyets (black lines) for the period 31 July–2 August 1976 are shown. Terrain contours (orange lines) are in feet above mean sea level. The precipitation summary and isohyetal map were prepared by the National Weather Service Central Region Headquarters in cooperation with other Federal agencies.

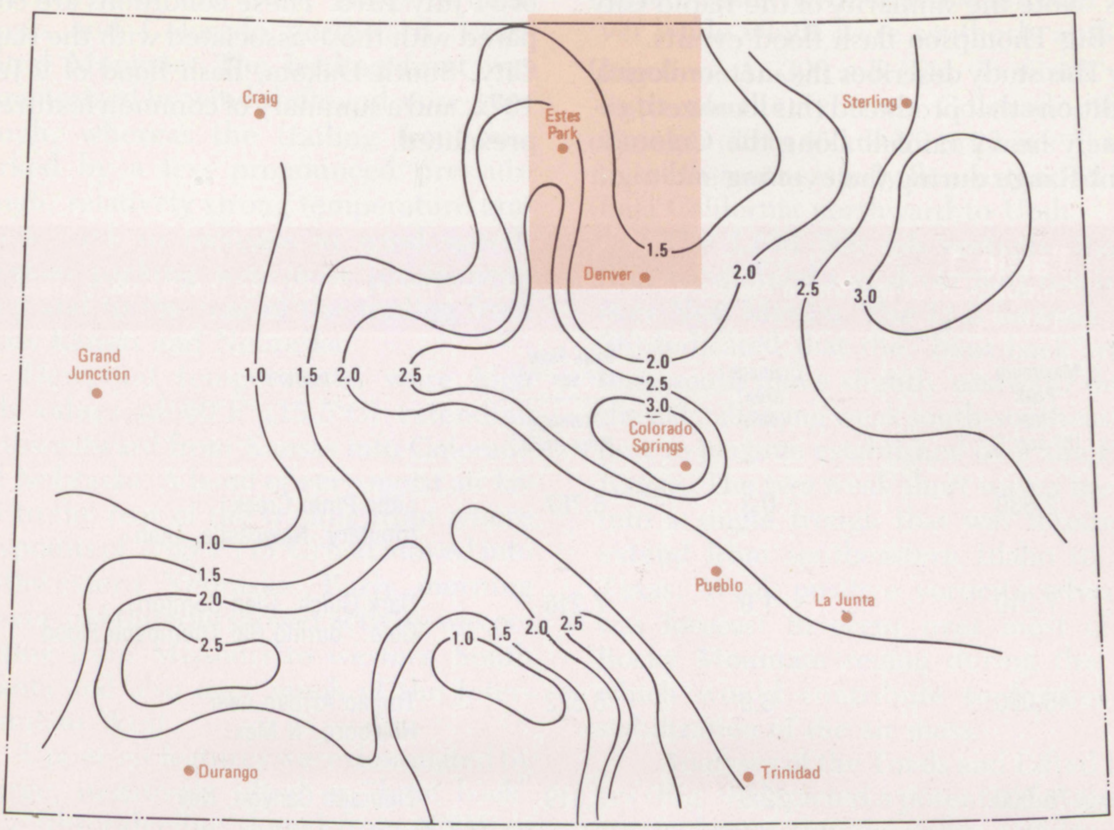

Figure 3. Mean July rainfall (inches) for Colorado (data from NOAA–EDS Climatological Summary for Colorado). The area shown in Fig. 2 is shaded.

by the flash flooding, and cumulative rainfall isohyets are depicted in Fig. 2. The precipitation summary covered the period 31 July through 2 August 1976. Mean July precipitation for Colorado is shown in Fig. 3. Note that within a few hours the Big Thompson storm produced rain amounts 5 to 10 times that normally expected for the entire month of July.

On July 31 a large thunderstorm complex developed over the mountains from west of Ft. Collins to southeast Estes Park just before dark when strong, unusually moist, easterly winds pushed upslope into the Front Range of the Rocky Mountains. The thunderstorm intensified very rapidly and by 0045 GMT radar measured tops exceeded 62,000 ft MSL (18.9 km) (NWS radar at Limon, Colorado) and reflectivities exceeded 60 dBZ (National Hail Research Experiment radar at Grover, Colorado). During its intense phase, the storm complex remained nearly stationary for 2 to 3 h; subsequently, it moved slowly northward into Wyoming. The behavior and characteristics of the Big Thompson storm were markedly different from those of typical summer afternoon storms in northeastern Colorado. These storms usually develop over the mountains and ridges in early afternoon and then move eastward across the plains. Rainfall is most often localized and of short duration, and is frequently accompanied by hail.

Stream flow records (Grozier et al., 1976) indicate that the precipitation that produced the flood crest on the main fork of the Big Thompson River at Drake probably fell within the first 2 h of the storm. Grozier et al. also reported a maximum measured stream flow on the Big Thompson River at the mouth of the canyon of 31,200 $ft^3\ s^{-1}$ (884 $m^3\ s^{-1}$) from an effective drainage basin of approximately 60 mi^2 (155 km^2). Table 1 compares maximum measured stream flows with drainages of varying sizes. Note the similarity of the Rapid City and Big Thompson flash flood events.

This study describes the meteorological conditions that produced this localized, extremely heavy rainfall along the Colorado Front Range during the evening and night of 31 July 1976. These conditions are compared with those associated with the Rapid City, South Dakota, flash flood of 9 June 1972, and a summary of common features is presented.

Table 1.
Comparison of maximum measured peak flows during flood events with the drainage areas involved

Maximum Peak Flow ($ft^2\ sec^{-1}$)	Drainage Area (mi^2)	Peak Flow ($ft^2\ sec^{-1}$) / Drainage Area (mi^2)	Location
2,630	0.3	8,767	Little Pinto Creek tributary, Newcastle, Utah
7,210	1.0	7,210	Dark Gulch, Glen Comfort, Colo., during Big Thompson Flood
45,000	6.9	6,522	Trujillo Arroyo near Hillsboro, N.Mex.
76,000	22.9	3,319	Eldorado Canyon, Nev.
31,200	60	520	Big Thompson River at mouth of canyon
50,600	91	556	Rapid Creek at Rapid City, S.Dak.
25,000	692	36	Animas River near Durango, Colo.

*Many of the data are from Williams (1976).

2. Meteorological Conditions Prior to Storm Development

A series of upper-air analyses was used, in conjunction with hourly surface analyses, upper-air soundings, radar scope and satellite photographs, and stability charts, to study the evolution of meteorological conditions that culminated in the development of the Big Thompson storm.

2.1 Synoptic Scale Analyses for 1200 GMT, 31 July 1976

Detailed surface and upper-air analyses for 700, 500, and 300 mb are presented in Figs. 4 through 7. Important surface features included a strong polar high pressure area centered over southern Canada, and a weak low pressure area located near Grand Junction in western Colorado. A double frontal structure at the periphery of the polar air mass (Fig. 4) stretched from the Great Lakes through Kansas and Colorado northward across central Montana. The leading front was characterized by wind shifts and a pressure trough, whereas the trailing front was marked by a less pronounced pressure trough, relatively strong temperature gradients, and an increase in wind speed. Thermal packing was most pronounced along and to the rear of the trailing front across Kansas and Nebraska.

Dewpoint temperatures were high with values of 60°F (15.5°C) extending northwestward from Kansas into Colorado and Nebraska. A band of very moist air lay just to the rear of the trailing front where dewpoints of ≥65°F (18°C) had moved into southwestern Nebraska. Early morning shower and thundershower activity was occurring from Missouri to western South Dakota and also over much of the intermountain West.

Upper-air features were dominated by a large, negatively tilted or "bent back" ridge (the ridgeline sloped from NNW to SSE), which extended from southern Texas to western Canada. A closed high was present over the Central Plains. Moist conditions were present over the intermountain West and eastern slopes of the Rockies from 700 through 300 mb.

A weak short-wave trough at 700 mb (Fig. 5) arced from near Salt Lake City, Utah, to El Paso, Texas. Light southeasterly winds were present over southwestern Nebraska, northwestern Kansas, and much of eastern Colorado. Hot, dry conditions at 700 mb over the southern plains indicated that deep convection would probably be suppressed south of the polar air mass.

Two weak 500 mb (Fig. 6) short-wave troughs—one over Mexico and another over Arizona and New Mexico—were imbedded in the southerly flow west of the ridgeline. A broad area of falling heights with a weak fall center over the Four Corners area was associated with these troughs. A small, closed anticyclonic circulation over the Colorado mountains produced westerly winds at 500 mb over Denver while winds were southerly at Grand Junction. At 300 mb (Fig. 7) winds were light southerly over Colorado while stronger (20 to 45 kt—10 to 23 m s^{-1}) south to south-southeasterly flow extended from Baja California northward to Utah.

The LFM 500 mb vorticity analysis (Fig. 8a) defined a weak vorticity maximum over New Mexico. The 12 h forecast (Fig. 8b) indicated that the "bent back" ridgeline would move slightly eastward during the day, allowing weak south-southeasterly flow to become established over the Front Range. The two weak short waves merged into a single trough that was forecast to extend from southeastern Idaho to west Texas. Weak positive vorticity advection was forecast to occur over most of the Rocky Mountain region during the day, which would contribute to further destabilization of the air mass.

Analyses of the Totals and Lifted Indices (Fig. 9) depicted a potential for moderate to heavy thunderstorm activity over northern Arizona, much of Utah and Nevada, and from western Kansas into northeastern Colorado. The Totals Index is defined as $2(T_{850} - T_{500}) - D_{850}$, where T_{850} is the 850 mb temperature, T_{500} is the 500 mb temperature, and D_{850} is the 850 mb dewpoint depression, all expressed in °C. Values of this index ≥46 reflect favorable conditions for thunderstorm development, and values ≥50 indicate a potential for moderate to heavy storm activity. (See Miller, 1972, for a more complete discussion of this index.) The Lifted Index (L.I.) was computed by lifting a parcel possessing the mean thermodynamic characteristics of the lowest 100 mb layer adiabatically to 500 mb, and then subtracting its temperature from the environmental temperature at that level.

The 1200 GMT Denver sounding (Fig. 10) was very moist (average vapor mixing ratio for the lowest 100 mb layer was 12.0 g kg^{-1}) below a temperature inversion at 670 mb. Winds above the inversion were light and variable, and winds in the cool air mass

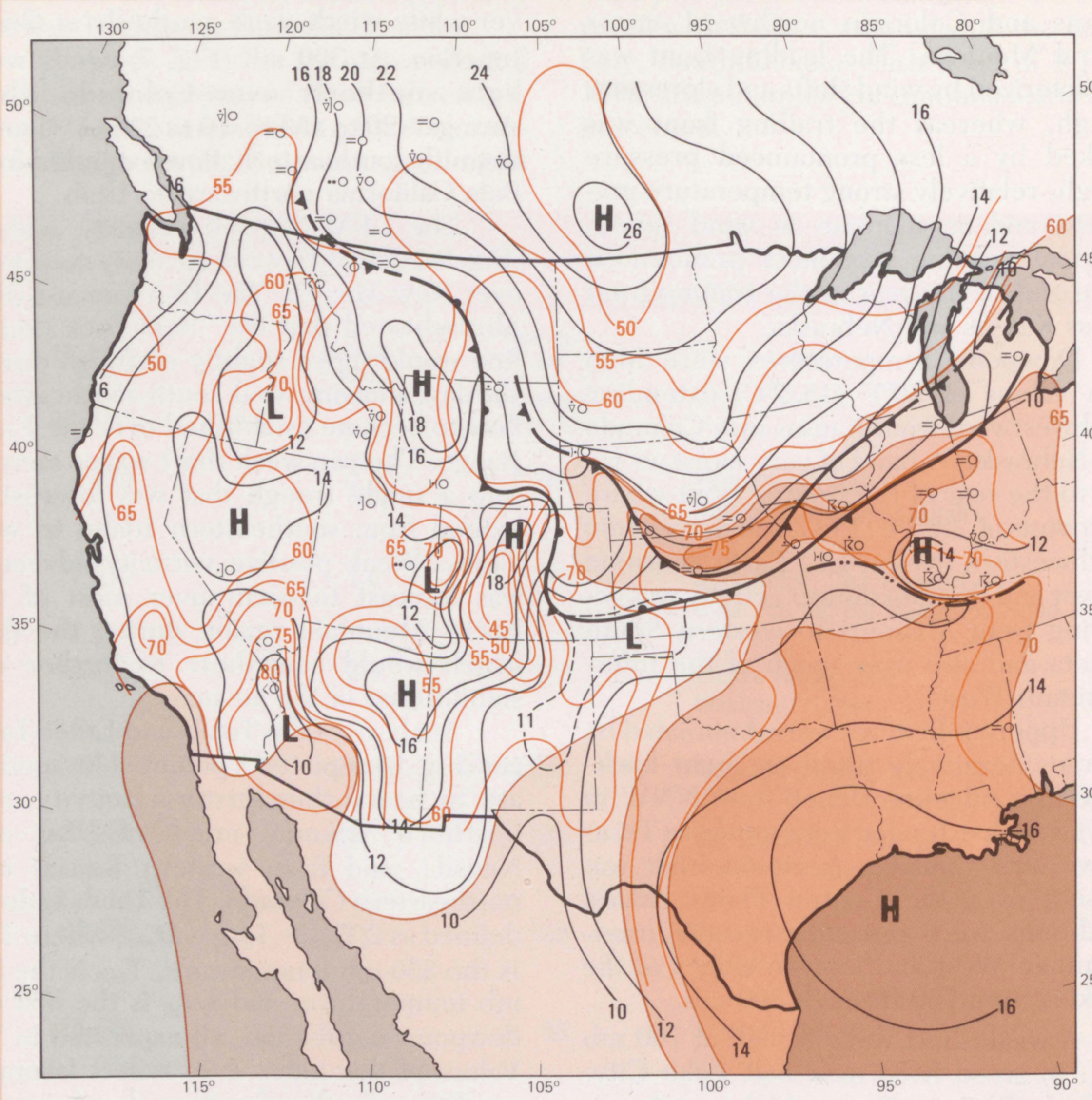

Figure 4. Synoptic scale surface analysis for 1200 GMT, 31 July 1976. Frontal positions, pressure centers, and isobars for 2 mb intervals (1012 = 12) are shown in black. Isotherms for 5° F intervals are in orange. Dewpoint temperatures ≥ 60°F are analyzed at 5°F intervals with the high dewpoint region shaded orange.

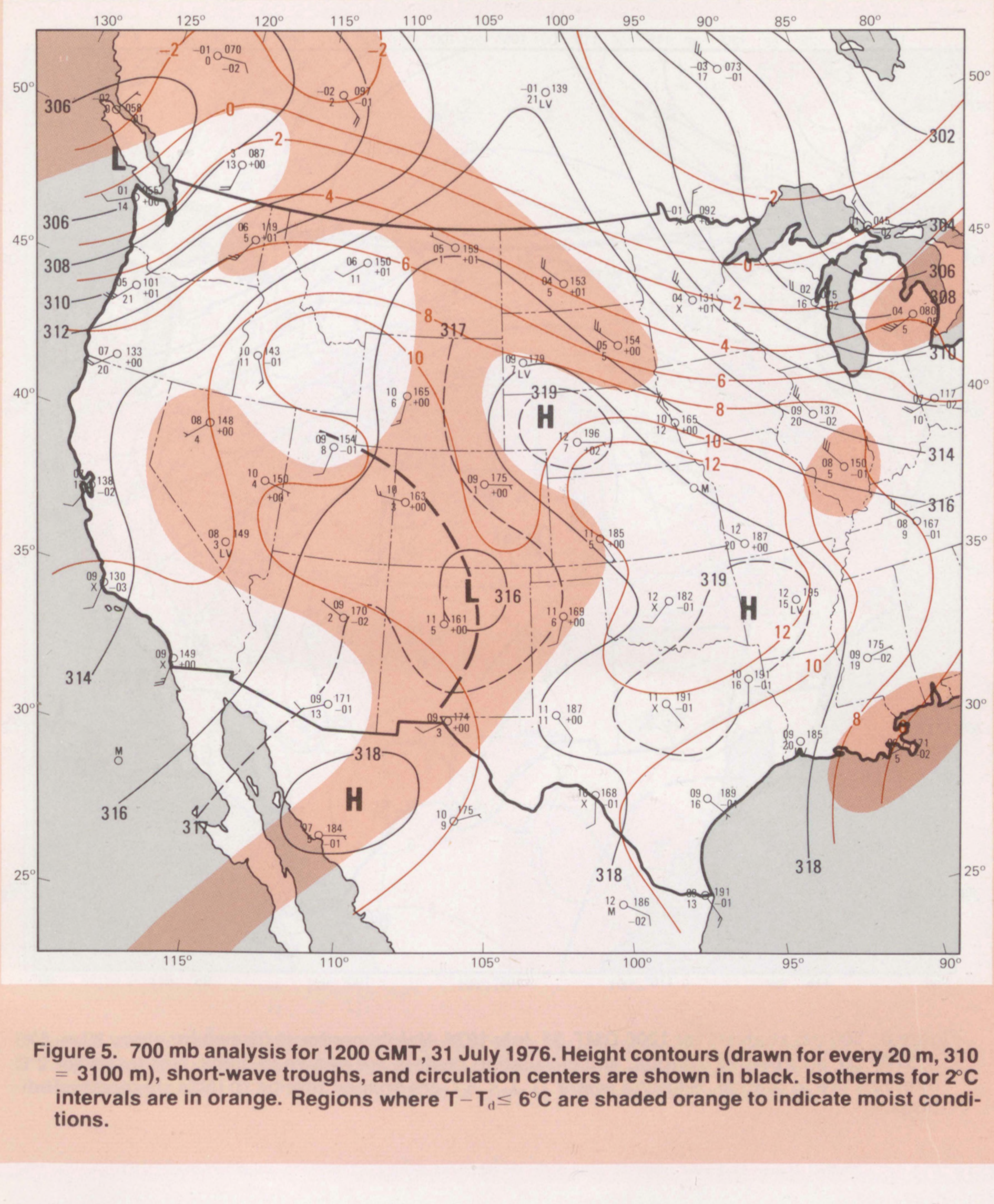

Figure 5. 700 mb analysis for 1200 GMT, 31 July 1976. Height contours (drawn for every 20 m, 310 = 3100 m), short-wave troughs, and circulation centers are shown in black. Isotherms for 2°C intervals are in orange. Regions where $T-T_d \leq 6°C$ are shaded orange to indicate moist conditions.

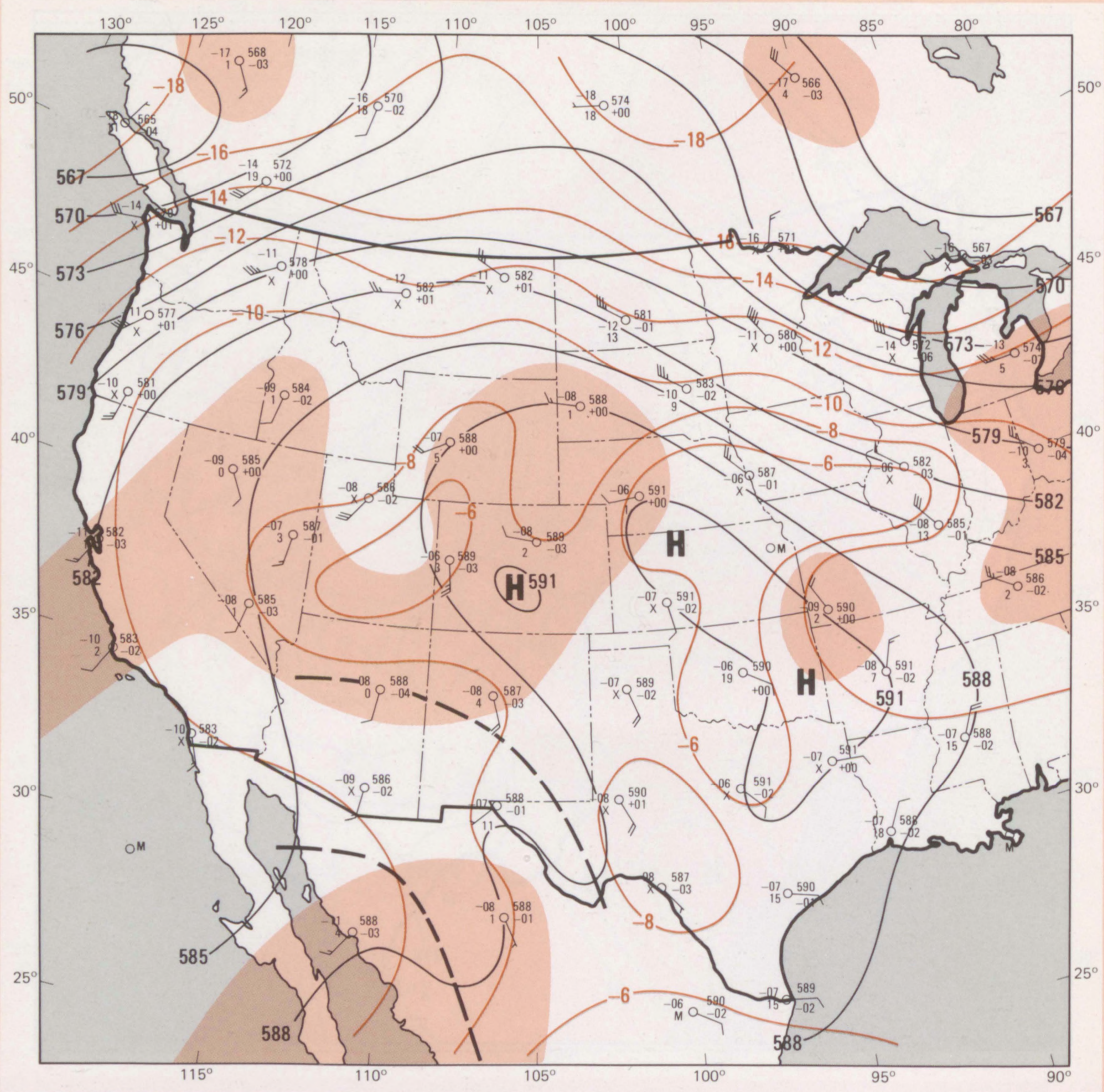

Figure 6. 500 mb analysis for 1200 GMT, 31 July 1976. Height contours (drawn for every 30 m, 570 = 5700 m), short-wave troughs, and circulation centers are shown in black. Isotherms for 2°C intervals are in orange. Regions where $T - T_d \leq 6°C$ are shaded orange to indicate moist conditions.

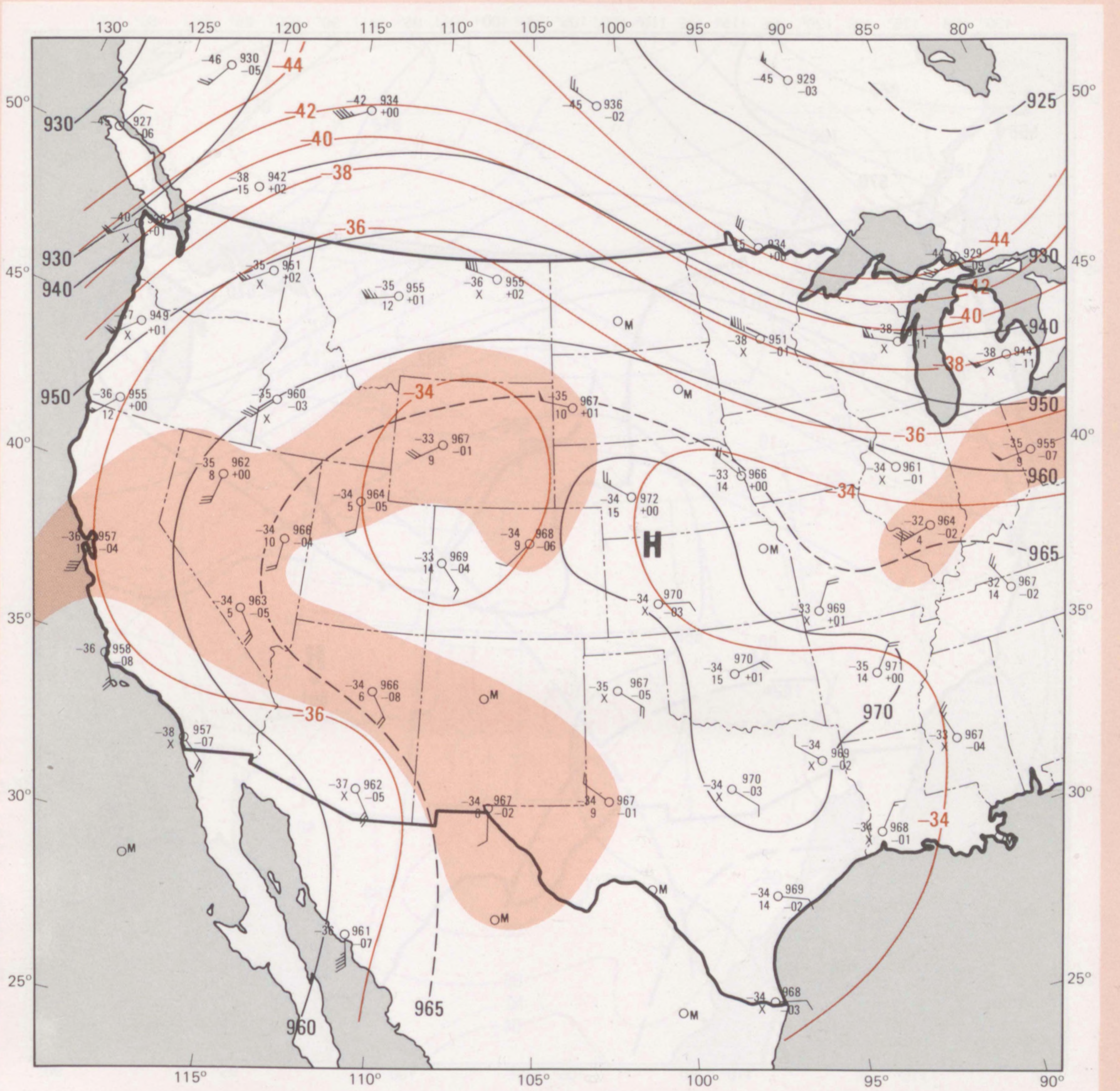

Figure 7. 300 mb analysis for 1200 GMT, 31 July 1976. Height contours (drawn for every 100 m, 960 = 9600 m) and circulation centers are shown in black. Isotherms for 2°C intervals are in orange. Regions where $T - T_d \leq 10°C$ are shaded orange to indicate moist conditions.

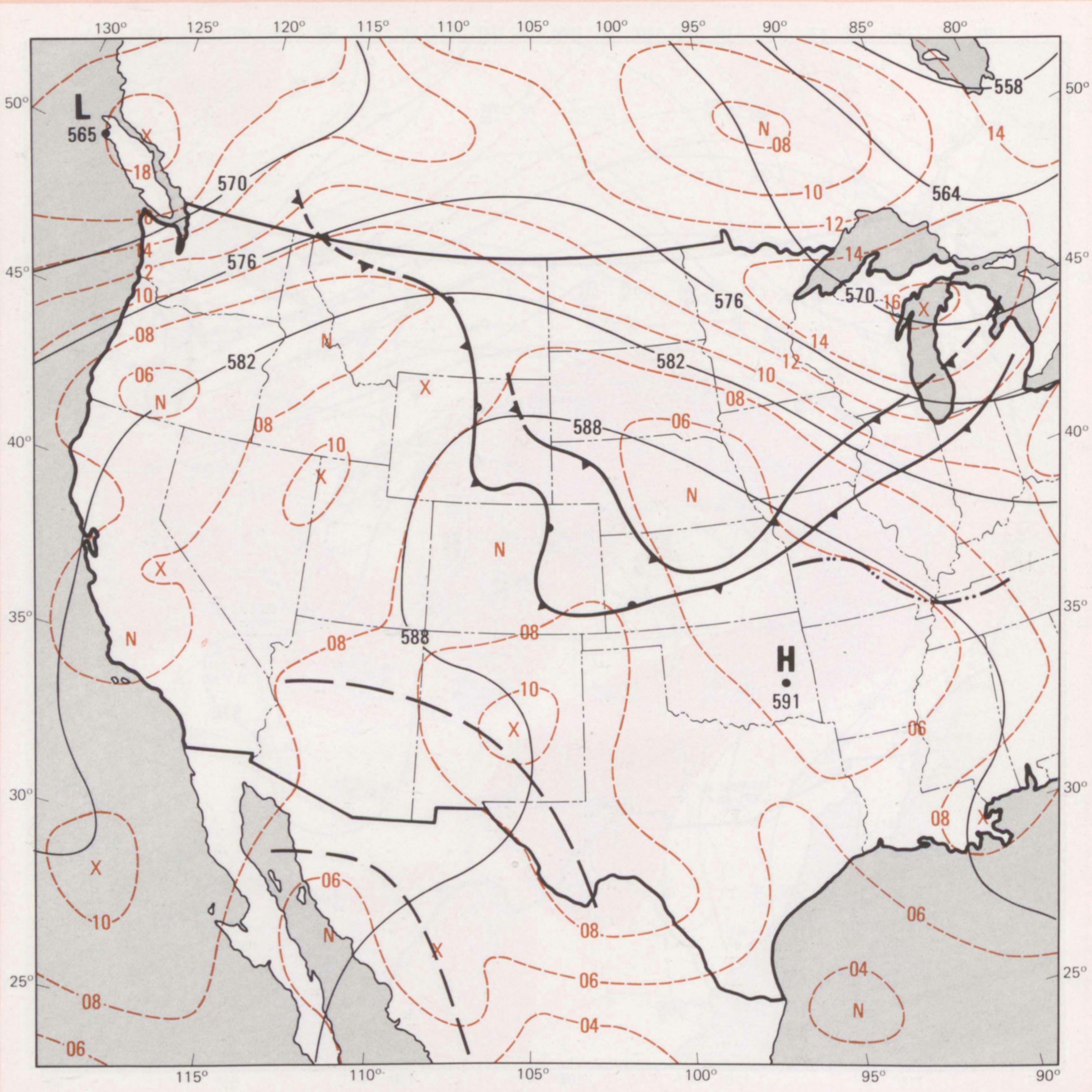

Figure 8a. National Meteorological Center (NMC) Limited Fine Mesh (LFM) vorticity analysis for 1200 GMT, 31 July 1976. Vorticity field is shown in orange; LFM 500 mb height analysis, surface frontal positions, and 500 mb short-wave troughs are shown in black. Surface analysis and trough positions are from Figs. 4 and 6.

below were easterly with speeds of less than 10 kt (5 m s^{-1}). The L.I. was -1, but the height of the Level of Free Convection (LFC) found at 530 mb indicated considerable lifting and/or heating would be needed to initiate deep convection. The high moisture content was the most unusual feature of the sounding. Precipitable water contents of 0.67 in (1.71 cm) in the lowest 150 mb layer and 1.00 in (2.54 cm) in the layer from the surface to 500 mb, were approximately 50% above Denver July means (from Lott, 1976) of 0.40 in (1.02 cm) and 0.69 in (1.74 cm), respectively. A low overcast at 1200 ft AGL (366 m) was reported at Denver at sounding time.

The 1340 GMT Sterling, Colorado, sounding (Fig. 11) was taken during operations of the National Hail Research Experiment (NHRE). A pronounced radiational

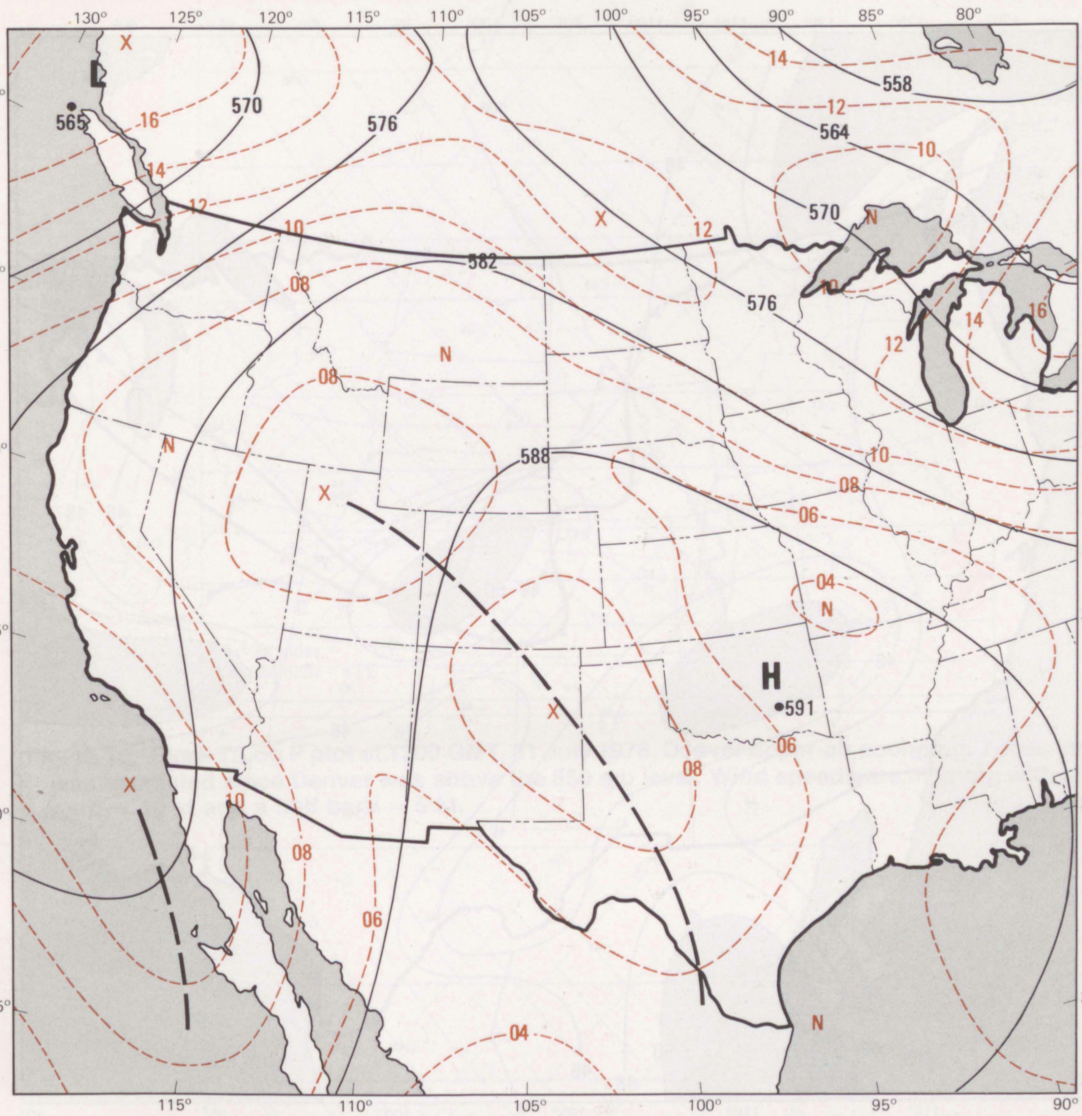

Figure 8b. NMC–LFM 12 h forecast of 500 mb heights (black) and vorticity (orange), valid 0000 GMT, 1 August 1976.

inversion near the surface was topped by a weaker inversion at 725 mb. Winds in the cool air mass were light easterly. The L.I. was +1 and the LFC was at 480 mb. Precipitable water contents of 0.59 in (1.49 cm) in the lowest 150 mb layer and 1.04 in (2.64 cm) in the surface-to-500 mb layer were similar to the Denver values. Middle level cloudiness was present in the Sterling area at the time of the sounding.

The 1200 GMT synoptic analyses suggested that the stage was set for the development of significant thunderstorm activity over much of the western part of the country. Abundant moisture, a potentially unstable atmosphere, and weak upward motion did combine to trigger numerous storms during the afternoon and evening of 31 July west of the Continental Divide. Some of these reached severe

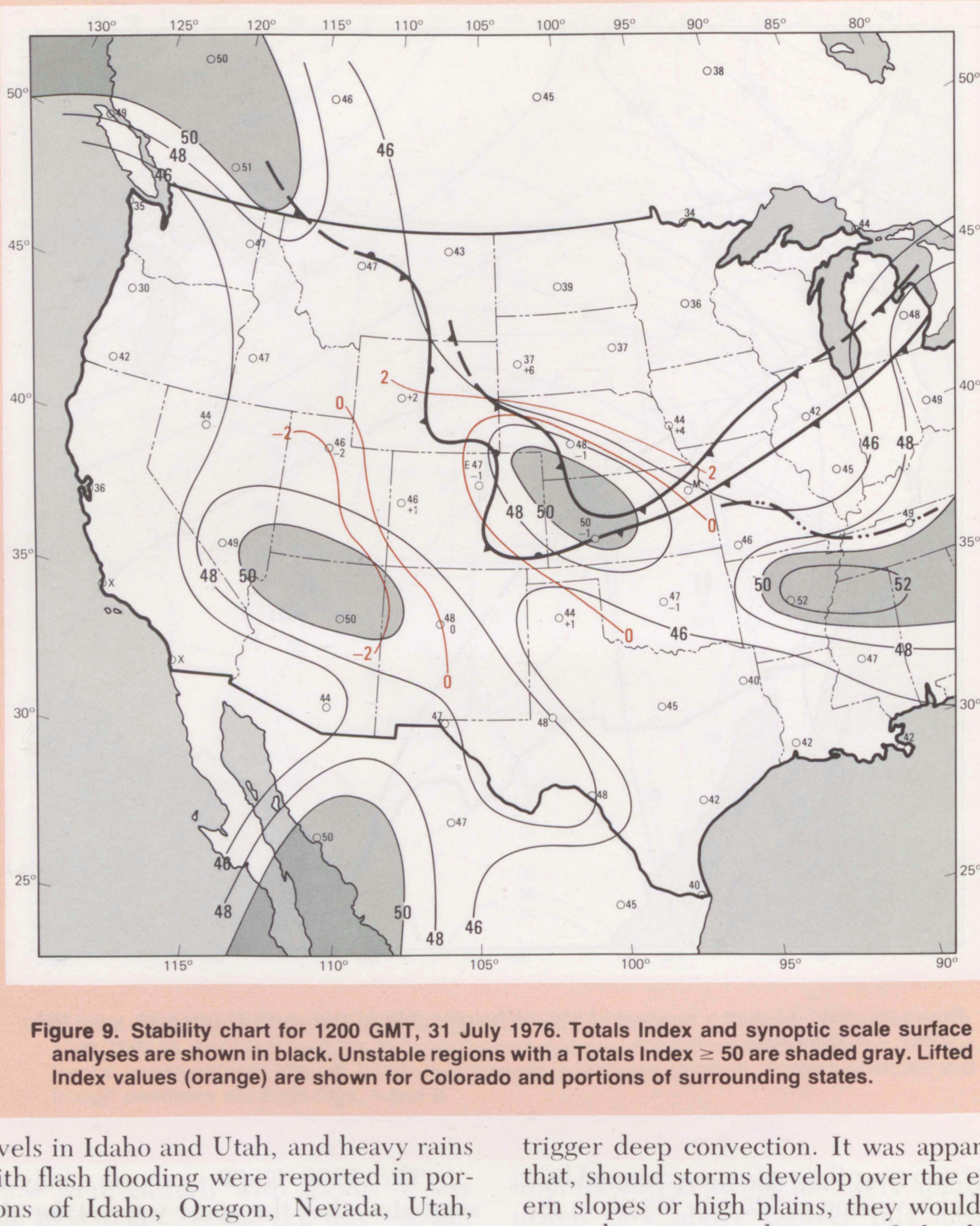

Figure 9. Stability chart for 1200 GMT, 31 July 1976. Totals Index and synoptic scale surface analyses are shown in black. Unstable regions with a Totals Index ≥ 50 are shaded gray. Lifted Index values (orange) are shown for Colorado and portions of surrounding states.

levels in Idaho and Utah, and heavy rains with flash flooding were reported in portions of Idaho, Oregon, Nevada, Utah, Wyoming, and Colorado. Synoptic weather conditions were quite similar to those associated with the Las Vegas flood of 3 July 1975 (Randerson, 1976).

East of the Continental Divide the atmosphere was conditionally unstable, but high LFC's indicated that considerable lifting and/or heating would be needed to trigger deep convection. It was apparent that, should storms develop over the eastern slopes or high plains, they would be very slow moving because of the light winds aloft. Unusually large amounts of precipitable water, combined with slow storm movement, suggested that thunderstorms would have the potential to produce heavy precipitation over localized areas.

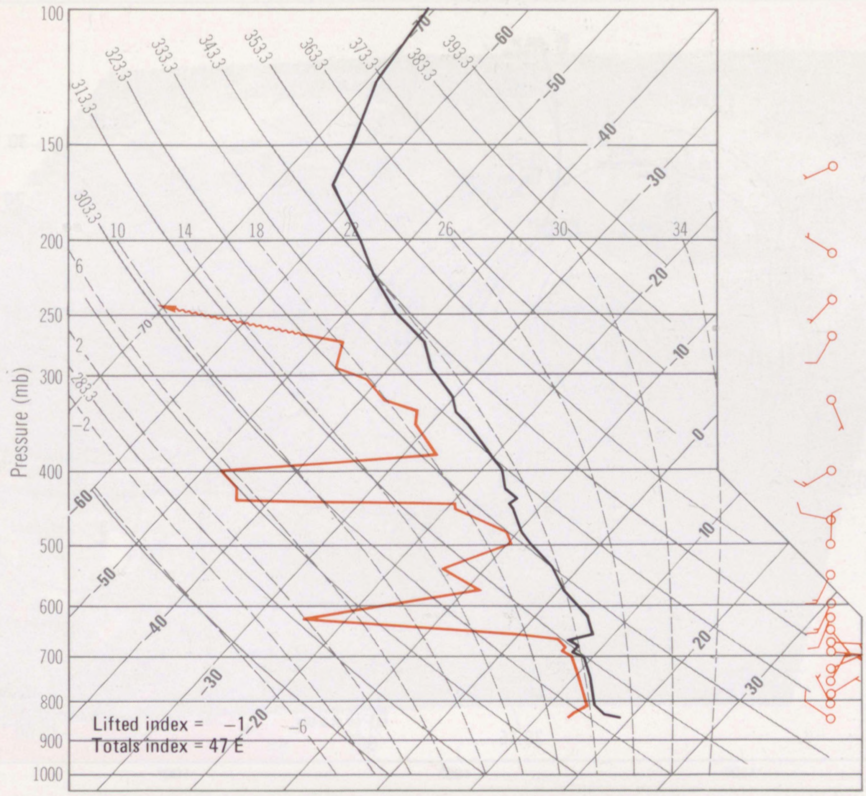

Figure 10. Skew T/Log P plot of 1200 GMT, 31 July 1976, Denver upper-air sounding. Totals Index was estimated since Denver was above the 850 mb level. Wind speeds are in knots with a full barb = 10 kt and a half barb = 5 kt.

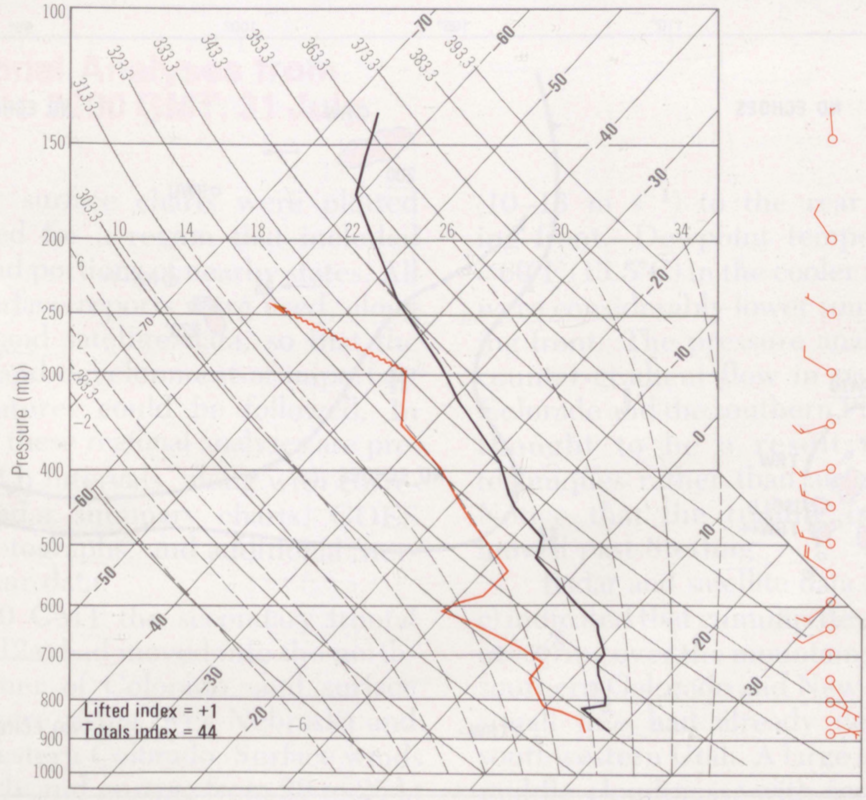

Figure 11. Skew T/Log P plot of Sterling, Colorado, upper-air sounding taken at 1340 GMT, 31 July 1976.

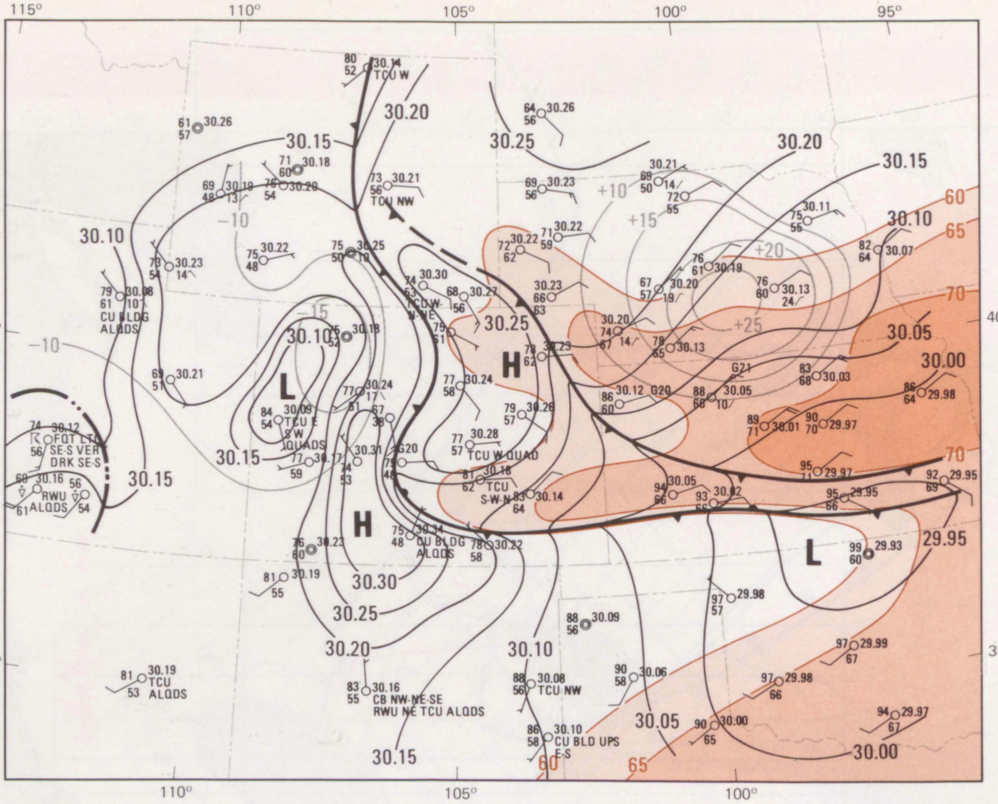

Figure 12a. Regional surface analysis for 1800 GMT, 31 July 1976. Frontal positions, squall lines, and pressure analysis (altimeter setting shown at 0.05 in intervals) are in black. The 3 h pressure change field (at 0.5 mb intervals) is shown in gray. Dewpoints ≥ 60°F are analyzed at 5°F intervals and shaded orange. Surface observations and pertinent remarks are plotted.

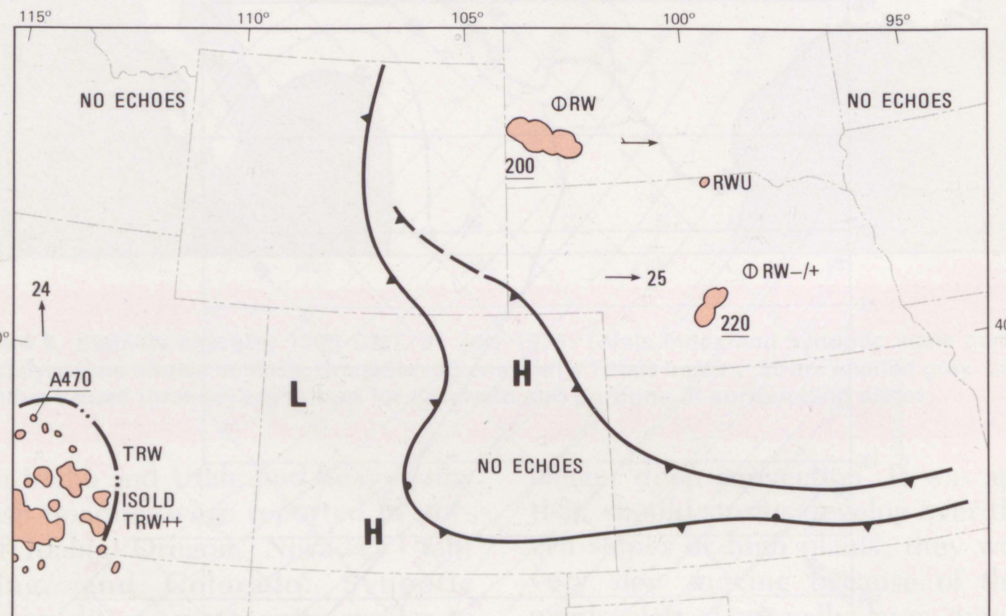

Figure 12b. Radar summary chart for 1735 GMT, 31 July 1976. Regional frontal positions are indicated.

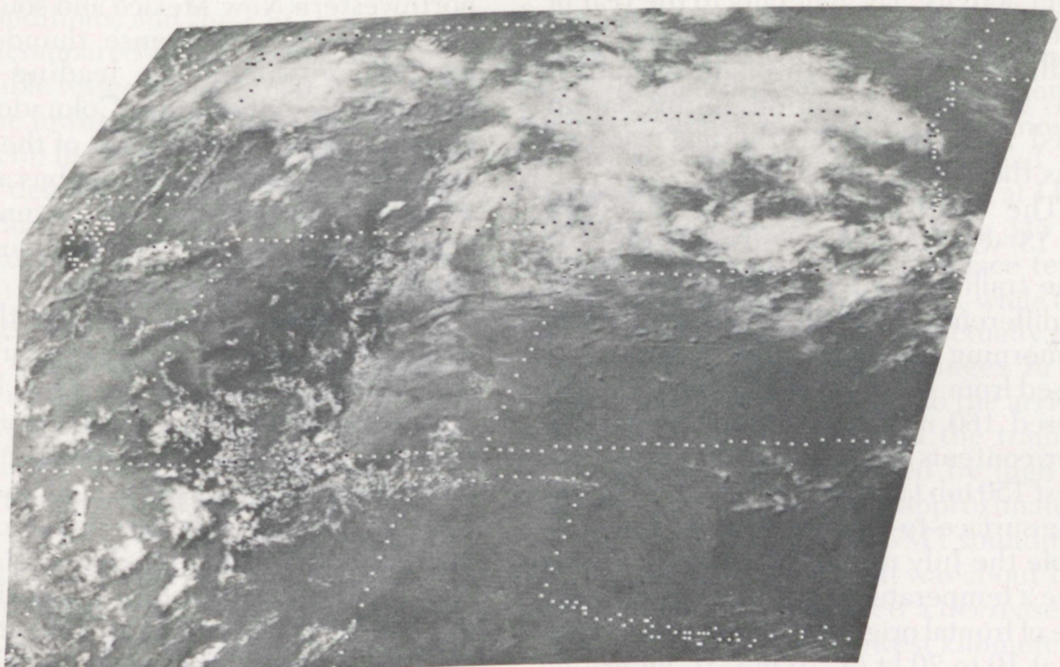

Figure 12c. GOES–1 photograph (visible channel, 1 km resolution at satellite sub-point) for 1800 GMT, 31 July 1976.

2.2 Regional Analyses from 1800 to 2200 GMT, 31 July 1976

Hourly surface charts were plotted and analyzed for a region that included Colorado and portions of nearby states. All available surface reports were used, along with radar and satellite data, so that the movement and development of important weather features could be followed. In Figs. 12–17 these regional analyses are presented, at 2 h intervals, along with corresponding radar summary charts, GOES satellite photographs, and additional Sterling upper-air data.

At 1800 GMT the secondary frontal surge (Fig. 12a) had moved into the northeastern corner of Colorado, and surface pressures were rising over Nebraska and falling in western Colorado. Surface winds were easterly and gusting from 20 to 25 kt (10–13 m s^{-1}) to the rear of this trailing front. Dewpoint temperatures were ≥60°F (15.5°C) in the cooler air masses but were considerably lower south of the leading front. The pressure analysis indicates counter-gradient flow in parts of eastern Colorado and the southern Plains. This was thought to be a result of reduction techniques rather than an actual feature. Notice that the trailing front had just moved past Sterling.

Radar and satellite data (Figs. 12b and c) indicated that cumulus development was occurring over the mountains, especially in southern Colorado and New Mexico, and a squall line had already developed over southwestern Utah. A large area of low and middle cloudiness, with some embedded shower activity, lay generally to the rear of the trailing front over the plains. This cloudiness persisted through the afternoon, and the reduction in insolation helped to maintain the thermal contrast across the trailing front.

The 1920 GMT Sterling sounding (Fig. 13) was taken about 40 km to the rear of the trailing front and exhibited important differences from the Sterling and Denver morning soundings. The L.I. had decreased from +1 to −4, while the LFC had lowered 160 mb to 640 mb. Precipitable water contents of 0.78 in (1.97 cm) in the lowest 150 mb layer and of 1.31 in (3.34 cm) in the surface-to-500 mb layer were almost double the July means for Denver. Winds above a temperature inversion (considered to be of frontal origin) at 720 mb were westerly at 10 to 20 kt (5–10 m s^{-1}), indicating that Sterling was very near the upper ridgeline. Easterly low level flow had increased to 10 to 15 kt (5–8 m s^{-1}). The Sterling sonde had sampled the air mass just behind the trailing front and found it to be conditionally very unstable with an unusually high moisture content. This air mass required lifting of approximately 140 mb to release its instability, and was moving westward and southwestward toward the Colorado Front Range at 15 to 20 kt (8–10 m s^{-1}).

The 2000 GMT regional analysis (Fig. 14a) showed that the leading front had remained nearly stationary except over southwestern Kansas and southeastern Colorado. Veering winds and decreasing dewpoints at Garden City and Dodge City, Kansas, indicated that the leading front had retreated northward in this region. The trailing front had moved southward and westward and was about to overtake the leading front across southern Kansas.

Radar and satellite data (Figs. 14b and c) showed that convective cloud and thunderstorm activity had continued to increase. The Utah squall line had intensified and was moving north-northeastward. Large thunderstorms had developed over northwestern New Mexico and southwestern Colorado. An intense thunderstorm had formed along the leading frontal boundary in southeastern Colorado. Small cumulus clouds dotted most of the Plains, and a line of small cumulonimbus and towering cumulus clouds had begun to develop along the secondary frontal surge as it moved onto the Palmer Ridge.

By 2200 GMT (see Fig. 15a) the trailing front had overtaken and reinforced the leading front across Kansas. It had become better defined with higher dewpoints and stronger easterly winds behind it. High temperatures in eastern Colorado and Kansas had helped trigger a line of thunderstorms along and to the rear of the front. The large storm in eastern Colorado had a top indicated by radar (Fig. 15b) of 56,000 ft MSL (17 km). The storms in this line appeared nearly circular on the satellite photograph (Fig. 15c), which indicated that they had developed in a low wind shear environment.

Surface pressure had continued to fall west of the Continental Divide, and the surface low pressure area was centered north of Grand Junction. The pressure at Rawlins, Wyoming, only 150 n mi (278 km) to the northeast, was holding 10 mb higher than that at Grand Junction. Thunderstorm activity was widespread over the West with large, apparently intense storms indicated over northwestern New Mexico, southwestern Colorado, and central Utah. Some thunderstorms had developed over the north-central mountains in Colorado; however, they remained well west of the Big Thompson drainage.

A final sounding was taken at Sterling at 2202 GMT (Fig. 16) when the trailing front was located approximately 120 km to the west. During the 2 h and 40 min that had elapsed since the 1920 GMT sounding several important changes in the air mass had occurred. The mean vapor mixing ratio in the lowest 100 mb layer had decreased 1.3 g kg^{-1} to 12.5 g kg^{-1}. The L.I. had increased to a value of −2 (indicating more stable conditions) and the LFC was now at 600 mb (compared to the earlier 640 mb). Precipitable water amounts of 0.70 in (1.79 cm) in the lowest 150 mb layer and of 1.14 in (2.90 cm) in the surface-to-500 mb layer had also decreased slightly from the 1920 GMT values.

A plot of equivalent potential temperature (θ_e) vs. height for the three Sterling soundings (Fig. 17) demonstrates the differences in moisture and stability characteristics of the air masses ahead of, immediately behind, and well behind the trailing front. Of most interest are the changes that occurred within the lowest 2 km. The 1340 GMT sounding showed a layer of high θ_e values very near the surface with a rapid decrease to a minimum just above 2 km. Although Sterling was well within the cool air mass behind the leading front, the moist layer was actually very shallow. The 1920 GMT sounding indicated a dramatic increase in θ_e throughout a layer extending from the surface to almost 4 km. Values of θ_e at the surface had increased from 343 K to 353 K, and θ_e at 1 km AGL had increased from 334 K to 345 K. During the same period the surface temperature had increased only 5.9°C, while the temperature at 1 km AGL had actually decreased 0.9°C. The large changes in θ_e were therefore primarily due to the arrival of the more moist air behind the trailing front. The zone characterized by high θ_e and a deep moist layer was approximately 100 km in width. The 2202 GMT sounding, taken when the trailing front was about 120 km west of Sterling, showed a decrease of 4.5 K in mean θ_e for the lowest kilometer.

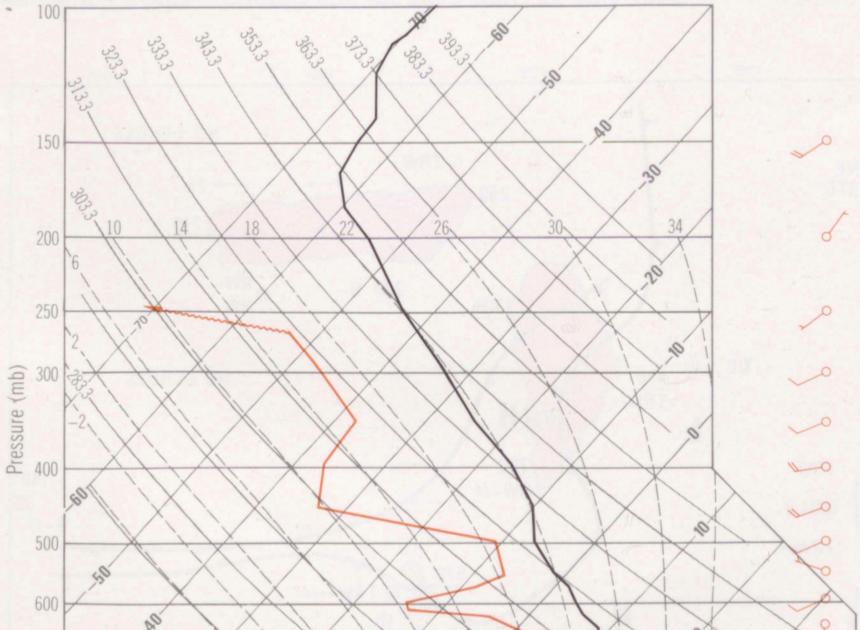

Figure 13. Skew T/Log P plot of Sterling, Colorado, upper-air sounding taken at 1920 GMT, 31 July 1976.

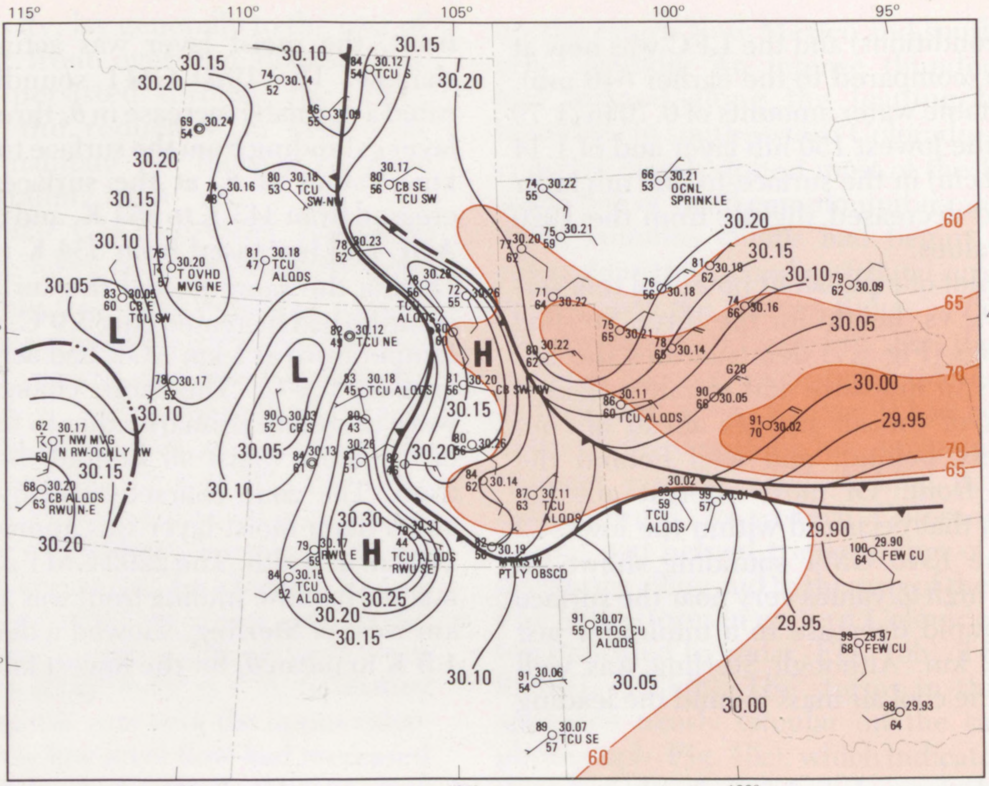

Figure 14a. Regional surface analysis for 2000 GMT, 31 July 1976. Refer to legend of Fig. 12a for details.

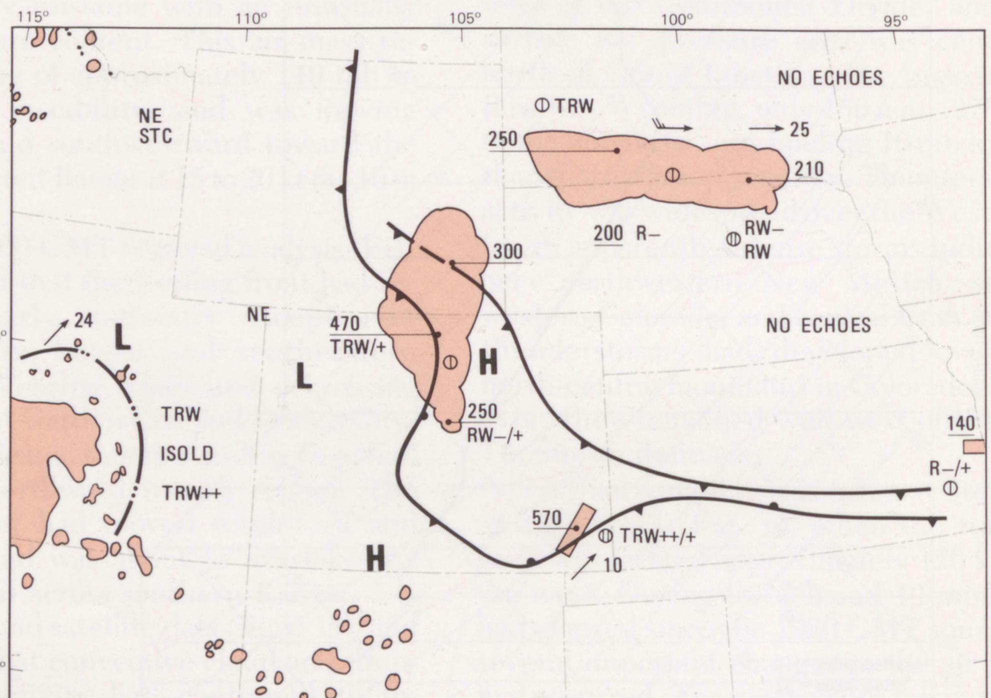

Figure 14b. Radar summary chart for 1935 GMT, 31 July 1976.

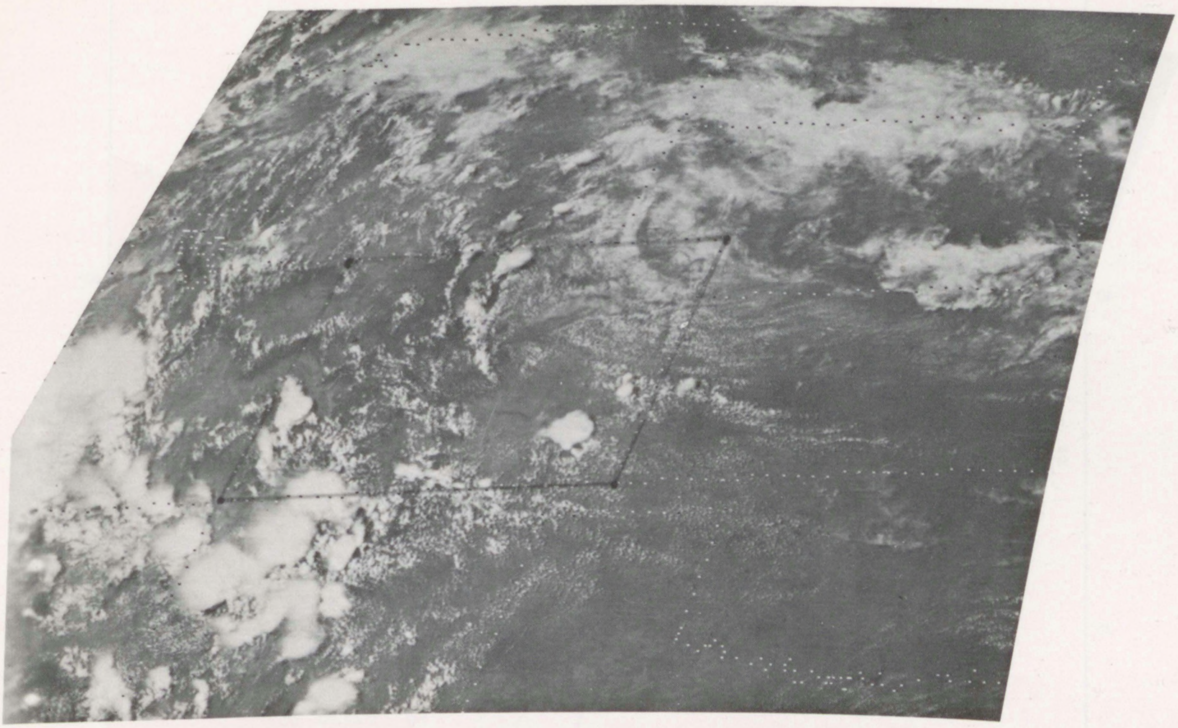

Figure 14c. GOES–1 photograph for 2000 GMT, 31 July 1976.

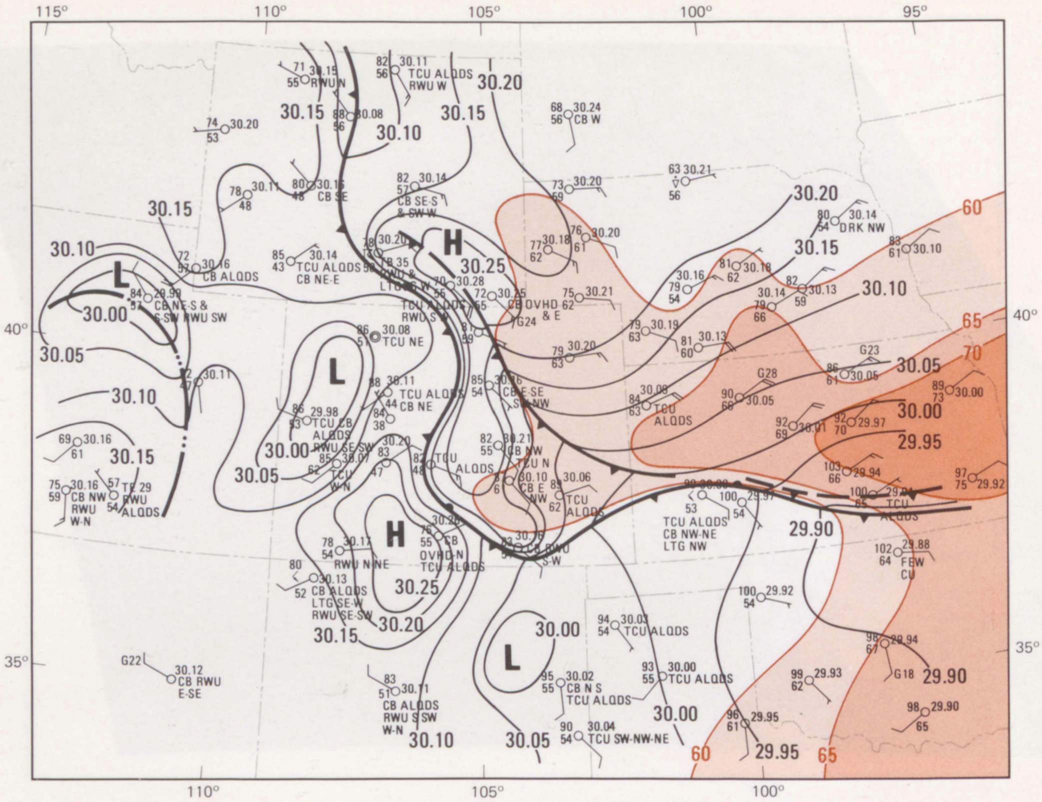

Figure 15a. Regional surface analysis for 2200 GMT, 31 July 1976. Refer to legend of Fig. 12a for details.

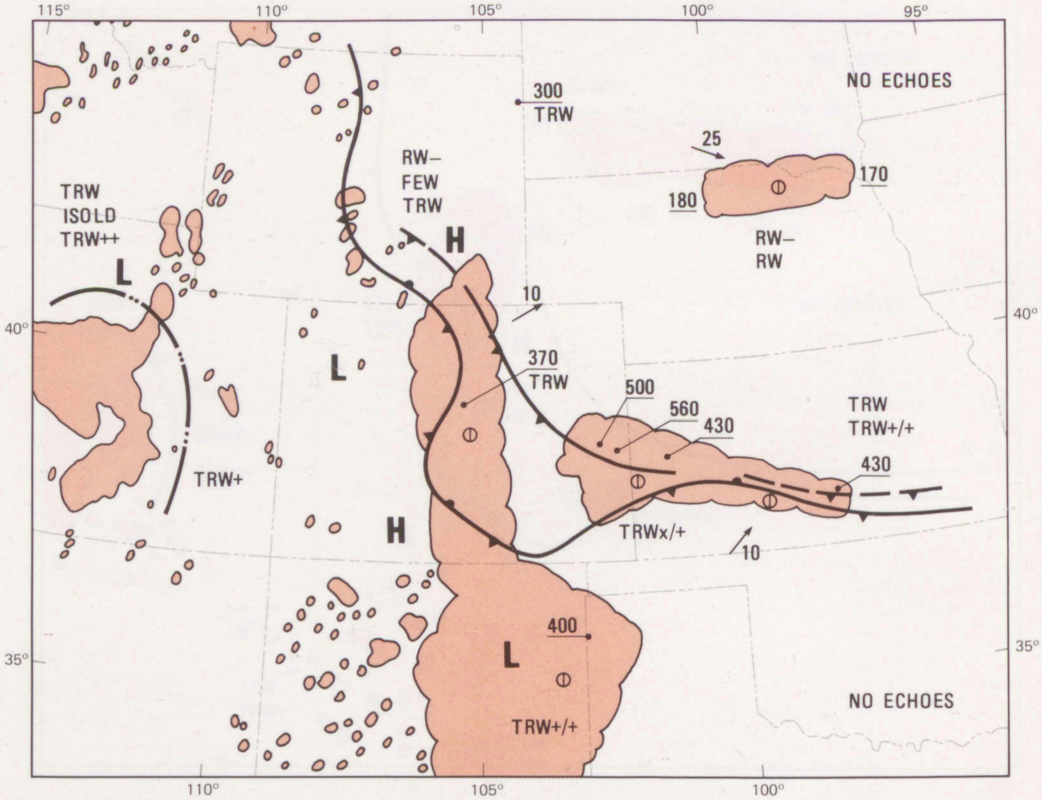

Figure 15b. Radar summary chart for 2135 GMT, 31 July 1976.

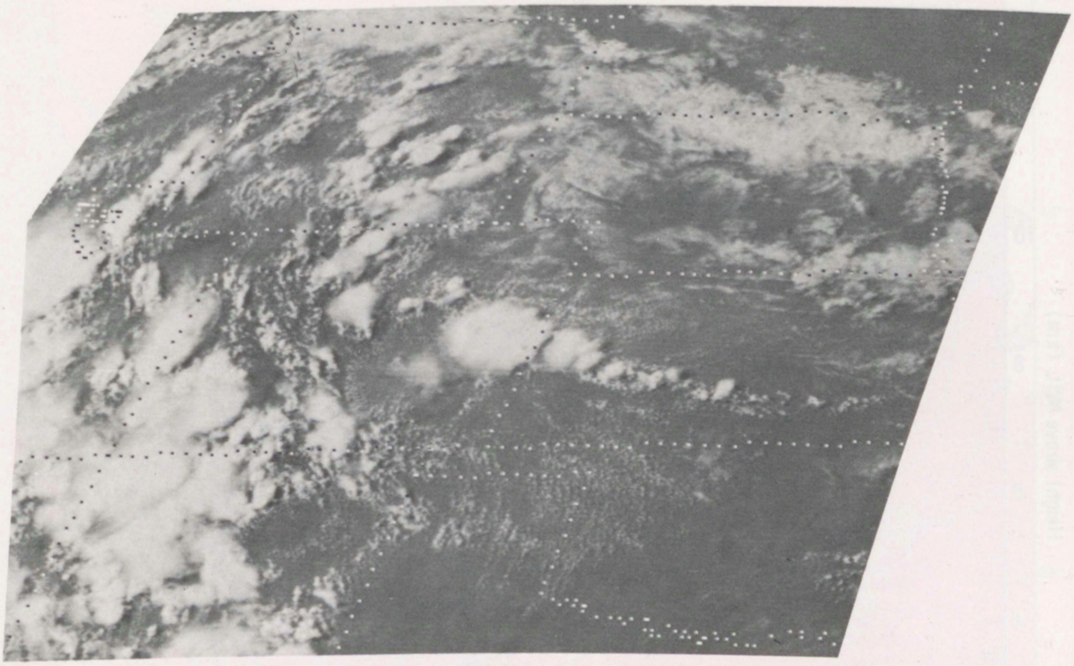

Figure 15c. GOES-1 photograph for 2200 GMT, 31 July 1976.

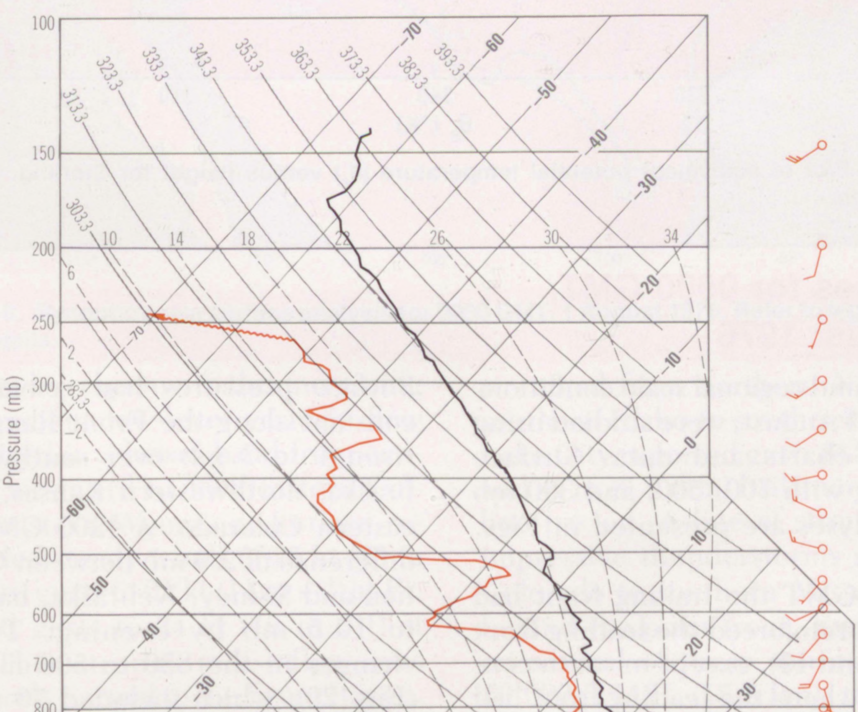

Figure 16. Skew T/Log P plot of Sterling, Colorado, upper-air sounding taken at 2202 GMT, 31 July 1976.

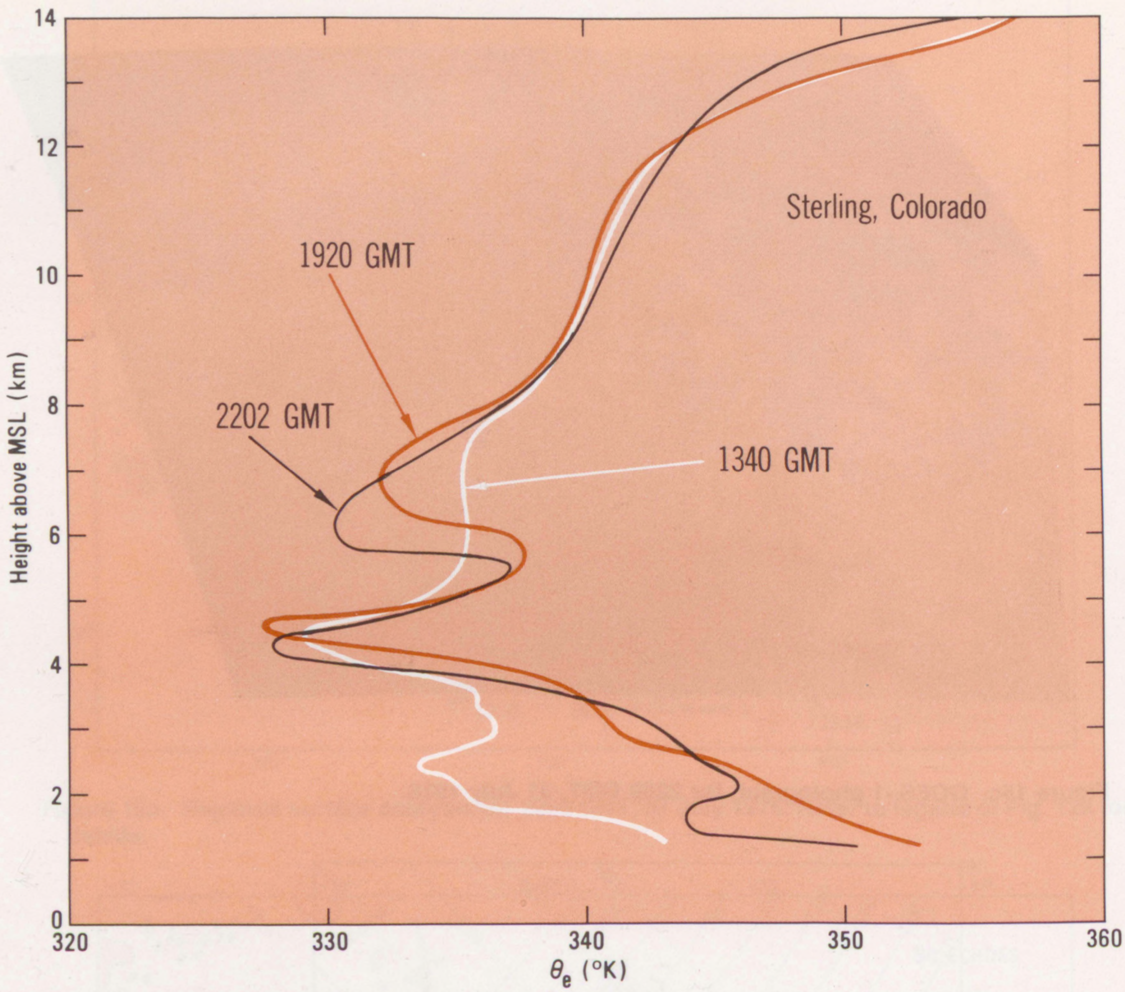

Figure 17. Plot of equivalent potential temperature (θ_e) versus height for Sterling, Colorado, soundings.

2.3 Analyses for 0000 GMT, 1 August 1976

Synoptic and regional scale conditions at 0000 GMT, 1 August, were studied using a variety of charts and data. Surface analyses along with 700, 500, and 300 mb upper-air analyses are presented in Figs. 18 through 23.

By 0000 GMT the trailing front had overtaken and reinforced the leading front (see Figs. 18 and 19), except in south central Colorado where the leading front had become diffuse and was analyzed as undergoing frontolysis. The low pressure center in western Colorado had deepened to 1005 mb and was located just north of Eagle. Surface pressures had remained nearly constant along the Front Range, and had risen 1 to 3 mb over southwestern Nebraska, northwestern Kansas, and northeastern Colorado. A 1200 GMT pressure difference of 2.9 mb between Grand Junction and Sidney, Nebraska, had increased to 10.5 mb by evening. Twelve-hour changes in the 850 to 500 mb thickness (Fig. 20), which included 70 m increases over northwestern Colorado and 20 m decreases over southern Nebraska, indicated a strengthening of the easterly pressure gradient through a large depth of the

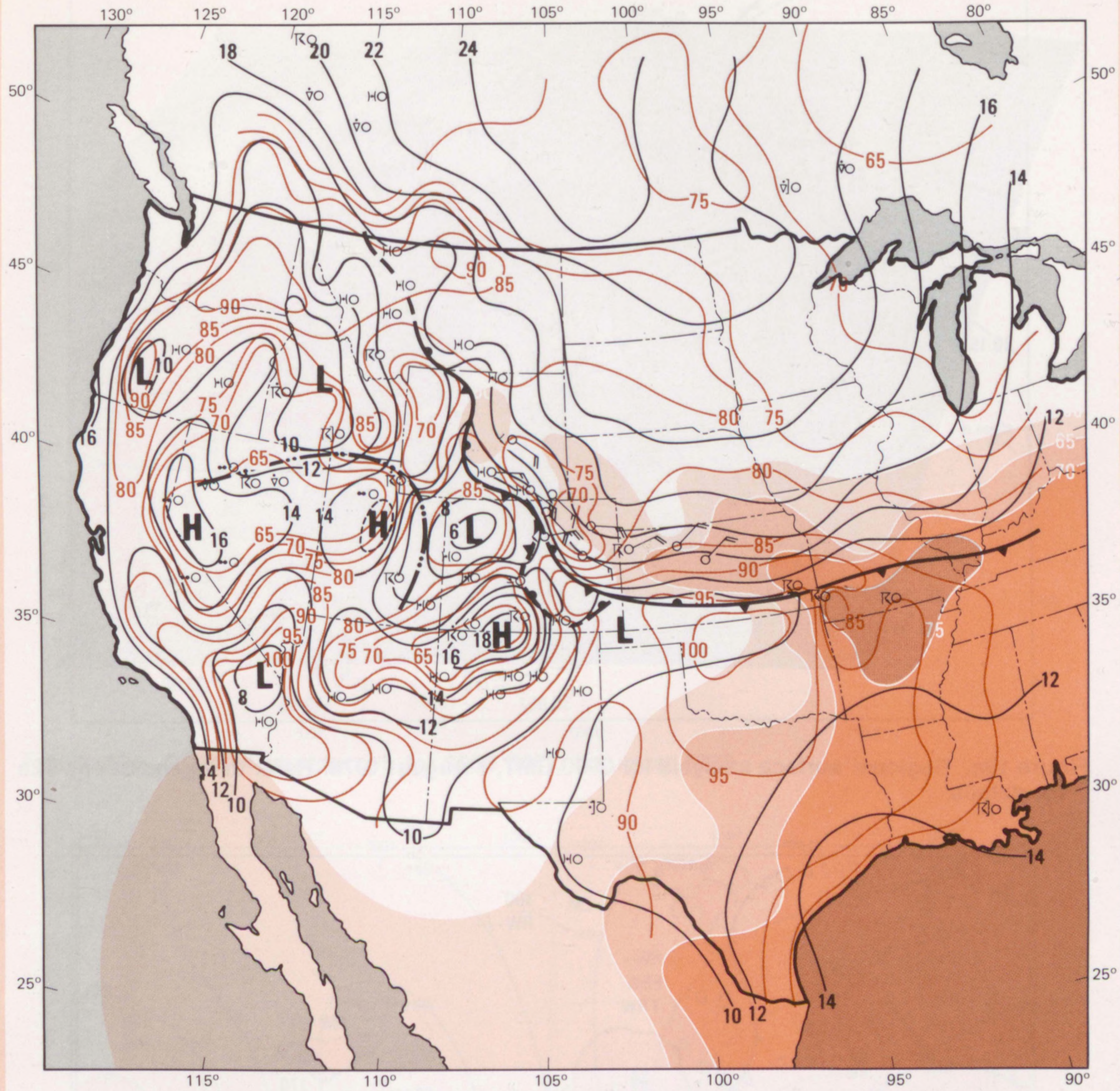

Figure 18. Synoptic scale surface analysis for 0000 GMT, 1 August 1976. Refer to legend of Fig. 4 for details.

troposphere. In response to this increasing pressure gradient low-level easterly flow had maximized in a broad band from central Kansas westward to northeastern Colorado and eastern Wyoming. Surface reports included steady winds of 25 kt (13 m s^{-1}) at Akron, gusts to 21 kt (11 m s^{-1}) at Ft. Collins, and gusts to 24 kt (12 m s^{-1}) at Denver. This strong, moist flow was oriented nearly normal to the Front Range.

Surface observations and the radar and satellite data shown in Figs. 19b and c indicated widespread mountain thunderstorm activity. A large squall line stretched from northern Nevada through southern Idaho to southeastern Utah. Salt Lake City reported gusts to 52 kt (27 m s^{-1}) and ⅜ in (9.5 mm) hailstones as this squall line passed. A line of strong and visually impressive thunderstorms stretched from Colorado to southern Missouri along and behind the polar front. Even though tops on several of these storms grew to over 50,000 ft MSL (15.3 km), their intensities remained below severe limits although locally heavy rains were likely produced.

A large area of thunderstorms had developed over east central Wyoming to the

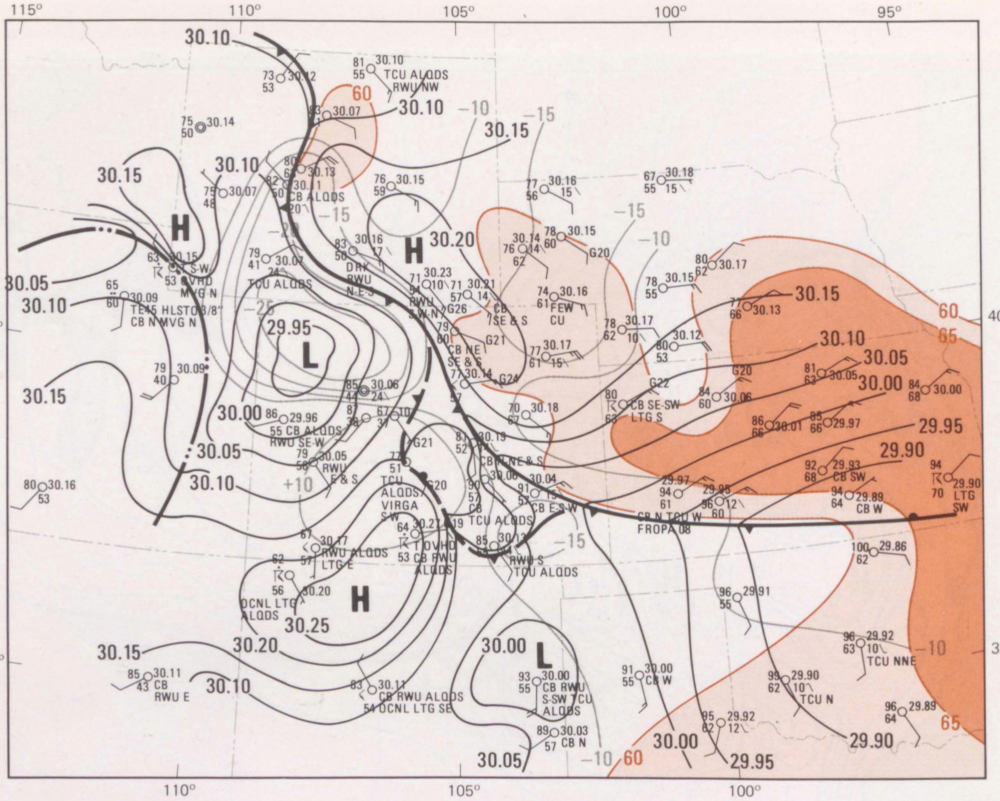

Figure 19a. Regional surface analysis for 0000 GMT, 1 August 1976. Refer to legend of Fig. 12a for details.

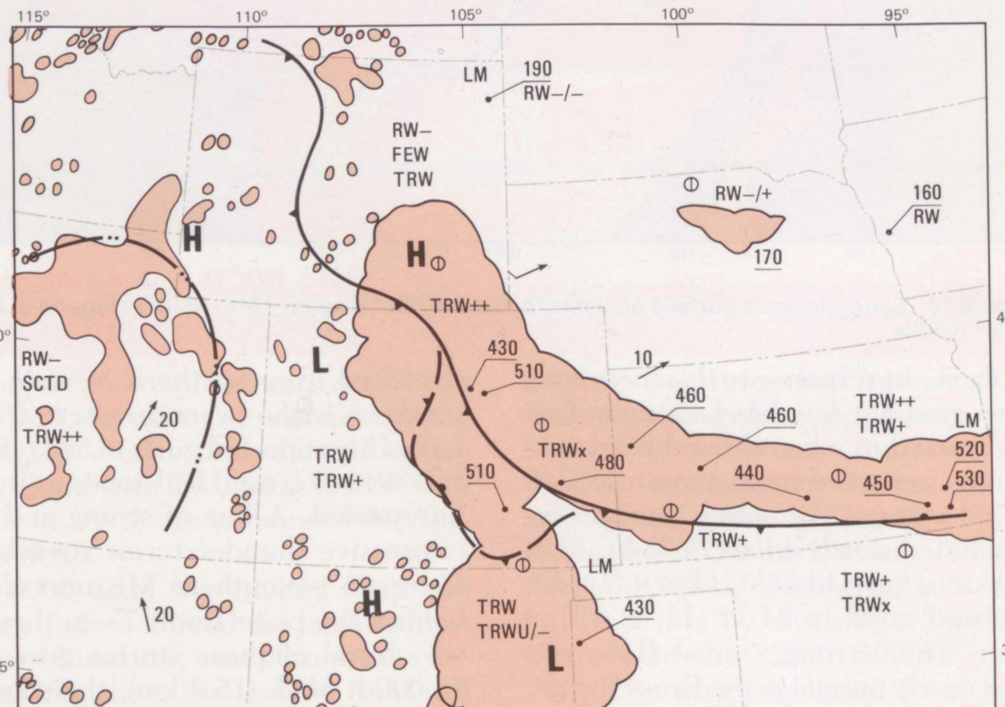

Figure 19b. Radar summary chart for 2335 GMT, 31 July 1976.

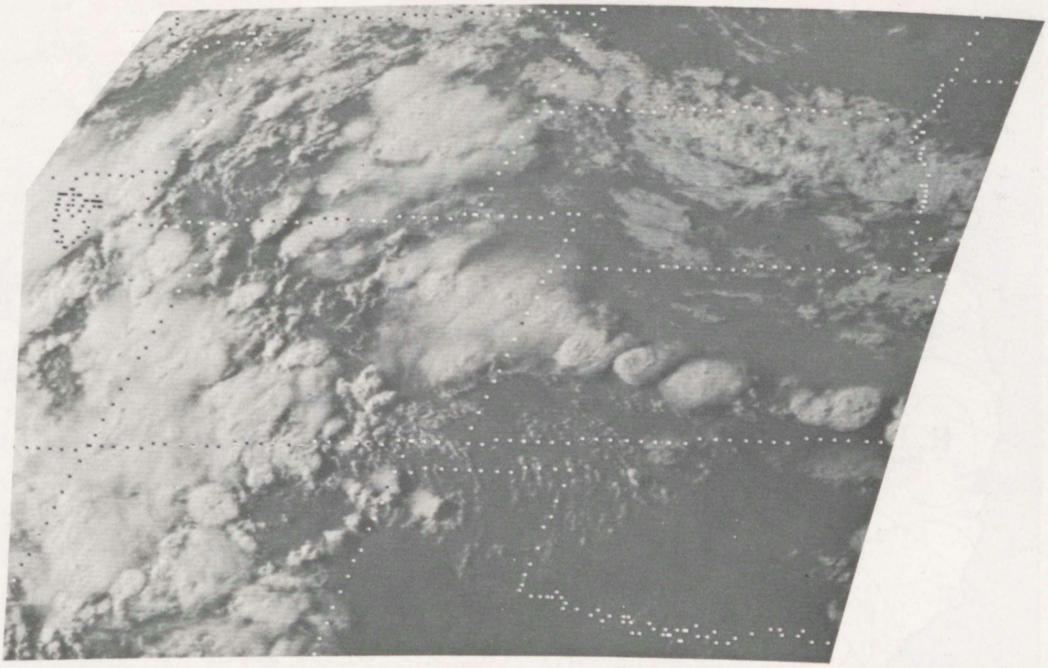

Figure 19c. GOES-1 photograph for 0000 GMT, 1 August 1976.

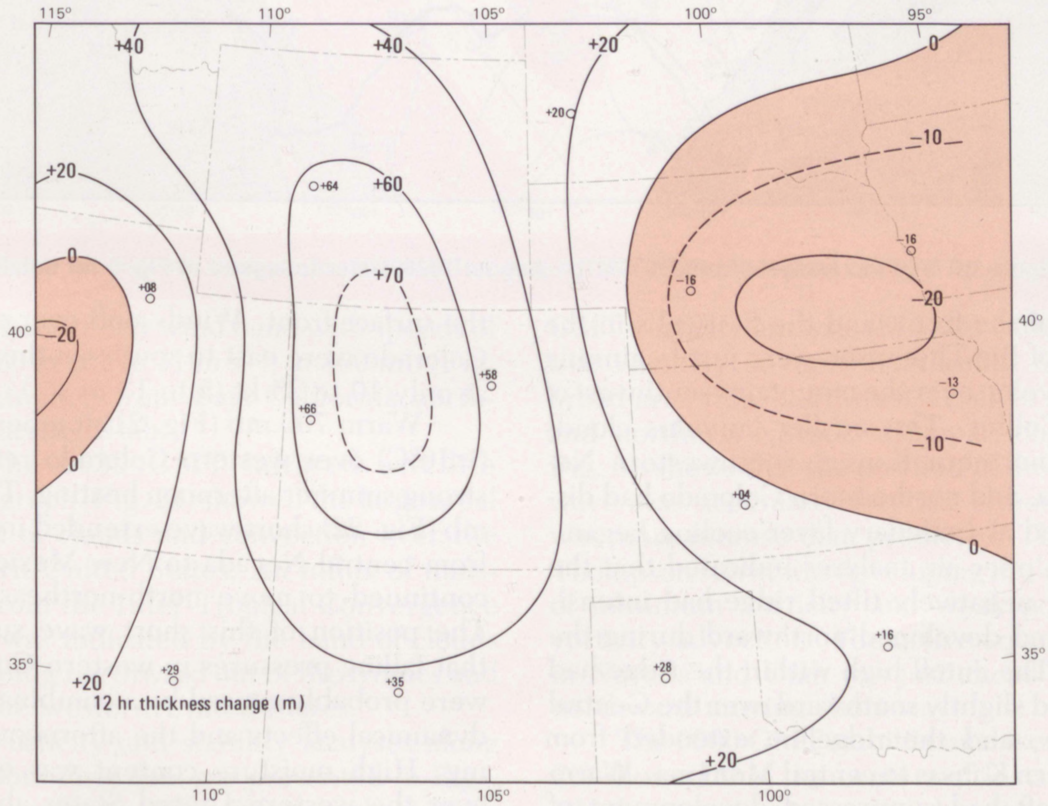

Figure 20. Changes in 850–500 mb thickness (in meters) from 1200 GMT on July 31 to 0000 GMT on August 1. Regions where thickness decreased are shaded orange.

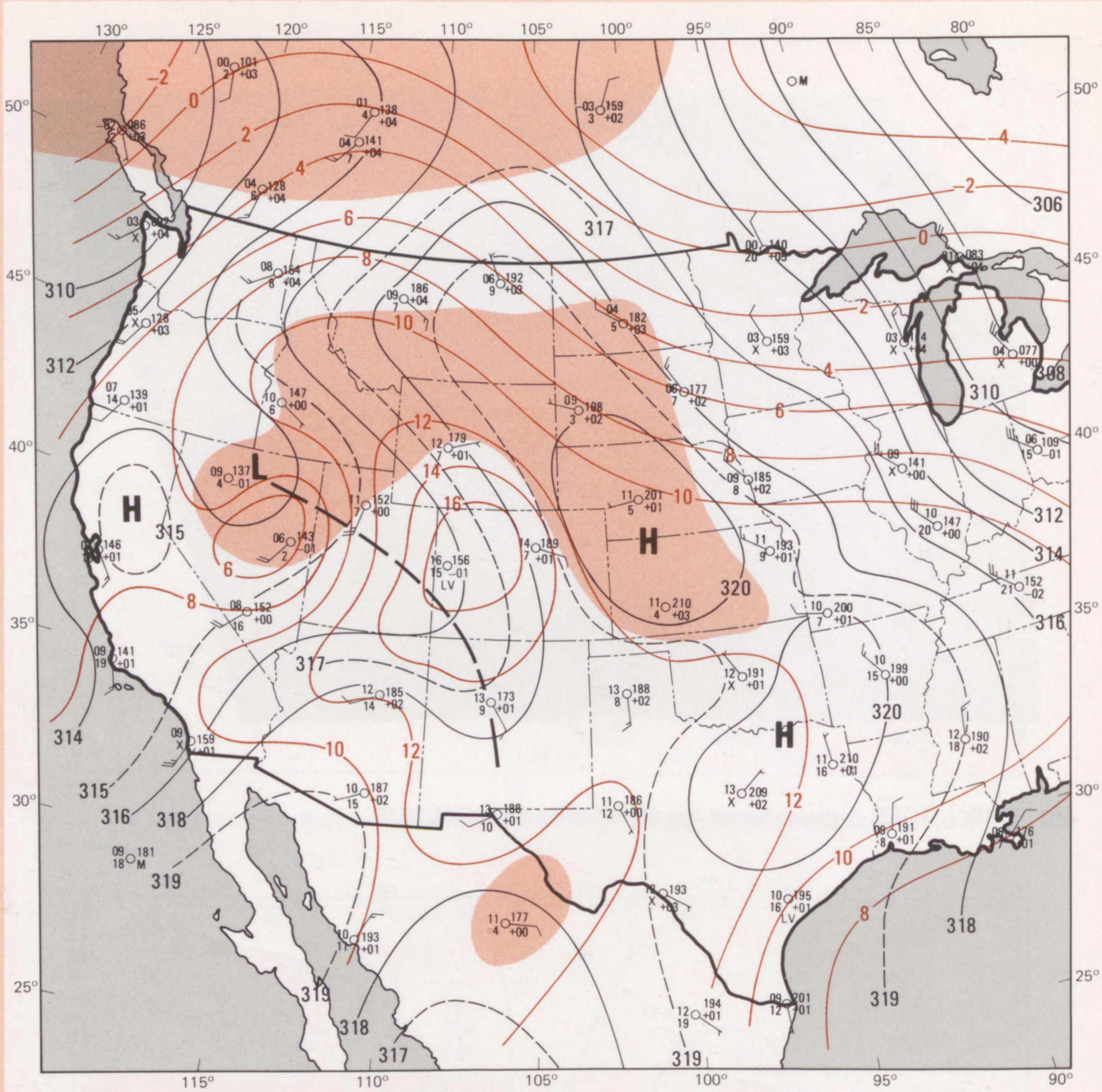

Figure 21. 700 mb analysis for 0000 GMT, 1 August 1976. Refer to legend of Fig. 5 for details.

rear of the front, and the first cells in the area of Big Thompson were just beginning to develop over the mountains southwest of Ft. Collins. The smaller cumulus clouds over northern Kansas, southwestern Nebraska, and northeastern Colorado had dissipated as boundary layer cooling began.

Upper-air analyses indicated that the large, negatively tilted ridge had intensified and developed northward during the day. The cutoff high within the ridge had drifted slightly southward over the Central Plains, and the ridgeline extended from western Kansas to central Montana. Warm air aloft had suppressed development of deep convection over the plains south of the surface front. Winds aloft over eastern Colorado were east to south-southeasterly at only 10 to 25 kt (5 to 13 m s^{-1}).

Warm 700 mb (Fig. 21) temperatures ($\geq$16°C) over western Colorado reflected strong summer afternoon heating. The 500 mb (Fig. 22) short wave extended in an arc from central Nevada to New Mexico as it continued to move north-northeastward. The position of this short wave suggests that falling pressures in western Colorado were probably caused by a combination of dynamical effects and the afternoon heating. High moisture content was evident over the western United States ahead of the trough. An unusually strong (for the

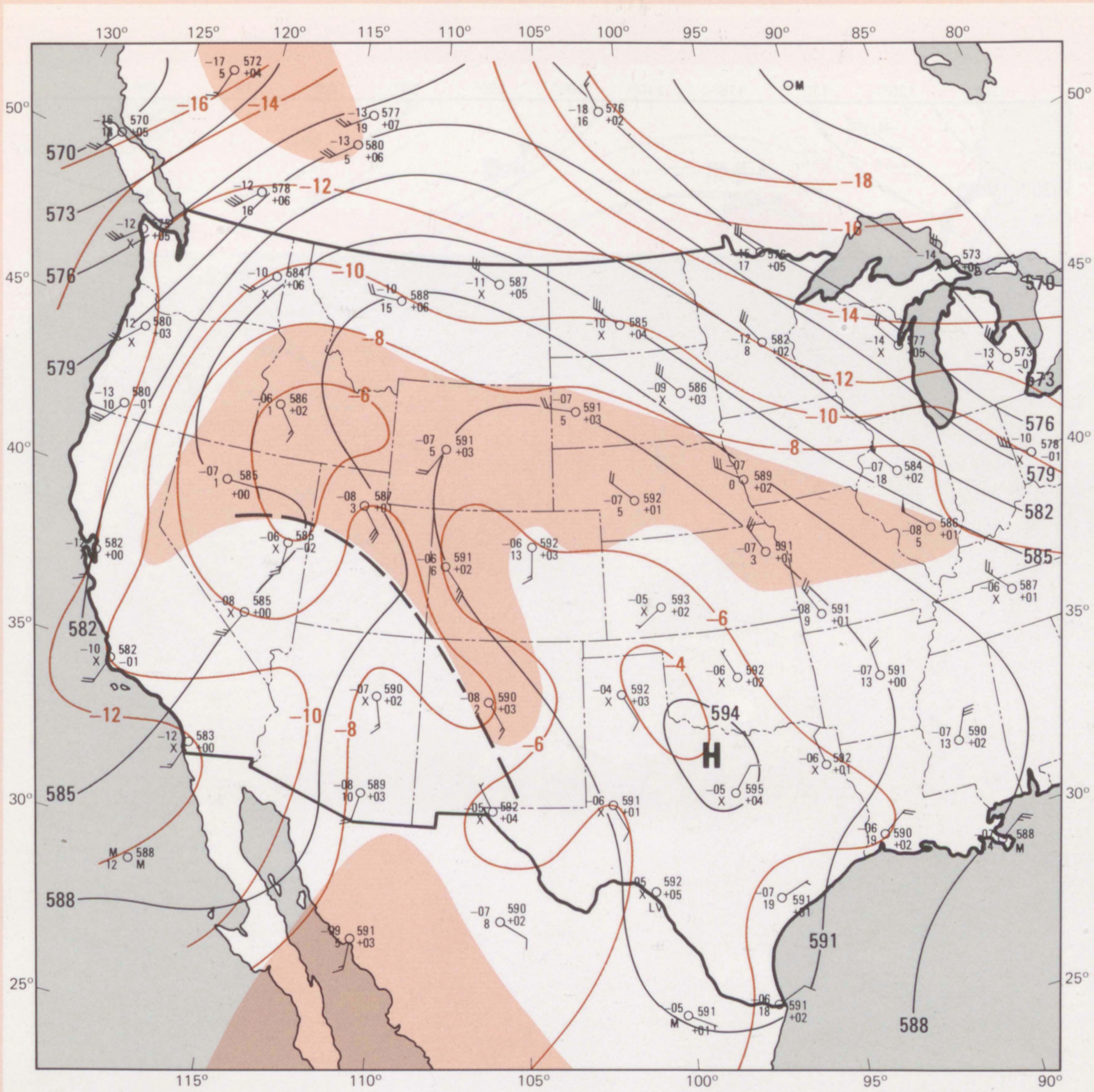

Figure 22. 500 mb analysis for 0000 GMT, 1 August 1976. Refer to legend of Fig. 6 for details.

season) southerly wind band with speeds of 40 to 60 kt (21 to 31 m s^{-1}) at 300 mb (Fig. 23) extended from Baja California northward across Utah.

The 0030 GMT infrared satellite photograph (Fig. 24) showed the large areal extent of clouds and convection over the western United States. An influx of moisture from the Inter-Tropical Convergence Zone was indicated by the band of clouds streaming northward out of the tropics and into the western United States.

Vorticity and stability analyses along with sounding data are presented in Figs. 25 through 27. The 500 mb short-wave trough was clearly depicted on the 0000 GMT vorticity analysis (Fig. 25) with positive vorticity advection indicated over a broad area from northwest Texas to Idaho and northern Nevada. Comparison with Fig. 8b shows that the position of the short wave was accurately forecast although it was more intense than predicted. The Big Thompson storm was developing in a region of minimum vorticity and weak positive vorticity advection. The active squall line in Nevada and Utah was just ahead of the northward moving short wave.

The 0000 GMT stability analyses (Fig. 26) showed that the centers of instability, which were over Arizona and western Kansas in the morning, had merged to form one

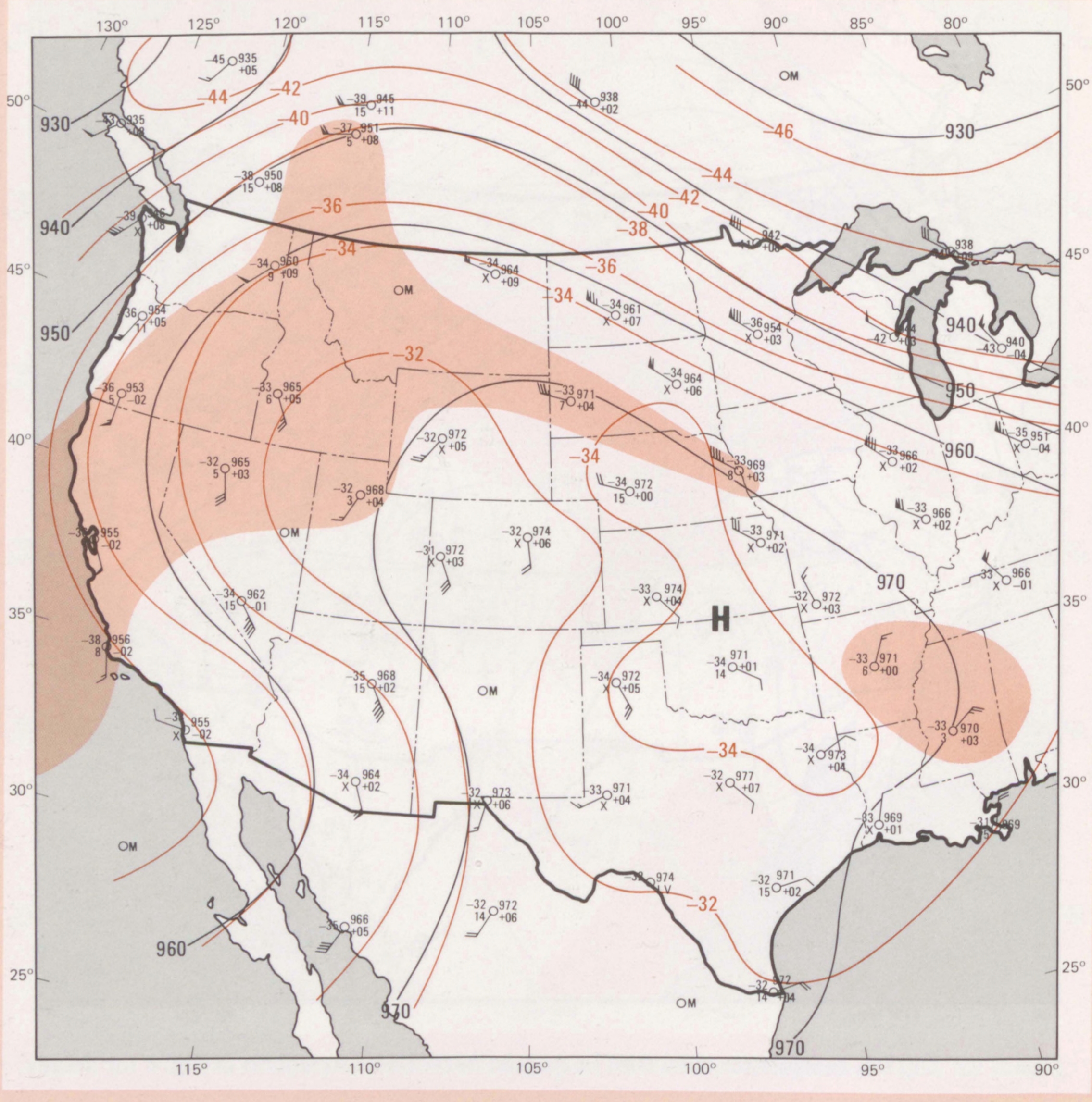

Figure 23. 300 mb analysis for 0000 GMT, 1 August 1976. Refer to legend of Fig. 7 for details.

large area of unstable conditions that stretched from New Mexico to Montana. Thunderstorms were occurring throughout this region and Totals of 50 to 52, along with L.I. values of −2 to −4, indicated the potential for moderate to heavy storm activity.

The 0000 GMT Denver sounding (Fig. 27) showed that the air mass structure had modified significantly during the day. The temperature inversion had lifted 80 mb to the 590 mb level. Strong diurnal heating was probably responsible for this lifting since a dry adiabatic lapse rate existed below the inversion. The low cloud layer had dissipated during the morning, and the mean vapor mixing ratio in the lowest 100 mb layer had decreased from 12.0 to 9.5 g kg^{-1}. Easterly flow had increased slightly and the LFC had lowered to 620 mb. The L.I. was −2 and thunderstorm activity was developing in the vicinity. Precipitable water for the surface-to-500 mb layer was 2.47 cm, little different from the 2.54 cm value at 1200 GMT. Strong afternoon heating and mixing had redistributed the moisture through a deeper layer. The Denver

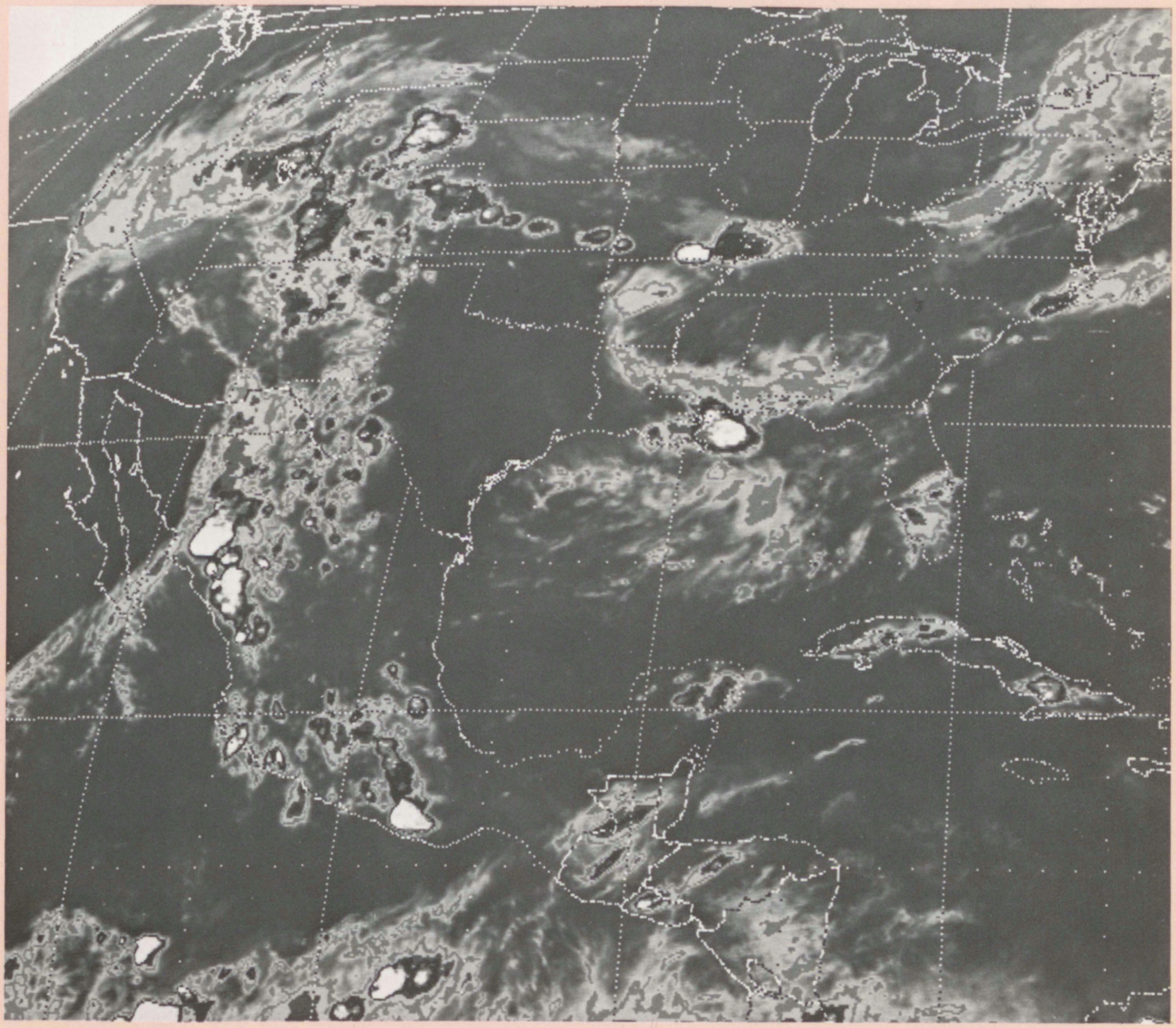

Figure 24. GOES–1 infrared (4 km resolution) satellite photograph for 0030 GMT, 1 August 1976.

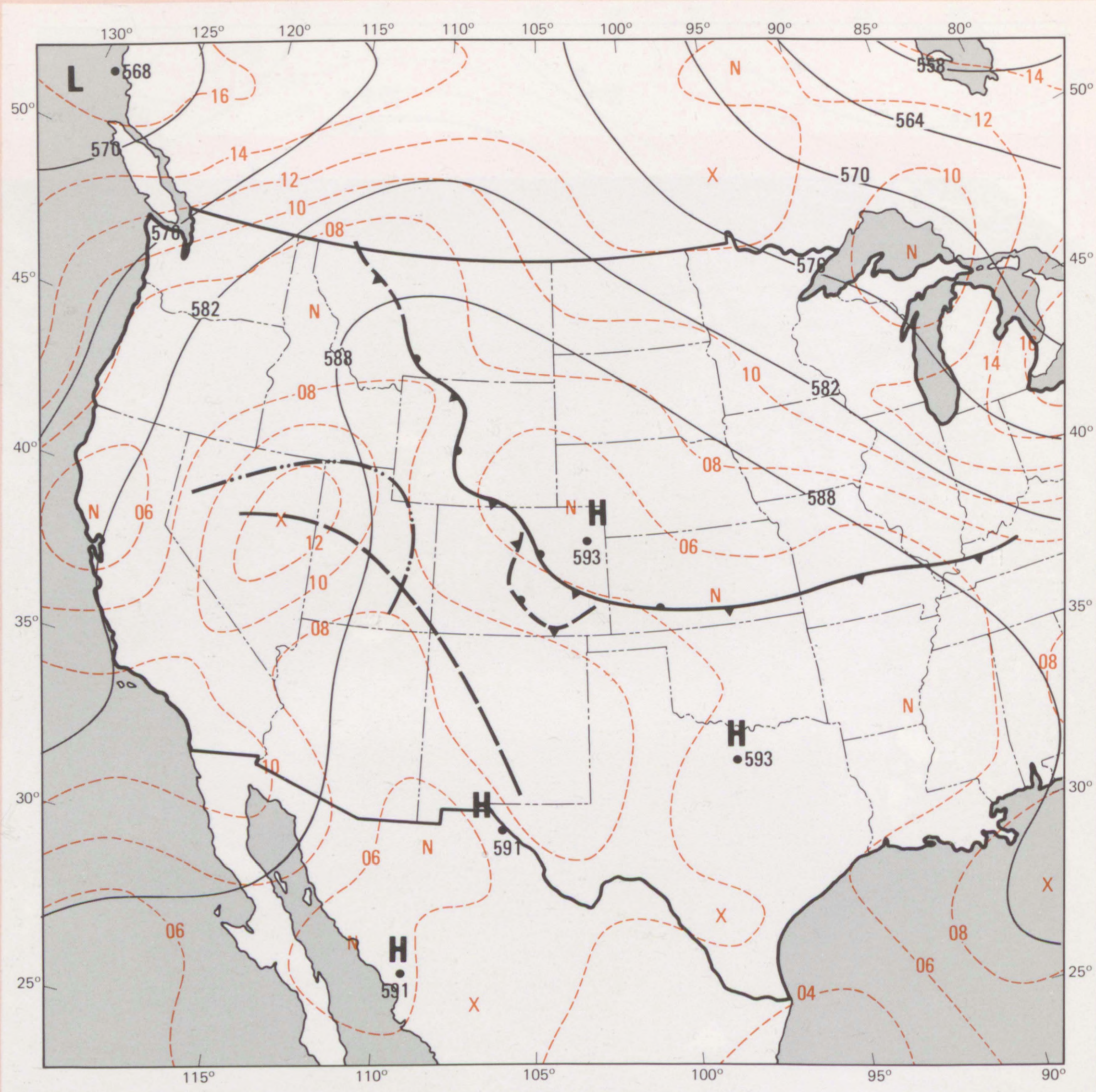

Figure 25. NMC–LFM vorticity analysis (orange) for 0000 GMT, 1 August 1976. Synoptic surface analysis and 500 mb height analysis are in black. Position of the important 500 mb short wave is also shown in black.

sonde was released at approximately 2315 GMT, **prior** to passage of the trailing front.

Table 2 compares soundings taken during the day of 31 July 1976. Note the considerable difference between the 1920 GMT Sterling sounding and the 0000 GMT Denver sounding. Precipitable water contents were about 50% higher at Sterling. While the Lifted Condensation Level (LCL) was much lower at Sterling (780 vs. 630 mb), the Denver air mass needed only 10 mb of additional lift to reach the LFC. This is in contrast with the air mass at Sterling in which 140 mb of lift was required to attain the LFC. Diurnal cooling could be expected to suppress the ongoing convection in the Denver area, and orographic lifting would be required to trigger storm development within the post-frontal air mass that was moving into the foothills of northern Colorado.

Denver and Dodge City soundings at

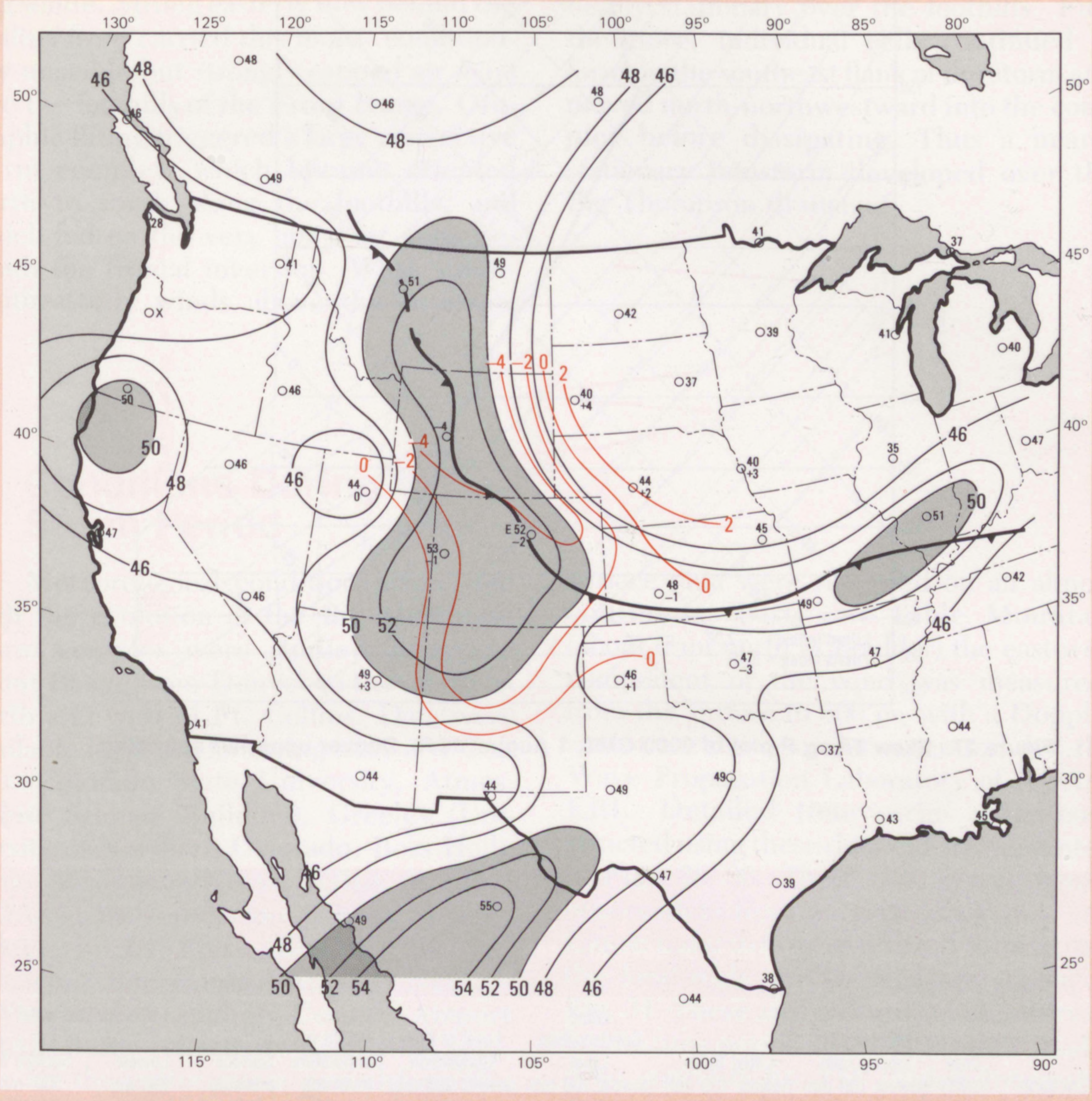

Figure 26. Stability chart for 0000 GMT, 1 August 1976. Refer to legend of Fig. 9 for details.

0000 GMT were similar and indicated that the air mass between the leading and trailing fronts had been modified by heating and mixing of boundary layer air; thus, little contrast remained across the leading front. The narrow band of very moist, conditionally unstable air, which played a vital role in the development of the Big Thompson storm, was not sampled by the synoptic rawinsonde network. Denver was located just south and west of the important air mass at 0000 GMT, and North Platte was located just east of the deep moist layer at 1200 GMT. However, surface reports from such locations as Imperial and McCook, Nebraska; Goodland, Kansas; and Akron, Limon, and Ft. Collins, Colorado, indicated the presence and helped delineate the extent of the moist tongue of air.

All available data suggest that the air mass that fed the Big Thompson storm was

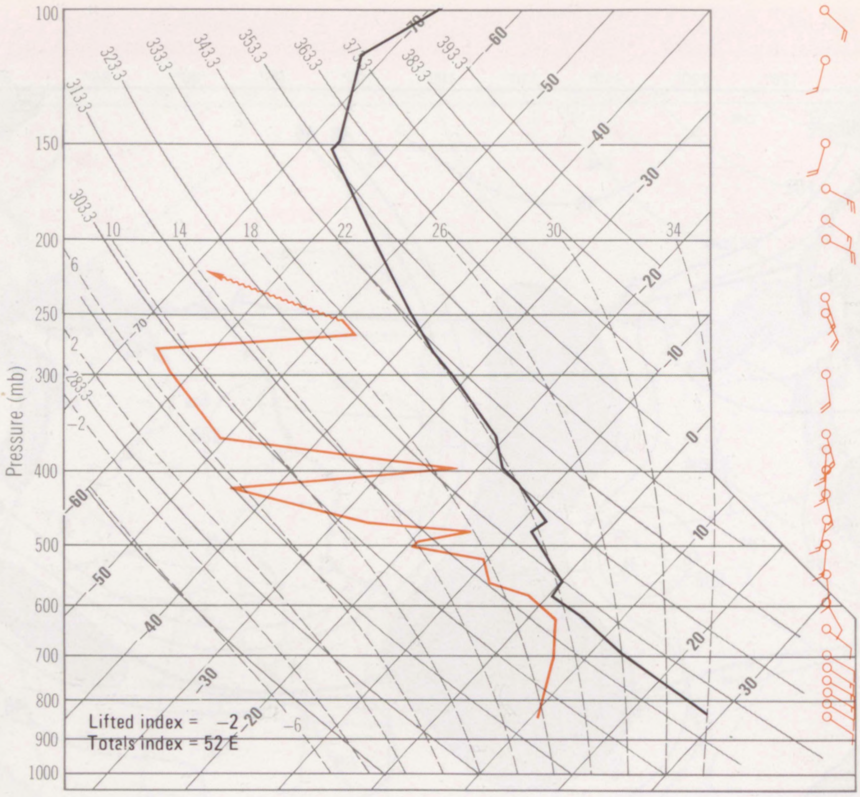

Figure 27. Skew T/Log P plot of 0000 GMT, 1 August 1976, Denver upper-air sounding.

Table 2.
Upper-air sounding parameters for several locations on 31 July 1976 and 1 August 1976

Location	Time (GMT)	Mean vapor mixing ratio (lowest 100 mb) (g kg^{-1})	Lifted Index (lowest 100 mb)	Lifted Condensation Level (lowest 100 mb) (mb)	Level of Free Convection (lowest 100 mb) (mb)	Height of temperature inversion (mb)	Surface pressure (mb)	Precipitable water: Lowest 150 mb (cm)	Precipitable water: Surface to 500 mb (cm)
Denver	1200	12.0	−1	785	530	670	843	1.71	2.54
Sterling	1340	11.0	+1	760	480	725	882	1.49	2.64
Sterling	1920	13.8	−4	780	640	720	882	1.97	3.34
Sterling	2202	12.5	−2	765	600	680	882	1.79	2.90
Denver	0000	9.5	−2	630	620	590	840	1.37 1.02*	2.47 1.74*
Grand Junction	0000	8.5	−1	615	550	none	850	1.21 0.90*	2.17 1.66*
Dodge City	0000	9.7	−1	650	650	none	935	1.45 1.43*	2.81 2.64*

*July mean precipitable water

like that sampled by the 1920 GMT Sterling sonde. Strong easterly flow behind the trailing front carried this moist, conditionally unstable but strongly capped air mass into the foothills of the Front Range. Orographic lifting triggered a large convective storm complex, which became oriented north to south along the foothills, and which fed on the very moist air mass beneath the frontal inversion. Weak south-southeasterly winds above the inversion allowed the storm complex to remain nearly stationary over the foothills. Furthermore, individual cells continued to form on the southeast flank of the storm and moved north-northwestward into the complex before dissipating. Thus a nearly stationary rainstorm developed over the Big Thompson drainage.

3. Conditions During the Storm Period

Meteorological conditions associated with the evolution of the Big Thompson storm complex were studied along the Front Range from Denver to the area just north and west of Ft. Collins. Data were available from the following sites: Ft. Collins (Colorado State University, Atmospheric Science Building), Greeley (University of Northern Colorado, Ross Hall), Table Mountain (NOAA–ERL), Boulder (NOAA–ERL), Jefferson County Airport (FAA), Rocky Flats (ERDA), Denver (Stapleton International Airport, NOAA–NWS), and Arapahoe County Airport (FAA). Radar reflectivity data were available for the entire storm period from the NWS WSR–57 radar at Limon, Colorado, (located approximately 205 km southeast of the Big Thompson area). Reflectivity data were also available from the NHRE 10 cm radar (located at Grover, Colorado, approximately 115 km east-northeast of the Big Thompson area) for a 45 min period near the beginning of the storm. Thunderstorms that produced flooding on the North Fork of the Cache la Poudre River were generally beyond the area of radar coverage.

3.1 Local Area Analyses

At three sites (Stapleton International Airport, Table Mountain, and Rocky Flats) surface data were recorded on an almost continuous basis. At Table Mountain (about 6 mi north of Boulder) the east-west component of the wind was measured, from the surface to 600 m, with a Doppler acoustic echo sounder operated by the Wave Propagation Laboratory of NOAA–ERL. Detailed time series were constructed using these data and are presented in Figs. 28–30. These time series, hourly observations from the remaining sites, and Limon radar data were utilized to construct the local-scale surface analyses shown in Fig. 31. These analyses are at ½ h intervals for the time period 2330–0100 GMT. Radar echo contours for VIP (Video Integrator Processor) levels 1, 2, and 3 are depicted. These contours correspond to the minimum detectable signal, 30 dBZ and 41 dBZ respectively.

In the Ft. Collins, Loveland, and Greeley areas an increase in wind speeds and gustiness were the only indications of the passage of the trailing front. These areas had remained partly cloudy with upslope southeasterly flow during the afternoon, resulting in little temperature difference across the front. In the Denver-Boulder area, however, afternoon cloudiness was minimal. The resulting heating and mixing had elevated surface temperatures and lowered dewpoints. Winds were also more

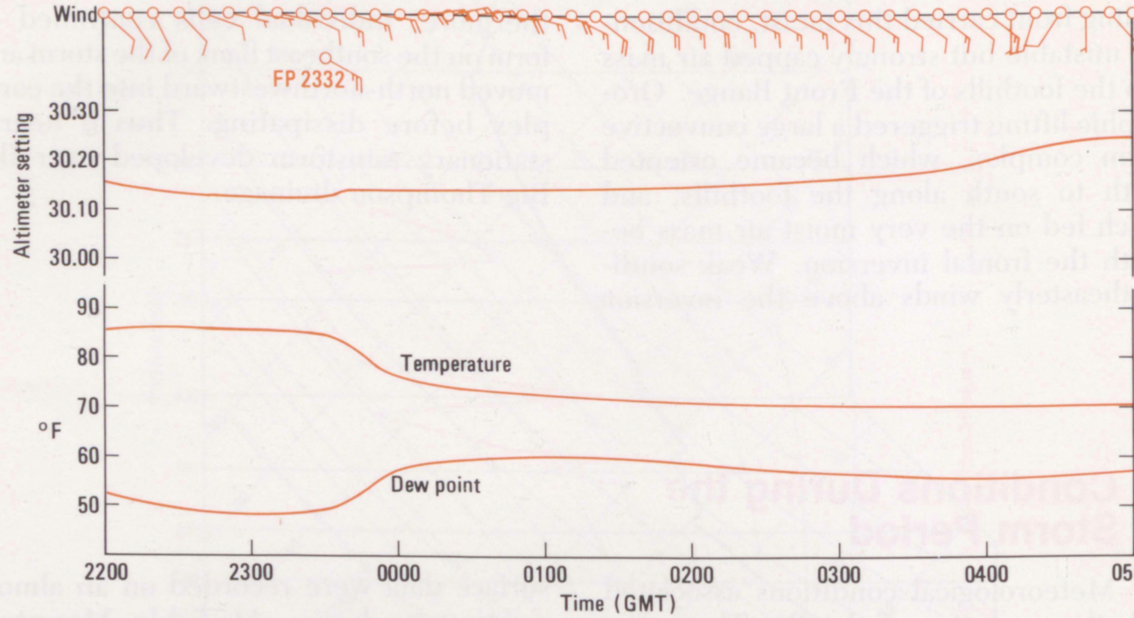

Figure 28. Time series plots of surface wind (in knots), altimeter setting (inches of mercury), and temperature and dewpoint temperature (°F) as recorded at Stapleton International Airport, Denver, Colorado. Time covered is from 2200 GMT, 31 July 1976 to 0500 GMT, 1 August 1976.

southerly. The trailing front passed both Stapleton (Fig. 28) and Table Mountain (Fig. 29) at about 2330 GMT. At both of these sites, the passage was accompanied by a significant increase in easterly or southeasterly winds. Dewpoint temperatures increased 10°–13°F (5.5°–7°C) and temperatures dropped 10°–12°F (5.5°–6.5°C) in a 30 min period.

Prior to 2330 GMT a large thunderstorm had developed along the higher terrain southeast of Denver as the trailing front moved into this region. This storm moved northwestward and merged with cells that formed between 2330–0000 GMT ahead of the front in the region west of Denver. The resulting arc of echoes (see Fig. 31) moved into the Boulder area around 0030 GMT.

A gust front and clouds of blowing dust were associated with this line of thundershowers. A strong cell moved across Rocky Flats, and the time series (Fig. 30) shows that wind gusts to 41 kt (21 m s^{-1}) occurred about 0015 GMT just ahead of a brief, but heavy rainshower. Temperature and dewpoint temperature changes comparable to those at Stapleton and Table Mountain also occurred. It is difficult to determine whether these changes were caused by passage of the trailing front or by the line of thundershowers.

Eyewitness accounts and the 0000 GMT Denver rawinsonde data indicated that the clouds that formed ahead of the trailing front had higher bases than the storms that developed along the foothills to the north. Between 0030 and 0100 GMT pressure rises of about 1 mb were observed at Rocky Flats and Boulder. These pressure changes were accompanied by a wind shift to the southwest. Evidently, rain showers and evaporative cooling in drier air along the foothills between Boulder and Golden had produced a small meso-high pressure area. The winds at both Boulder and Rocky Flats remained light southerly to westerly until about 0400 GMT.

That portion of the arc of echoes east of Boulder dissipated rapidly after 0030 GMT

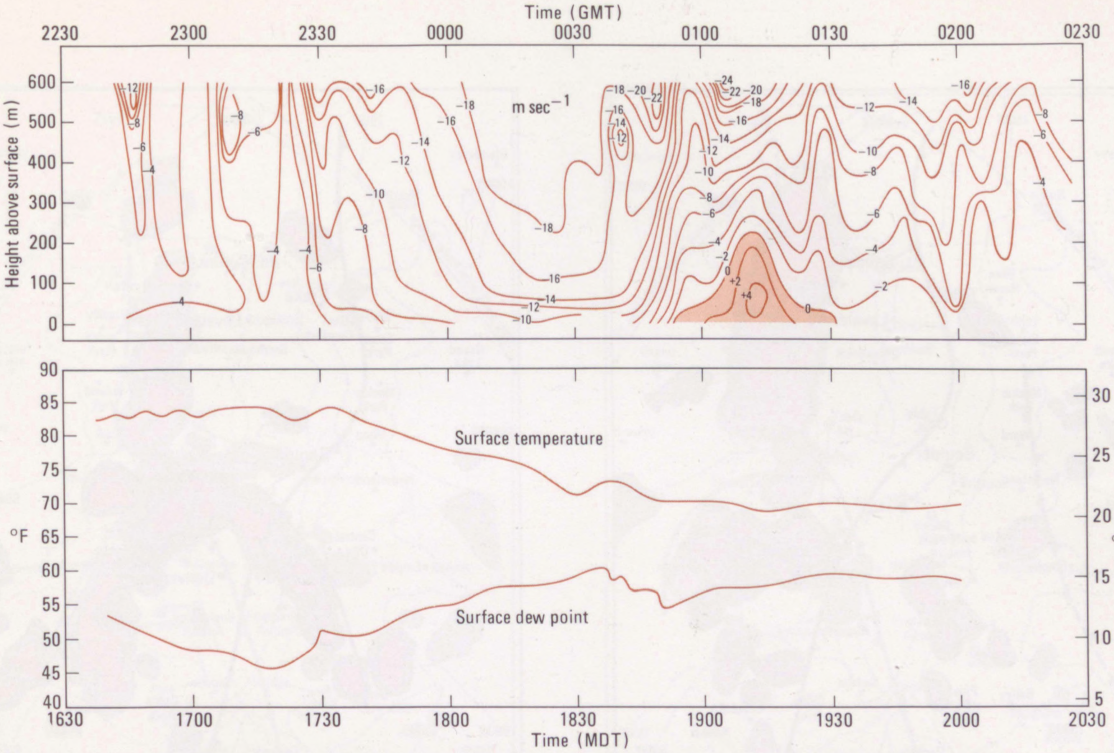

Figure 29. Time series of east-west component of wind (m s^{-1}), temperature, and dewpoint temperature (°F) from the Wave Propagation Laboratory site on Table Mountain. Negative values indicate easterly winds. Occurrence of light westerly winds near the surface is denoted by orange shading. Time covered extends from 2230 GMT, 31 July 1976 to 0230 GMT, 1 August 1976.

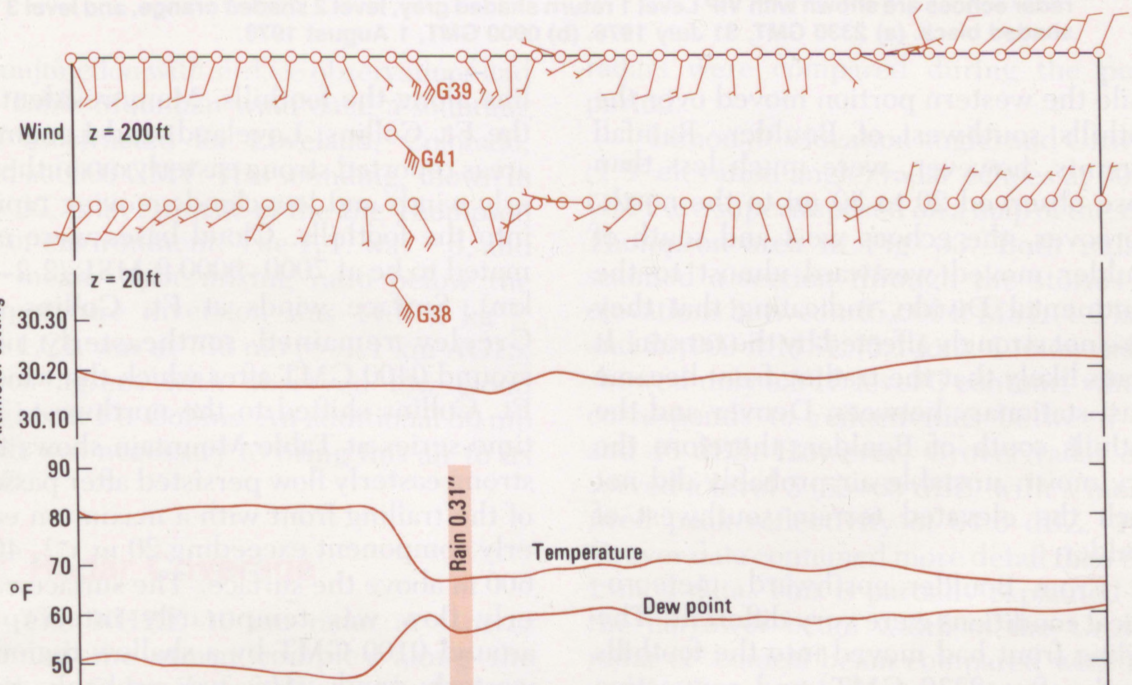

Figure 30. Time series plots, similar to Fig. 28, for Rocky Flats, Colorado. Winds were measured at 20 and 200 ft AGL on an instrumented tower. Time during which 0.31 in of rain fell is shaded orange.

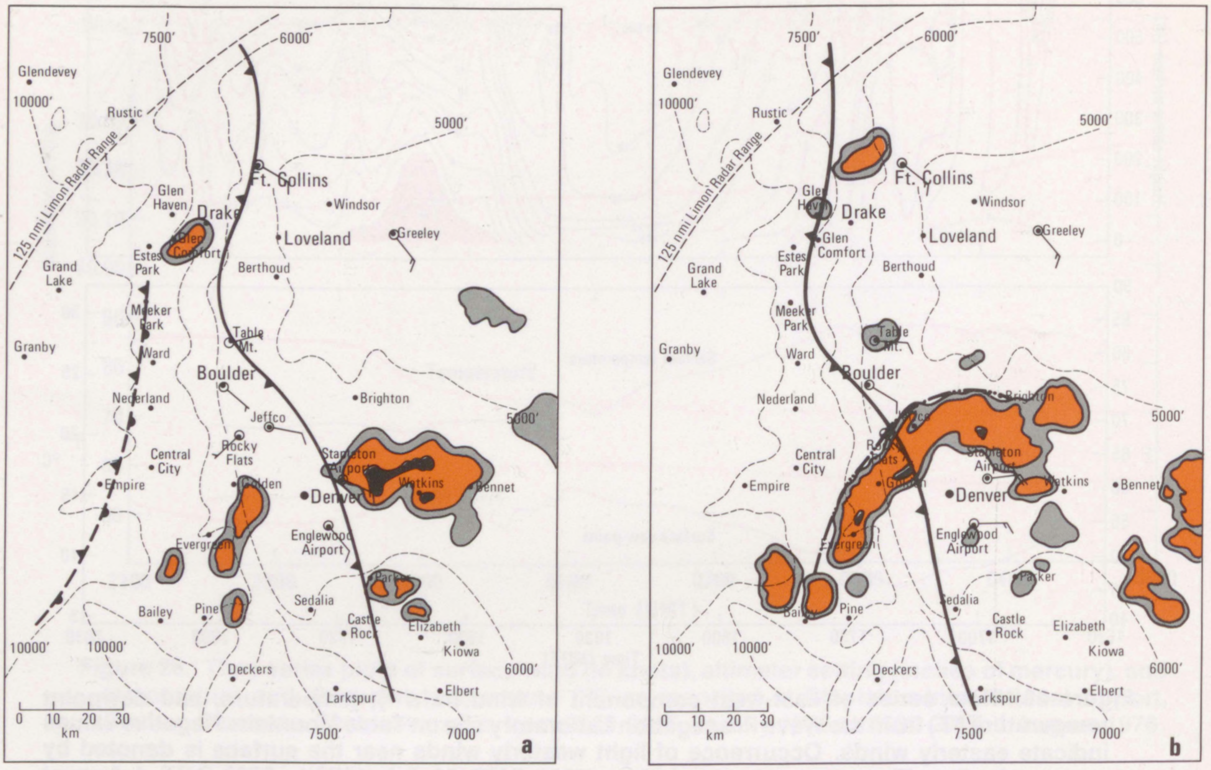

Figure 31. Local scale surface analyses. Frontal positions and reported winds are in black; Limon radar echoes are shown with VIP Level 1 return shaded gray, level 2 shaded orange, and level 3 shaded black. (a) 2330 GMT, 31 July 1976. (b) 0000 GMT, 1 August 1976.

while the western portion moved over the foothills southwest of Boulder. Rainfall amounts, however, were much less than those observed 20 to 80 mi to the north. Moreover, the echoes west and south of Boulder moved westward almost to the Continental Divide, indicating that they were not strongly affected by the terrain. It seems likely that the trailing front became quasi-stationary between Denver and the foothills south of Boulder; therefore the very moist, unstable air probably did not reach the elevated terrain southwest of Boulder.

From Boulder northward, meteorological conditions were very different. The trailing front had moved into the foothills shortly after 2330 GMT, and convective clouds developed very rapidly. By 0000 GMT a few echoes were detected by radar, and by 0030 GMT several strong thunderstorms were oriented in a north-south line along the foothills. Many residents of the Ft. Collins, Loveland, and Longmont areas reported strong easterly or southeasterly winds and low clouds moving rapidly into the foothills. Cloud bases were estimated to be at 7000–9000 ft MSL (2.2–2.7 km). Surface winds at Ft. Collins and Greeley remained southeasterly until around 0400 GMT after which the wind at Ft. Collins shifted to the northwest. The time series at Table Mountain shows that strong easterly flow persisted after passage of the trailing front with a maximum easterly component exceeding 20 m s^{-1}, 400–600 m above the surface. The surface easterly flow was temporarily interrupted around 0100 GMT by a shallow region of westerly winds. This was probably weak outflow from the large cell located a few miles to the west of the site.

Using the afternoon rawinsonde data from Sterling, Denver, and Grand Junction

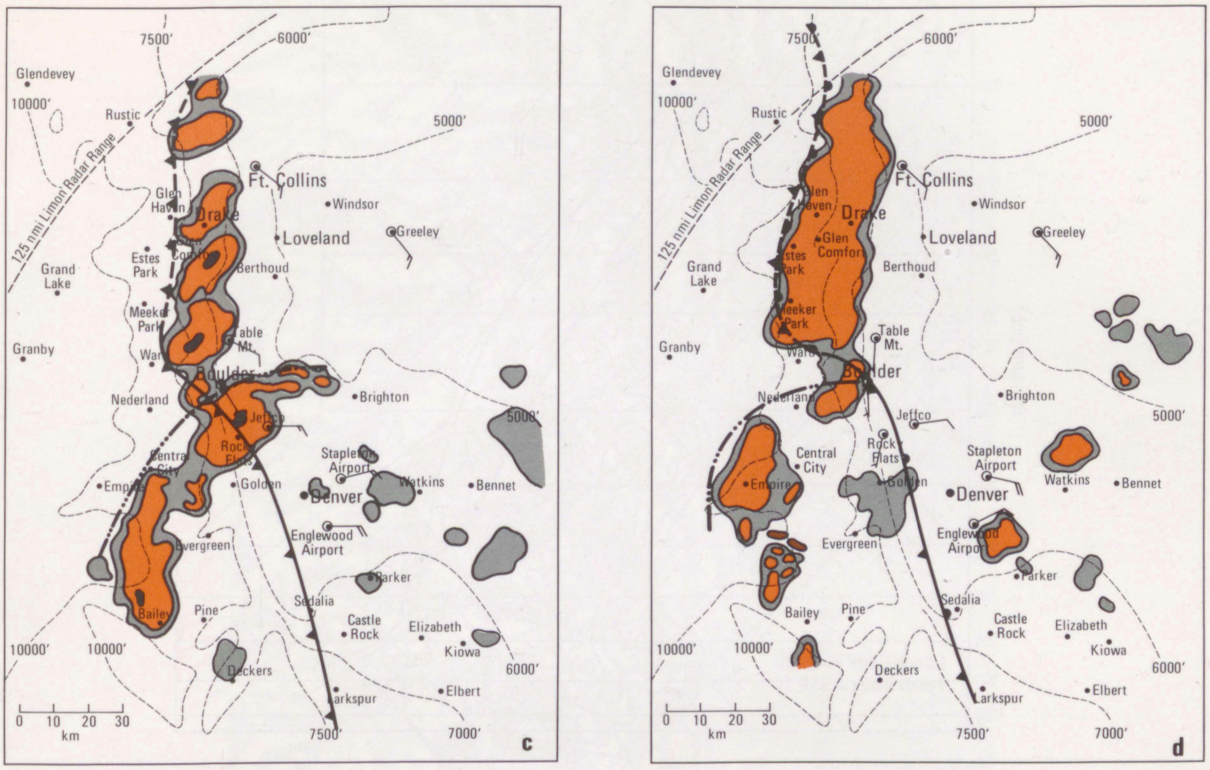

Figure 31. Continued. (c) 0025 GMT, 1 August 1976. (d) 0100 GMT, 1 August 1976.

in conjunction with surface observations and the Table Mountain wind data, a sounding was constructed for Loveland, Colorado, valid at 0000 GMT. This sounding, shown in Fig. 32, is an estimate of the Big Thompson storm environment. The L.I. was −6, and the mean vapor mixing ratio below the temperature inversion was 14.8 g kg^{-1}. The LCL was at 730 mb ($\approx$ 1.1 km AGL), which agrees with observed low cloud heights at Ft. Collins. An additional 80 mb of lift was necessary to bring this air to its LFC.

3.2 Radar Coverage

The NHRE 10 cm radar at Grover scanned the storm complex along the northern Colorado foothills until a few minutes after 0100 GMT. During this period the storm's intensity peaked about 0045 GMT and then weakened temporarily. Reflectivity data from Limon and Grover radars were compared during the peak period.

Limon (0° elevation angle) and Grover (1.9° elevation angle) radar echoes at 0045 GMT are superimposed on a map of the Big Thompson area in Fig. 33. Both radars scanned a section through the storms at elevations between 15,000 ft MSL (4.6 km) and 20,000 ft MSL (6.1 km). Limon radar showed only a VIP level 3 contour, which corresponds to reflectivities between 41 and 46 dBZ. However, Grover radar observed a level 5 (55–65 dBZ) with a measured peak reflectivity of 64.6 dBZ. The Grover data contained more detail than the Limon data. This is partially explained by the narrower beam width of the Grover radar (1° conical beam compared with Limon's 2° conical beam) and Grover's location closer to the storm area. Fig. 33 suggests that Limon radar underestimated the true intensity in the core of the storms by about 15 dBZ.

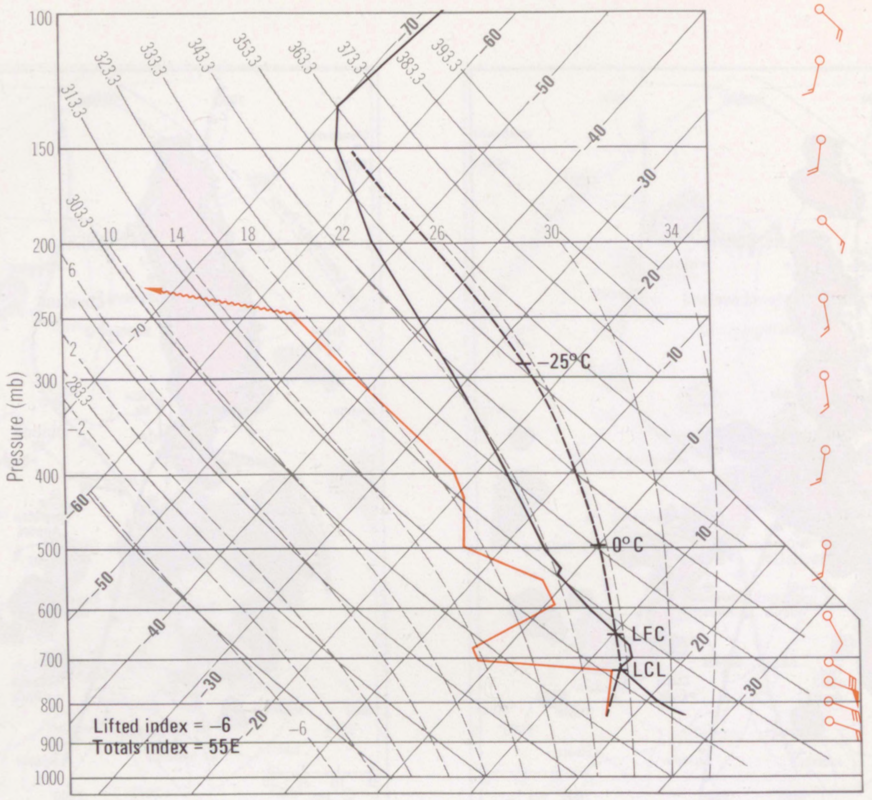

Figure 32. Skew T/Log P plot of upper-air sounding constructed for Loveland, Colorado, at 0000 GMT, 1 August 1976. LCL and LFC levels and moist adiabat are shown for a lifted parcel with mean thermodynamic characteristics of lowest 100 mb layer.

Although it underestimated rainfall intensities, Limon radar data still provide an excellent description of the temporal and spatial variation of precipitation over the Big Thompson drainage. Fig. 34 shows the radar echo locations and intensities for the period 2300–0400 GMT (20 min intervals prior to 0100 GMT and 10 min intervals thereafter).

The first cells that developed around 0000-0030 GMT were several miles east of the maximum rainfall zone. These storms reached their peak intensities near 0045 GMT. During the period 0100–0130 GMT the echoes in the foothills tended to merge, weaken slightly, and shift westward. The most intense rainfall was indicated southwest of the town of Drake by 0130 GMT. From about 0130 to shortly after 0300 GMT the "cloudburst" phase of the storm occurred in the Big Thompson drainage around Glen Comfort. After 0300 GMT the area of intense rain moved slightly northwest over the tributaries of the North Fork of the Big Thompson. The rainfall intensity decreased after 0400 GMT, and most of the precipitation shifted northward into the foothills west of Ft. Collins.

The rainfall amounts shown in Fig. 2 at the beginning of this report were for a 36 to 48 h period. Radar data and eyewitness accounts suggest that the intense rain in the Big Thompson drainage was over by 0400–0430 GMT; however, showers persisted throughout the night. Rain showers were present again the following afternoon and evening and were locally heavy, especially west of Ft. Collins. Therefore, the 36 to 48 h totals are an overestimation of the precipitation that contributed to the flash flooding.

It was shown above that Limon radar echoes of the Big Thompson storm understated the true intensity of the storm; however, if the reflectivity were off by a constant factor, it should be possible to correct

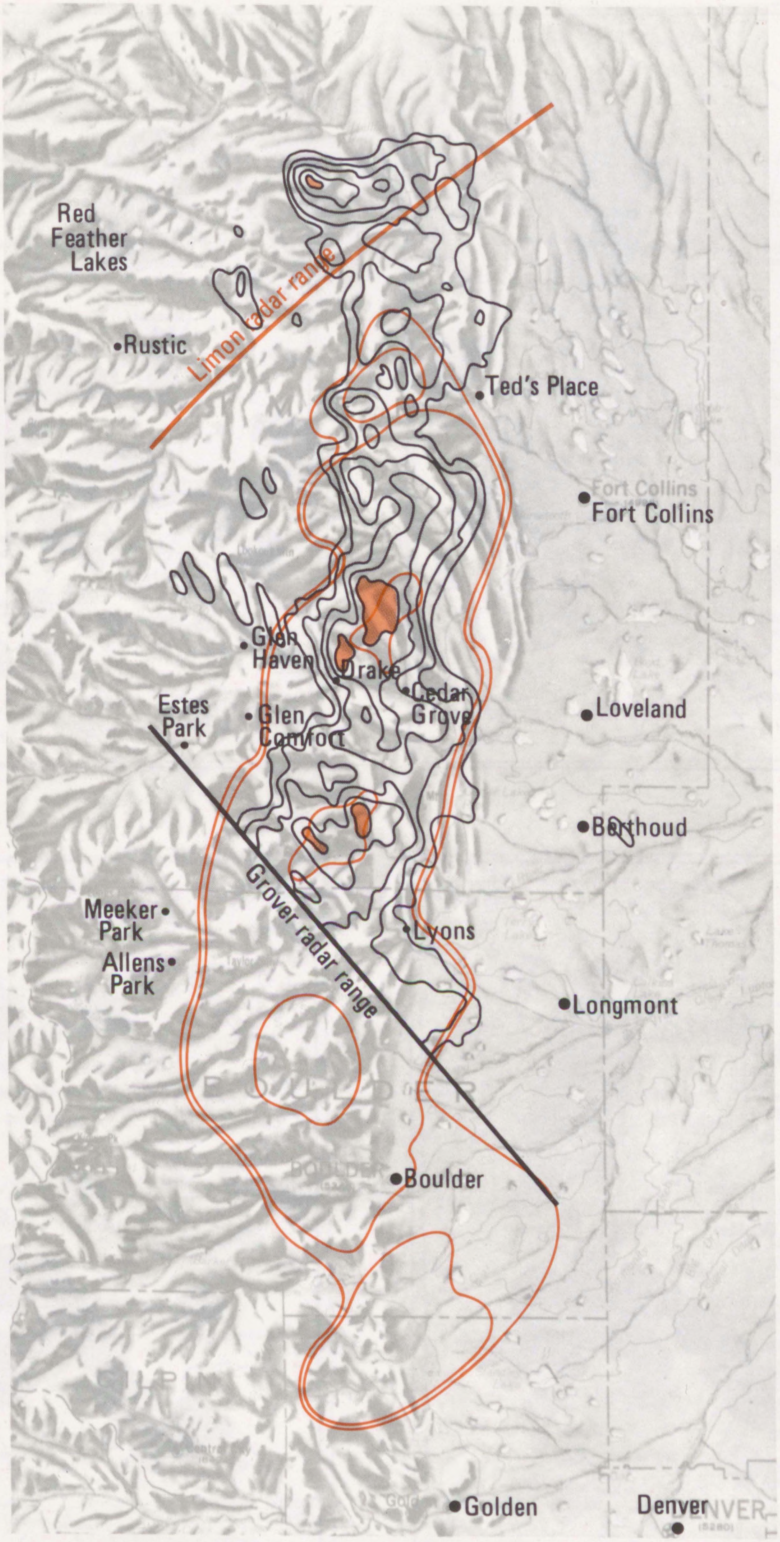

Figure 33. Relief map showing 0045 GMT radar echoes from NWS radar at Limon, Colorado (orange), and from NHRE radar at Grover, Colorado (black). Limon contours are for VIP levels 1, 2, and 3. Grover contours are at 10 dBZ intervals beginning at 15 dBZ with regions of reflectivity ≥ 55 dBZ shaded orange.

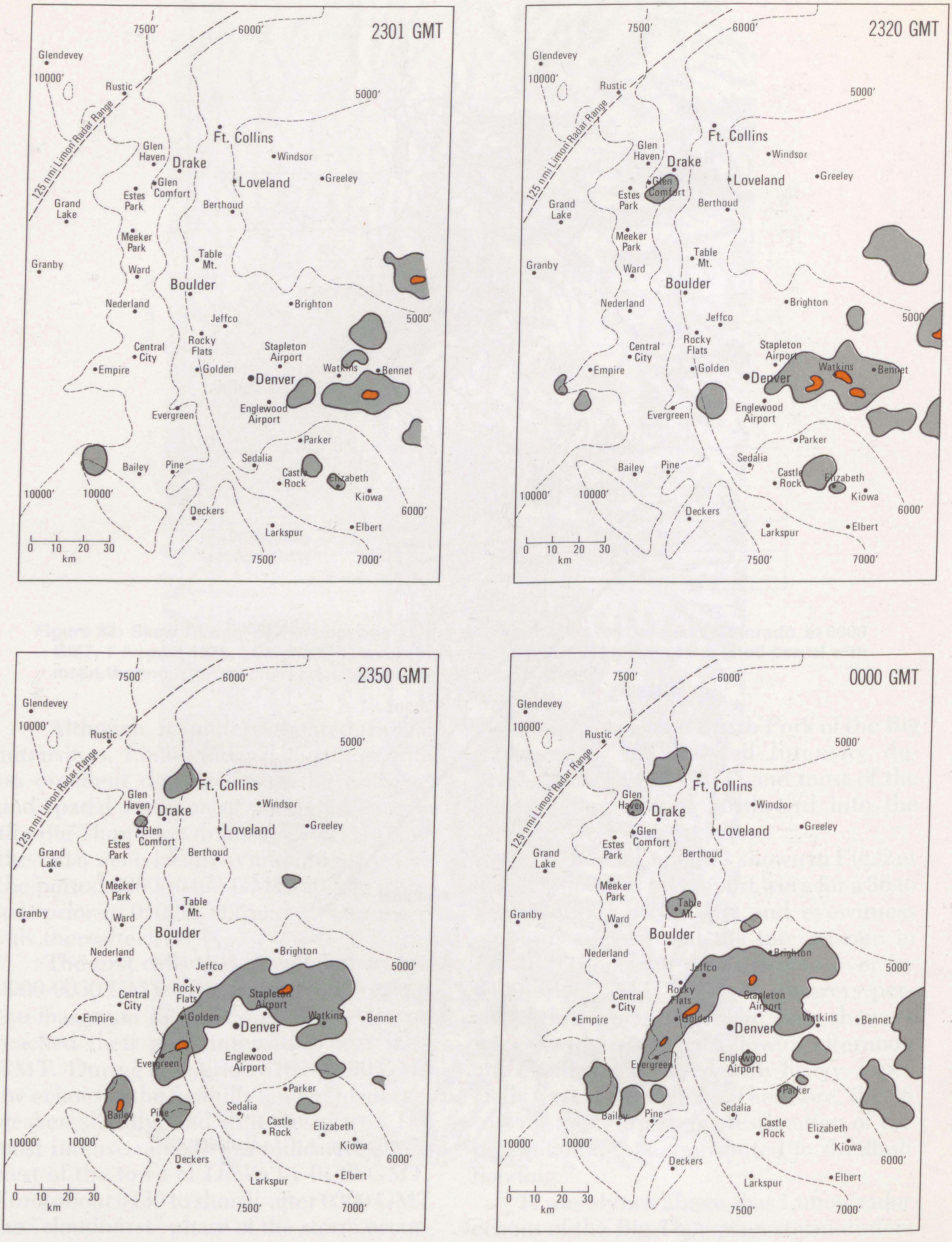

Figure 34. Time series plots of Limon radar echoes covering period 2301 GMT, 31 July 1976 through 0400 GMT, 1 August 1976. Time interval is approximately 20 min prior to 0100 GMT and approximately 10 min after 0100 GMT. Level 1 and 2 returns are shaded gray, and level 3 returns are shaded orange.

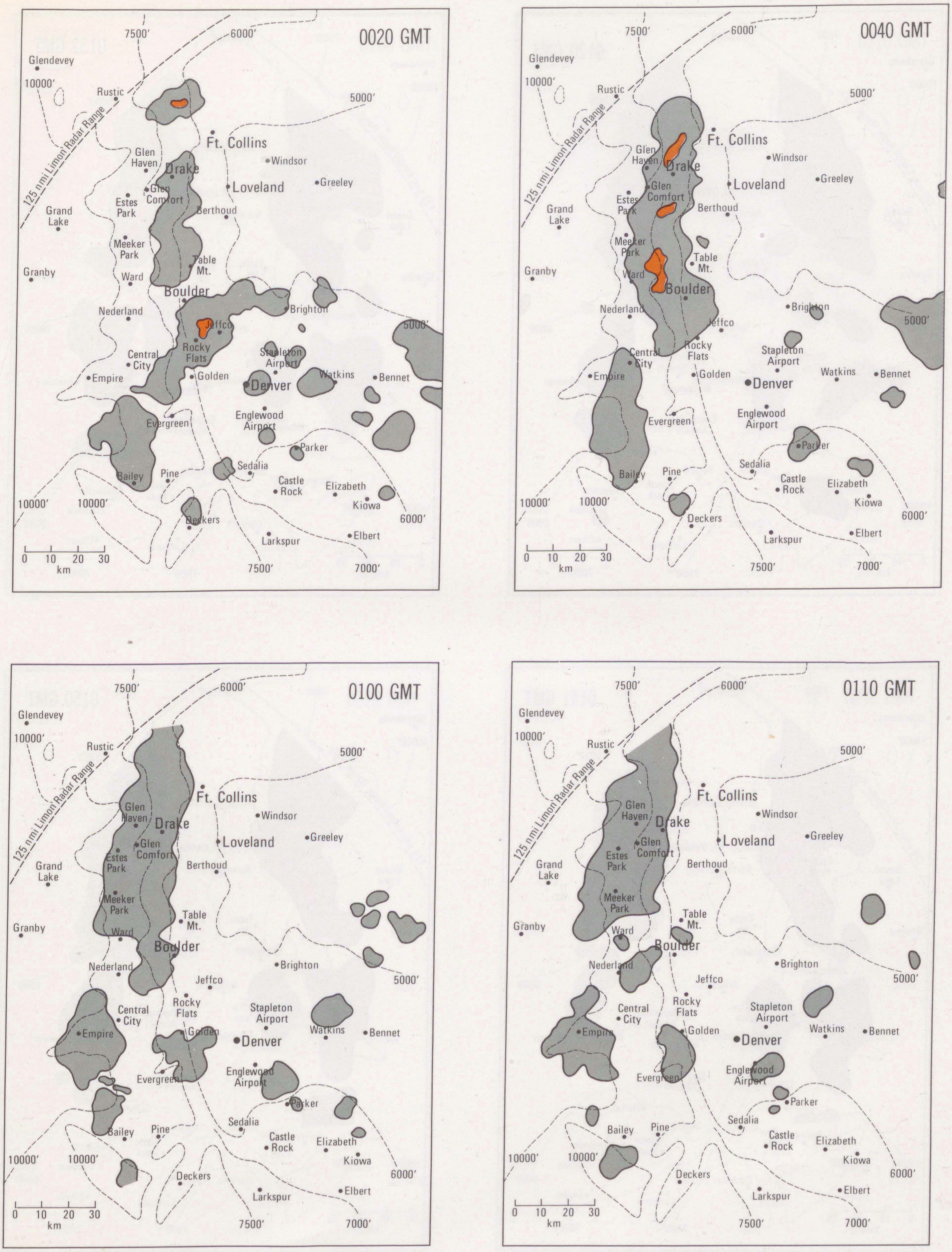

Figure 34. Continued.

Figure 34. Continued.

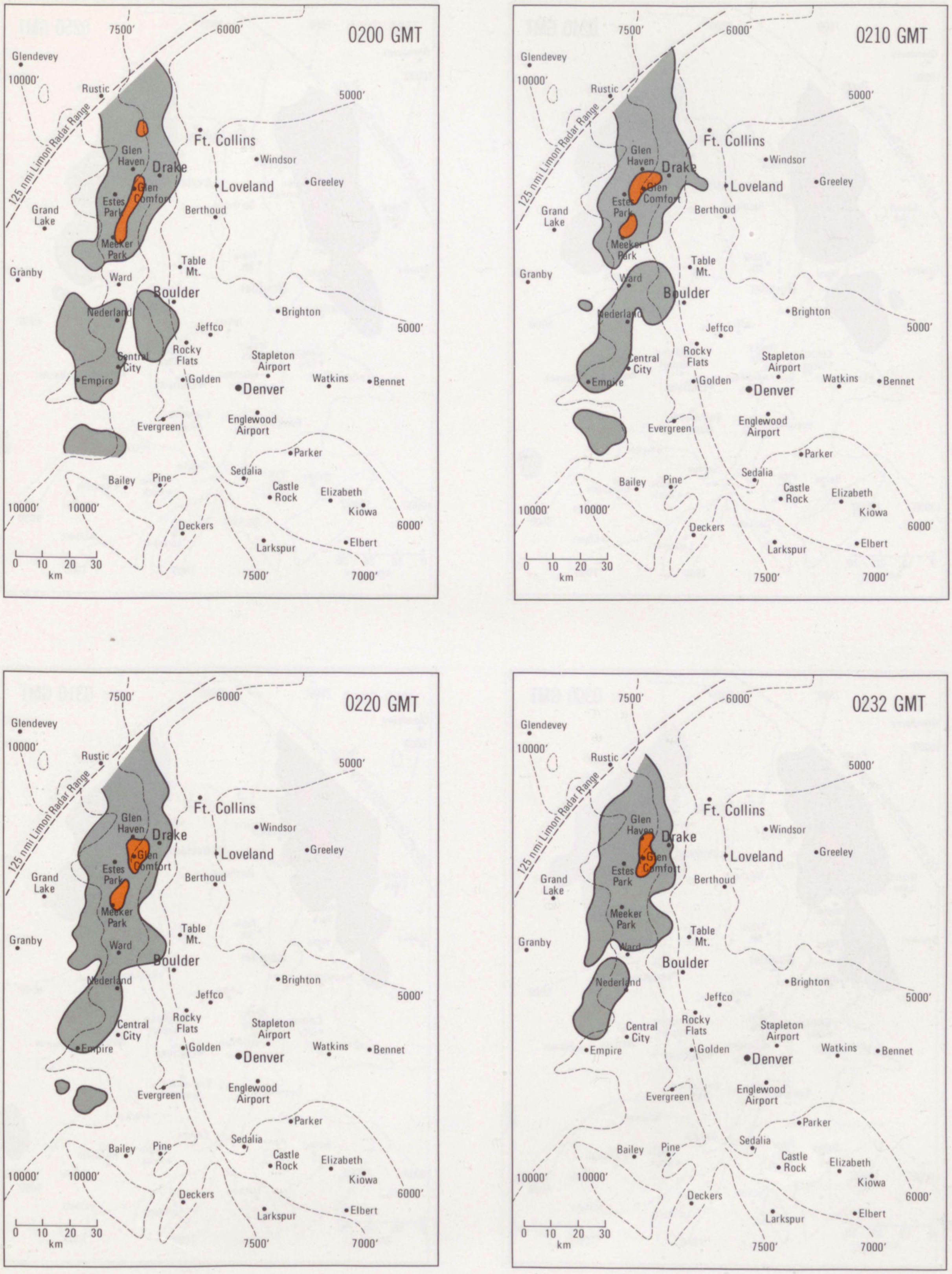

Figure 34. Continued.

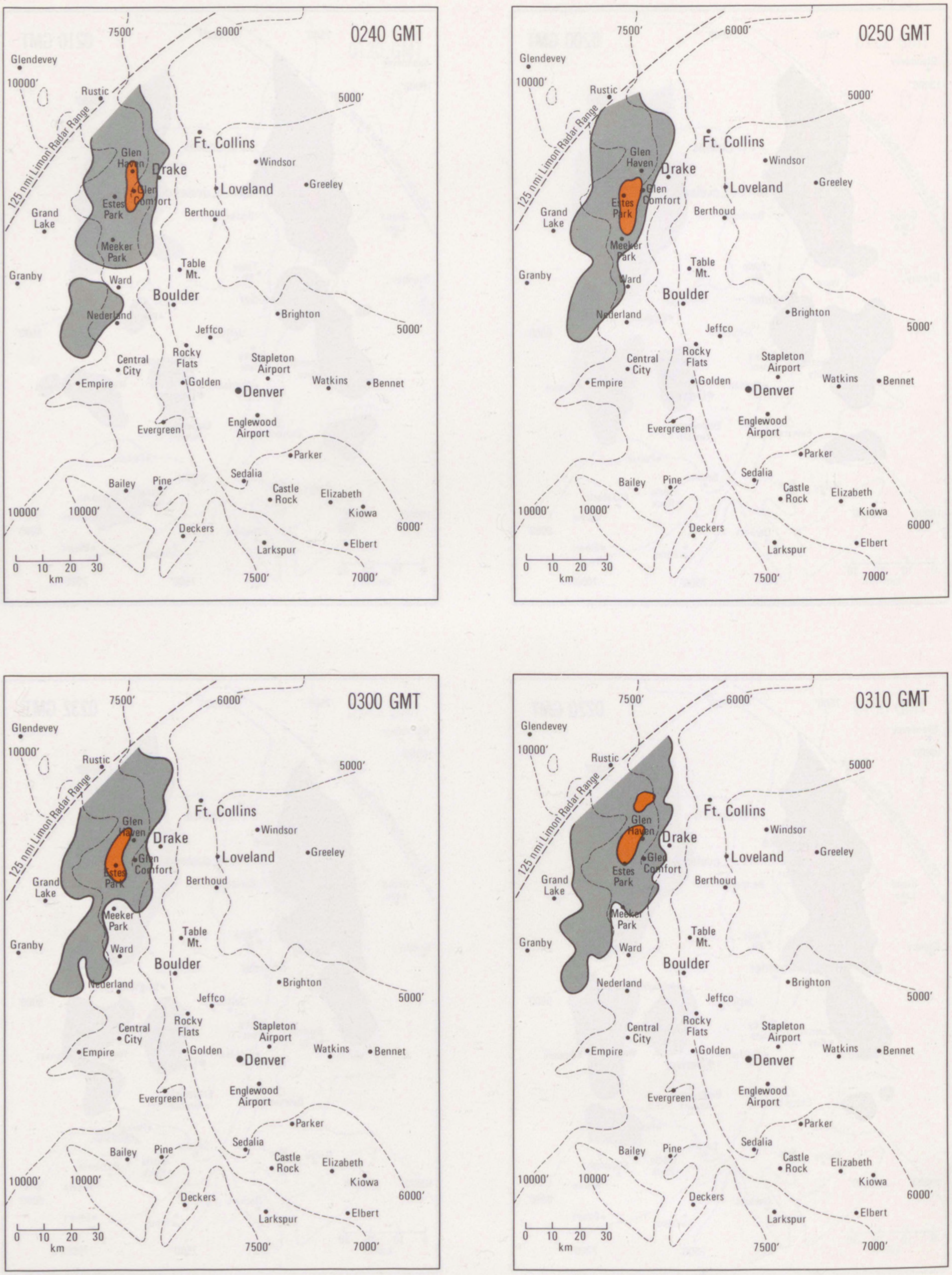

Figure 34. Continued.

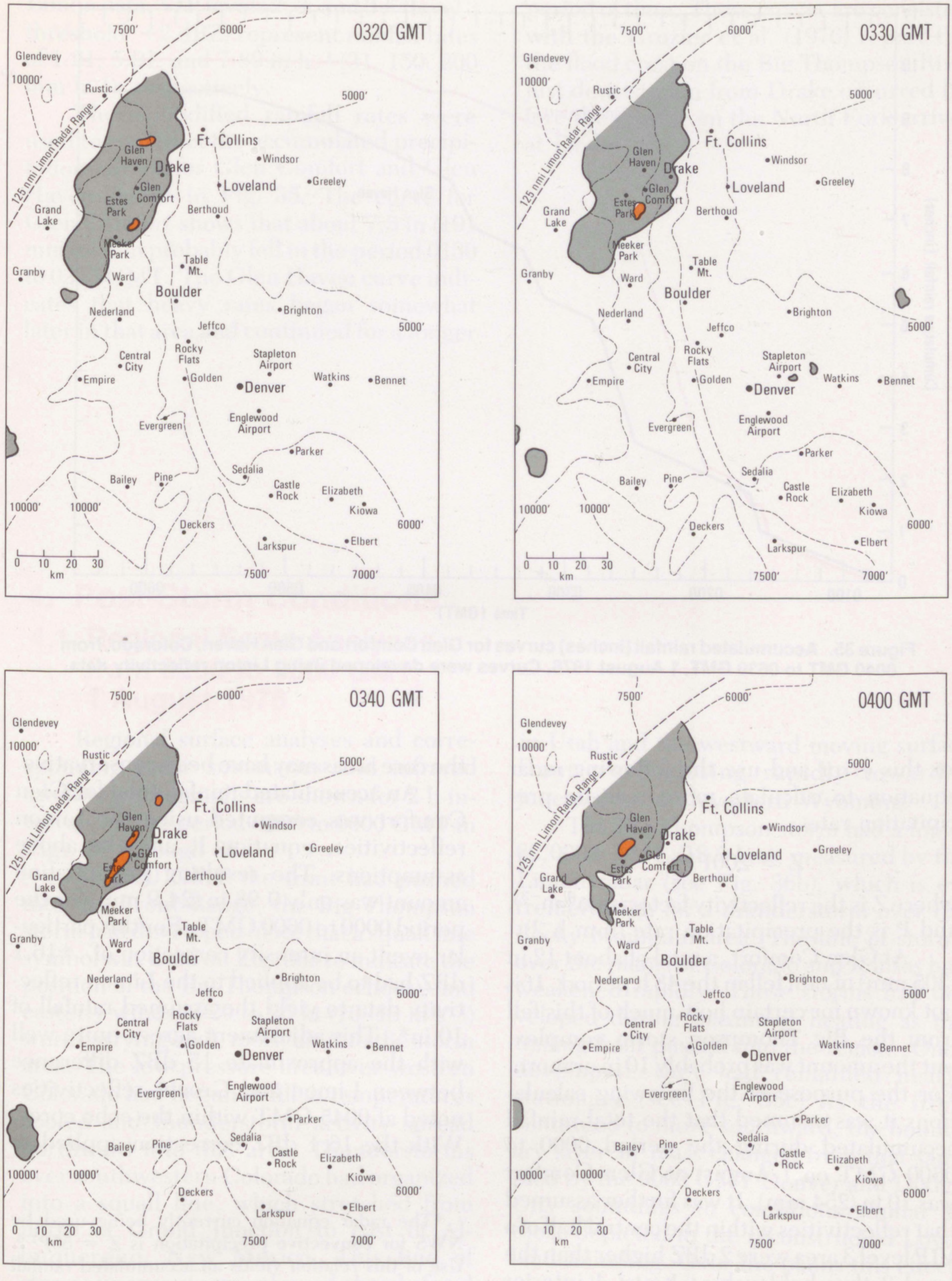

Figure 34. Continued.

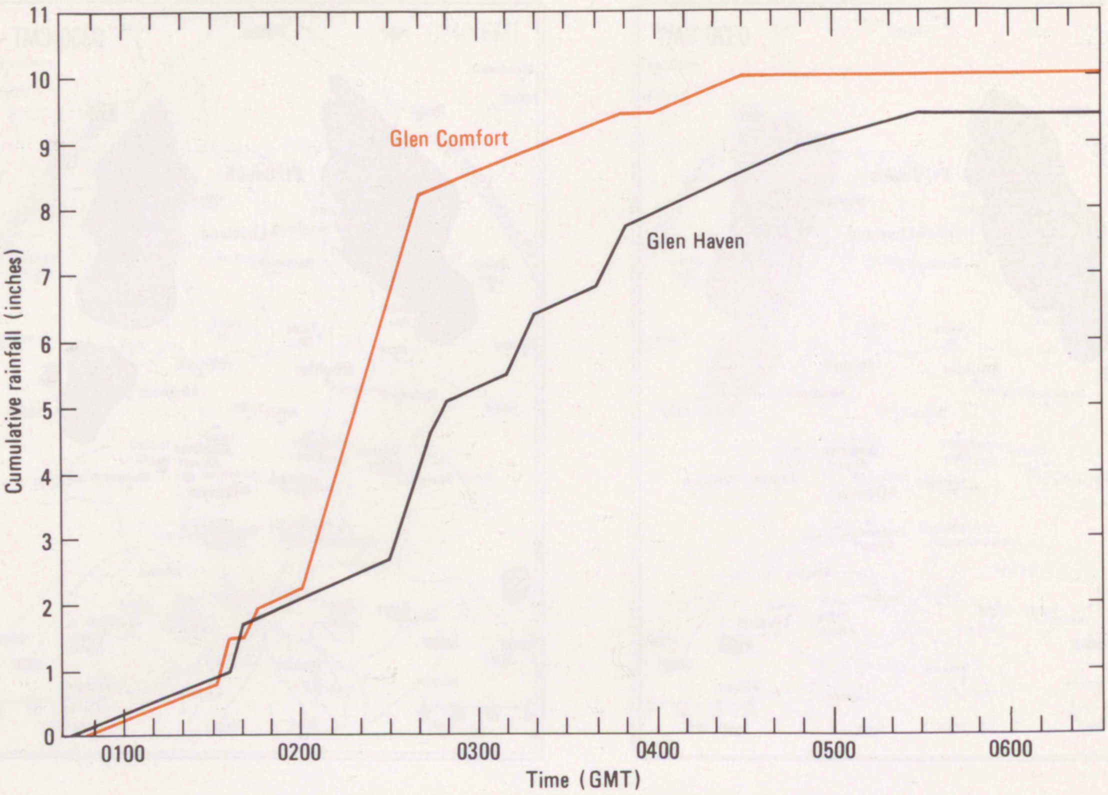

Figure 35. Accumulated rainfall (inches) curves for Glen Comfort and Glen Haven, Colorado, from 0040 GMT to 0630 GMT, 1 August 1976. Curves were developed using Limon reflectivity data.

for this error and use the following radar equation to calculate more realistic precipitation rates:

$$Z = 200P^{1.6}, \qquad (1)$$

where Z is the reflectivity factor ($mm^6\ m^{-3}$), and P is the precipitation rate ($mm\ h^{-1}$).

At Glen Comfort, a total of about 12 in (305 mm) of rain fell in the 48 h period. It is not known for certain how much of this fell from the Big Thompson storm complex, but the amount was probably 10 in or more. For the purpose of the following calculations it was assumed that the total rainfall accumulated during the period 0000 to 0600 GMT on 1 August at Glen Comfort was 10 in (254 mm). It was further assumed that reflectivities within the central half of a VIP level 3 area were 2 dBZ higher than the level 3 threshold value. Level 4 interior contours fleetingly occurred in the storm area indicating that the assumed 43 dBZ for the core areas may have been conservative.

An accumulated rainfall total for Glen Comfort was computed using the Limon reflectivities, equation 1, and the above assumptions. The resulting precipitation amount was only 0.98 in (24.9 mm) for the period 0000 to 0600 GMT. For this particular event an intensity correction of +16.1 dBZ had to be applied to the Limon reflectivity data to yield the assumed rainfall of 10 in*. This adjustment agrees quite well with the approximate 15 dBZ difference between Limon and Grover reflectivities noted at 0045 GMT within the echo cores. With the 16.1 dBZ correction applied to

*The radar equation currently being used by NWS for **convective** precipitation is $Z = 55P^{1.6}$. Use of this relation yields an accumulated rainfall of 2.19 in (55.6 mm) at Glen Comfort during the period 0000 to 0600 GMT. The required Limon reflectivity correction decreases to + 10.6 dBZ.

Limon data, VIP levels 2, 3, and 3+ (level 3 threshold +2 dBZ) represent rainfall rates of 1.21, 5.91, and 7.89 in h^{-1} (31, 150, 200 mm h^{-1}), respectively.

These modified rainfall rates were used to construct the accumulated precipitation curves for Glen Comfort and Glen Haven shown in Fig. 35. The curve for Glen Comfort shows that about 7.5 in (191 mm) of rain probably fell in the period 0130 to 0245 GMT. The Glen Haven curve indicates that heavy rains began somewhat later in that area and continued for a longer period of time. These curves are consistent with the Grozier et al. (1976) report that the flood crest on the Big Thompson River just downstream from Drake occurred before the crest from the North Fork arrived at Drake.

4. Post-Storm Conditions

4.1 Regional Scale Analyses from 0200 to 0600 GMT, 1 August 1976

Regional surface analyses and corresponding radar summaries and infrared satellite photographs are shown for 2 h intervals for the period 0200 to 0600 GMT in Figs. 36 through 38.

At 0200 GMT the front had pushed into the Front Range, the Big Thompson storm had developed (note that a squall line symbol was used on Fig. 36a to indicate the position of the Big Thompson echoes), and easterly winds of 20 to 26 kt (10–13 m s^{-1}) were carrying cool, moist air into the storm area. The low pressure area over western Colorado had begun to fill as temperatures cooled and thunderstorm activity spread northward into that area. Thunderstorms over southwestern Colorado had organized into a squall line, which stretched from north of Grand Junction to east of Albuquerque, New Mexico. This line of storms was moving northward ahead of and associated with the 500 mb short-wave trough. The northward moving squall line in Utah and the westward moving surface front were closing rapidly toward a juncture in southwestern Wyoming.

The Big Thompson storm had a top of 62,000 ft MSL (18.9 km), measured by the Limon radar (see Fig. 36b), which is extremely high for a thunderstorm over the Rocky Mountain area. The line of storms over the plains of Colorado and Kansas had weakened rapidly. These storms had developed during maximum heating as the trailing front pushed into the region. Once developed, they had remained nearly stationary (see Fig. 36c). As the front continued to move southward, the boundary layer air mass changed from that sampled by the 0000 GMT Denver and Dodge City soundings to conditions similar to those depicted in the reconstructed Loveland sounding. Over the plains this effect, coupled with slight diurnal cooling, caused dissipation of the storms. Even though the air mass had become conditionally much

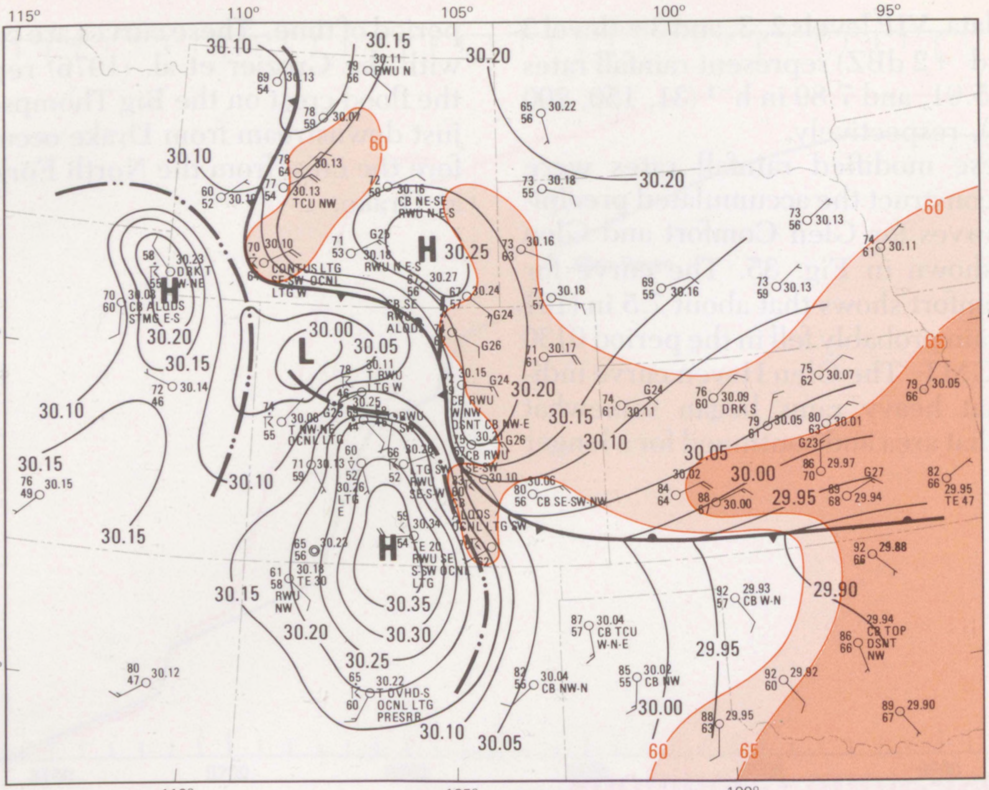

Figure 36a. Regional surface analysis for 0200 GMT, 1 August 1976. Refer to legend of Fig. 12a for details.

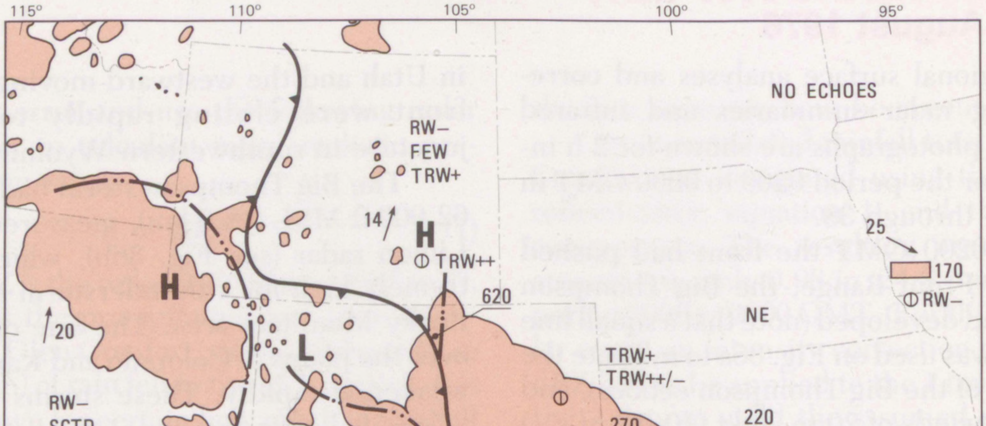

Figure 36b. Radar summary chart for 0135 GMT, 1 August 1976.

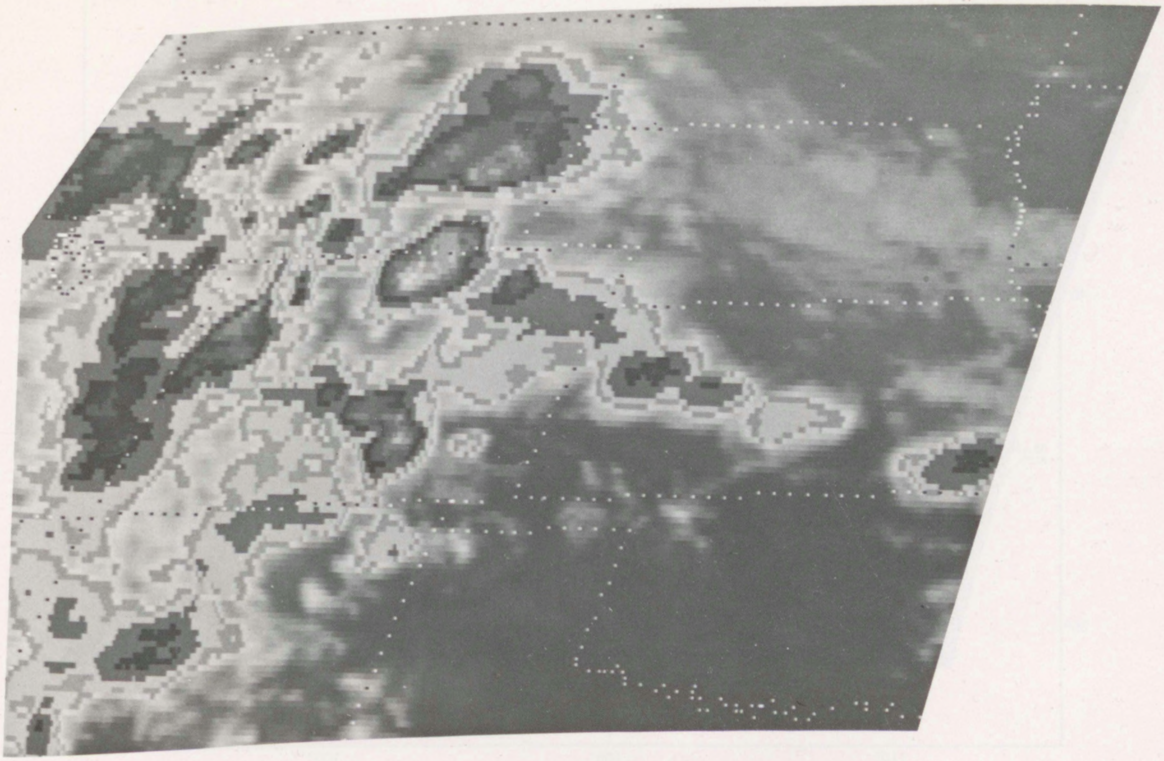

Figure 36c. GOES–1 infrared photograph for 0200 GMT, 1 August 1976.

more unstable, there was no mechanism acting over the plains to lift this air to its LFC and release the instability.

By 0400 GMT (refer to Figs. 37a, b, and c) the meso-high pressure system behind the Colorado squall line had intensified, and the low pressure area over northwestern Colorado had continued to fill. This squall line was moving northward toward the Big Thompson storm complex.

The squall line moving northward out of Utah and the moist air moving westward across southern Wyoming met near Rock Springs, Wyoming. A large thunderstorm intensified rapidly in the area where the two features interacted. The intense nature of both the Big Thompson and Rock Springs storms was indicated by continuous lightning reported by observers in these areas and by the very bright and cold storm tops in the infrared satellite photograph.

By 0600 GMT (Figs. 38a, b, and c) the Big Thompson storm had begun moving northward along the Front Range in response to the approaching short wave and associated squall line. The Rock Springs storm now appeared (in the satellite photograph) larger and more intense than the Big Thompson storm, as it moved northward across sparsely populated portions of western Wyoming. However, an important difference between this storm and the Big Thompson storm was that the stronger steering level winds over western Wyoming kept it moving steadily northward.

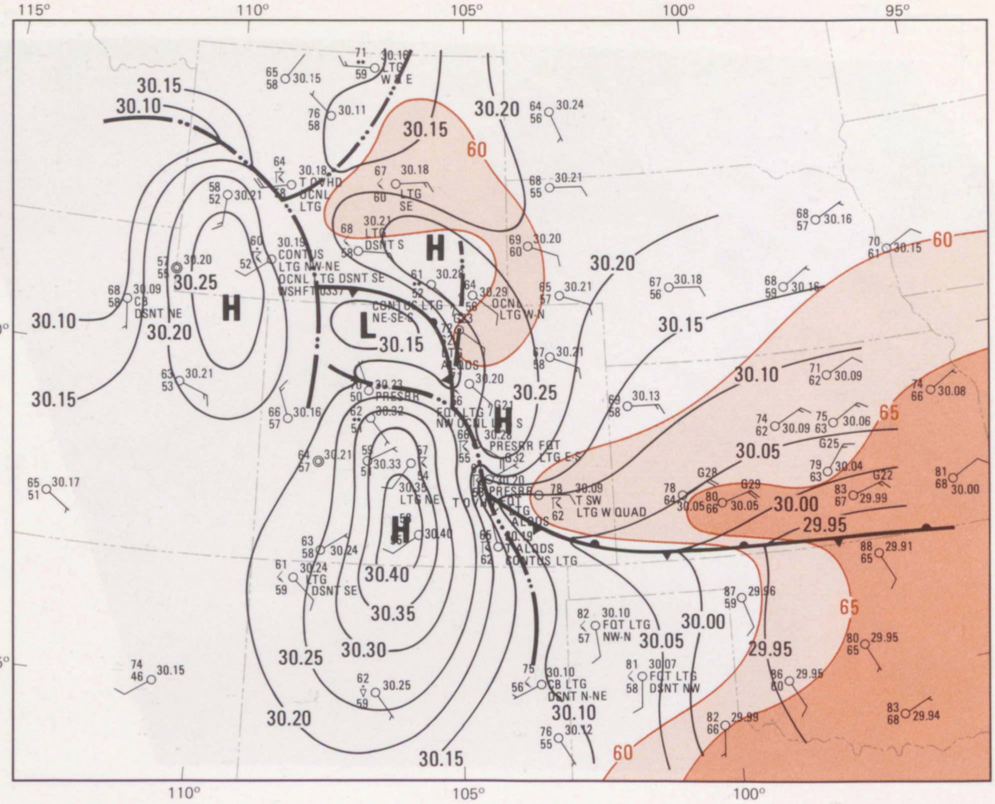

Figure 37a. Regional surface analysis for 0400 GMT, 1 August 1976. Refer to legend of Fig. 12a for details.

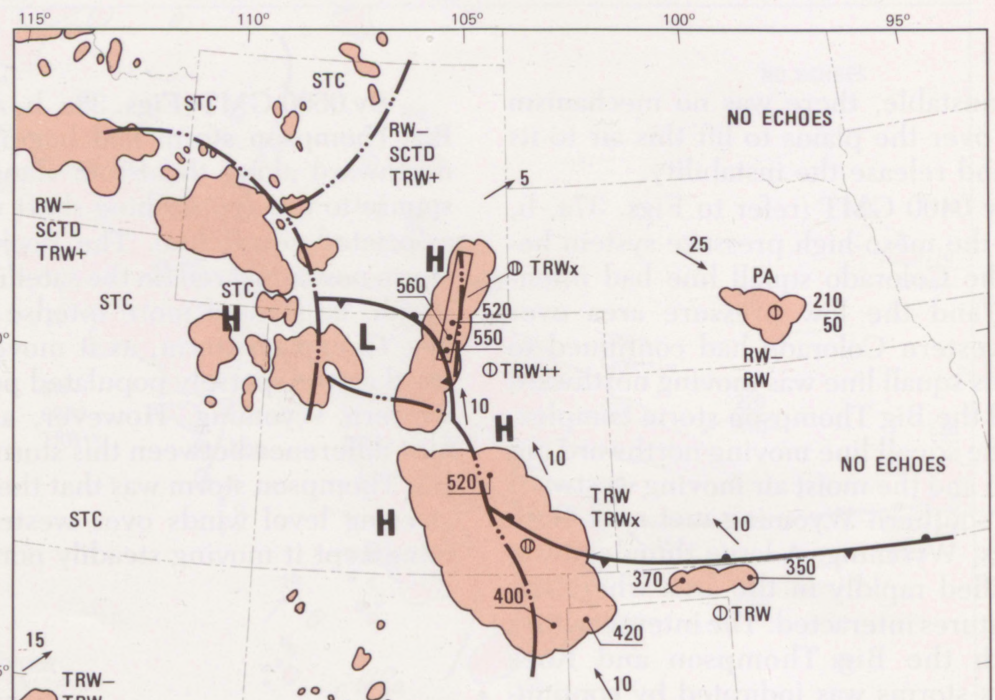

Figure 37b. Radar summary chart for 0335 GMT, 1 August 1976.

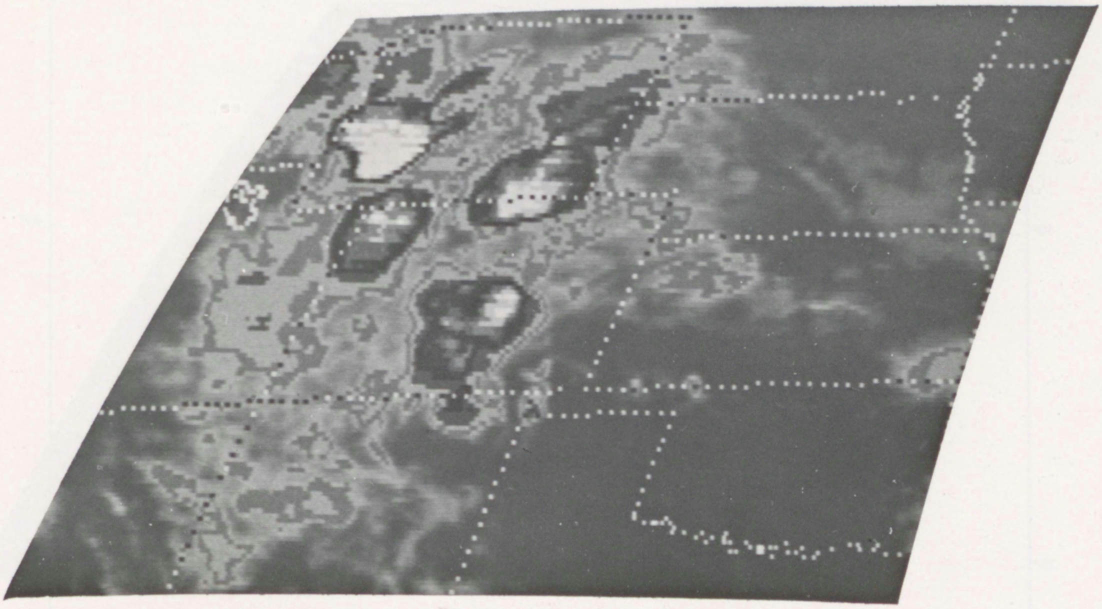

Figure 37c. GOES–1 infrared photograph for 0400 GMT, 1 August 1976.

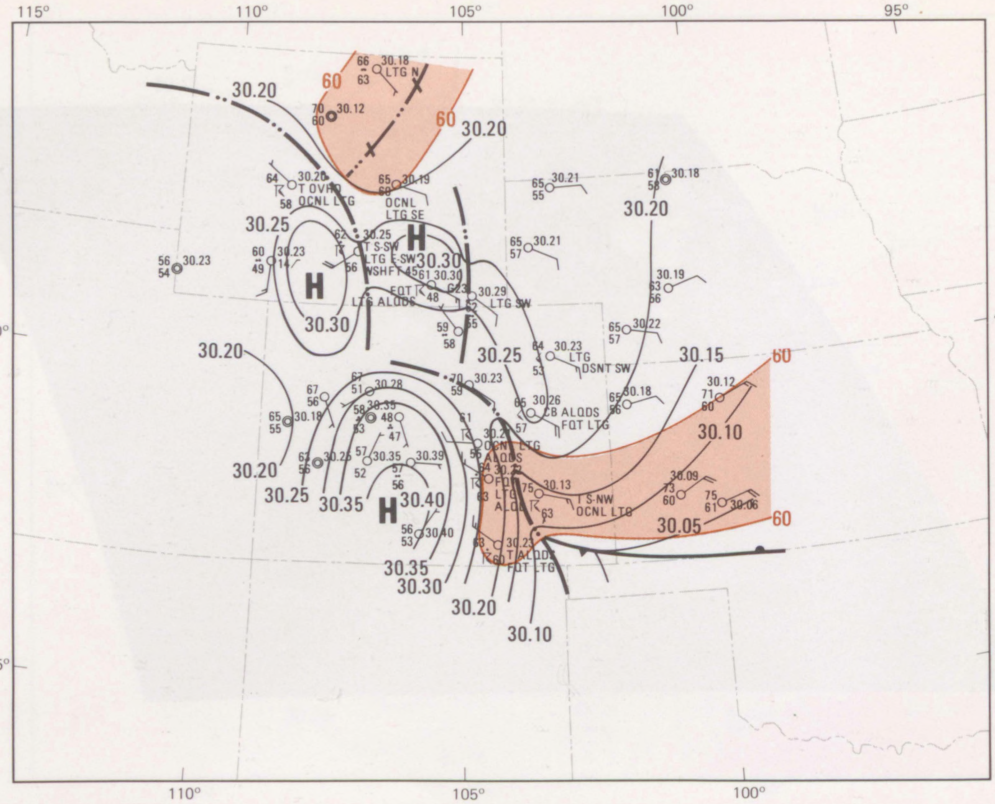

Figure 38a. Regional surface analysis for 0600 GMT, 1 August 1976. Refer to legend of Fig. 12a for details.

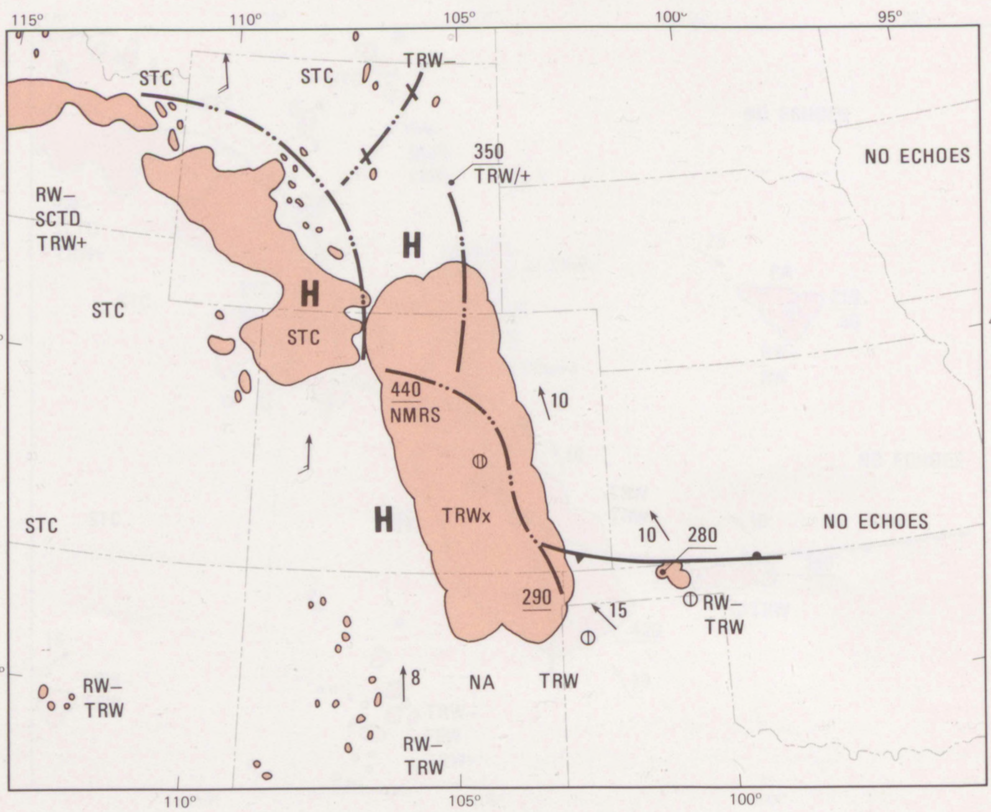

Figure 38b. Radar summary chart for 0535 GMT, 1 August 1976.

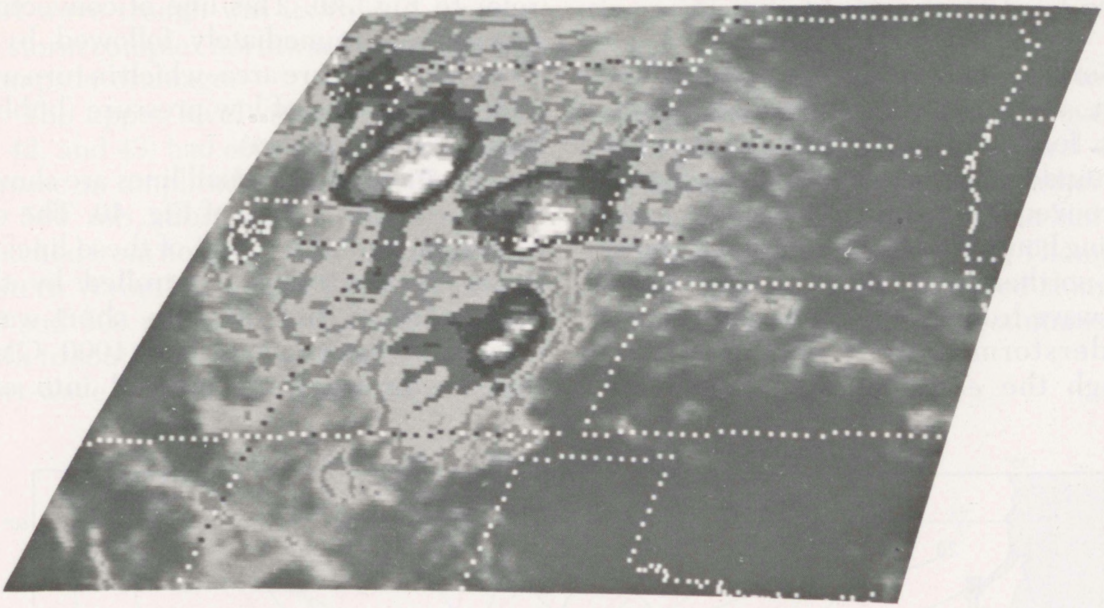

Figure 38c. GOES-1 infrared photograph for 0600 GMT, 1 August 1976.

4.2 Synoptic Scale Analyses for 1200 GMT, 1 August 1976

Surface and upper-air analyses are shown, along with vorticity and continuity charts, for 1200 GMT in Figs. 39 through 44. Thunderstorm activity had merged into one convective feature during the early morning hours, and had continued to move north-northeastward ahead of the 500 mb short-wave trough. This arc of shower and thunderstorm activity had persisted through the early morning hours and stretched from central Idaho through western South Dakota to western Kansas (refer to Fig. 39). This line of convective activity was immediately followed by a meso-high pressure area, which in turn was trailed by a wake of low pressure (bubble high/wake depression).

Positions of the squall lines are shown on the continuity map of Fig. 40. The organization and movement of these lines of storms were strongly controlled by the movement of the 500 mb short-wave trough. Between 0600 and 1000 GMT thunderstorm activity merged into one

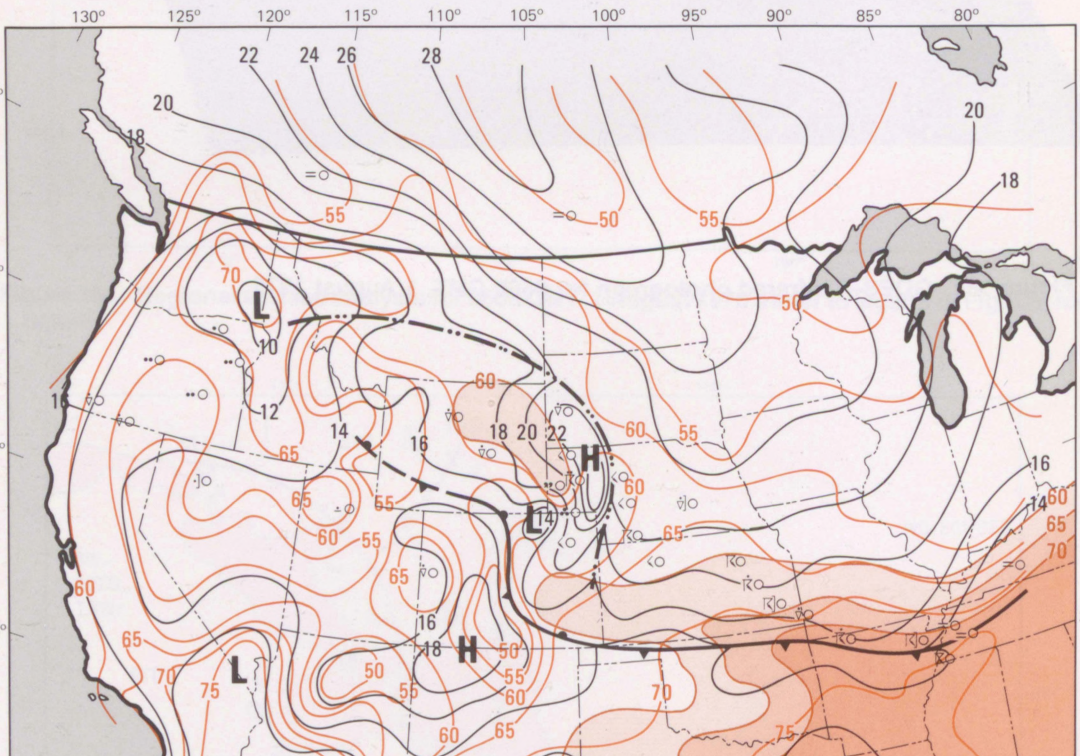

Figure 39. Synoptic scale surface analysis for 1200 GMT, 1 August 1976. Refer to legend of Fig. 4 for details.

large arc of storms along and ahead of the trough. One important effect of this short-wave trough was its role in moving the storm complex northward out of the Big Thompson drainage.

The upper level ridge (refer to Figs. 41, 42, and 43) had continued to build and increase in amplitude overnight ahead of the 500 mb short-wave trough, which stretched from northern California through western Wyoming to west Texas. Winds at 700 and 500 mb had veered and become south to southwesterly over Colorado. The short-wave trough was easily identifiable on the vorticity analysis shown in Fig. 44, and the squall line lay in the region of positive vorticity advection just ahead of the trough.

Although the synoptic scale pattern of a trough over the West and a ridge over the plains persisted for the next several days, the interaction of mesoscale weather features and orographic features that had produced the nearly stationary Big Thompson storm complex was not repeated along the Front Range of the Rocky Mountains.

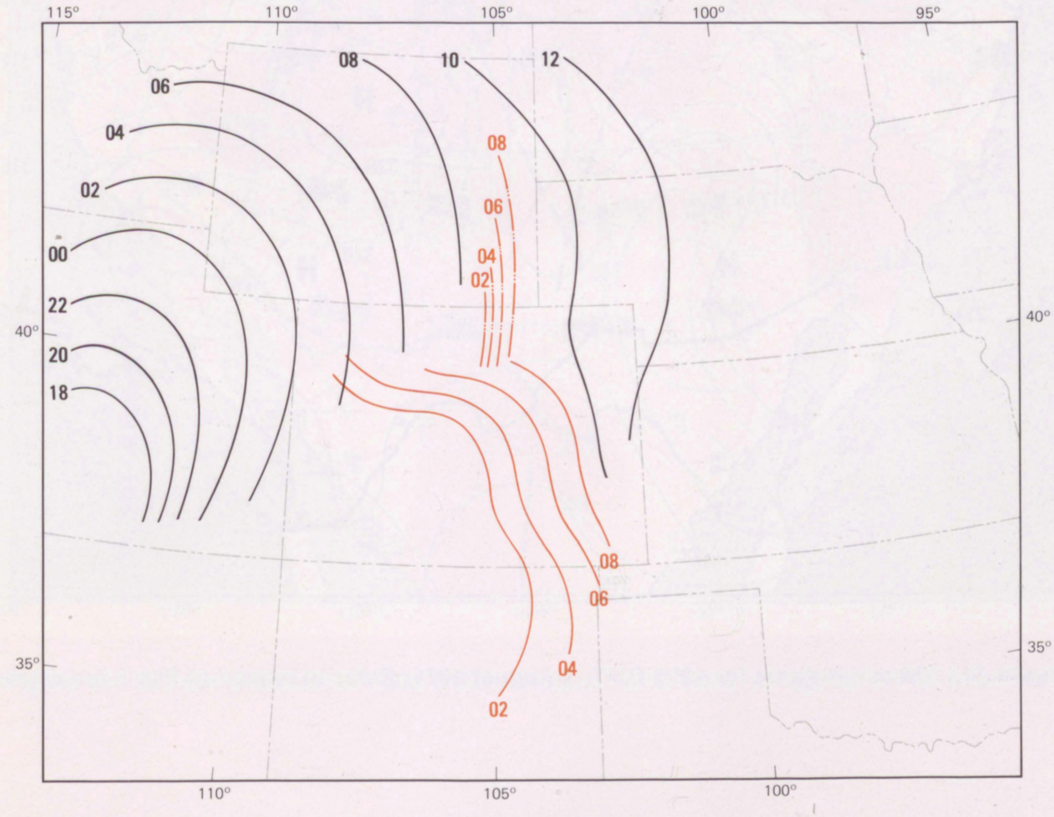

Figure 40. Continuity positions of Utah squall line (black), Colorado squall line (orange), and Big Thompson storm complex (broken orange). Time in GMT is given for each line.

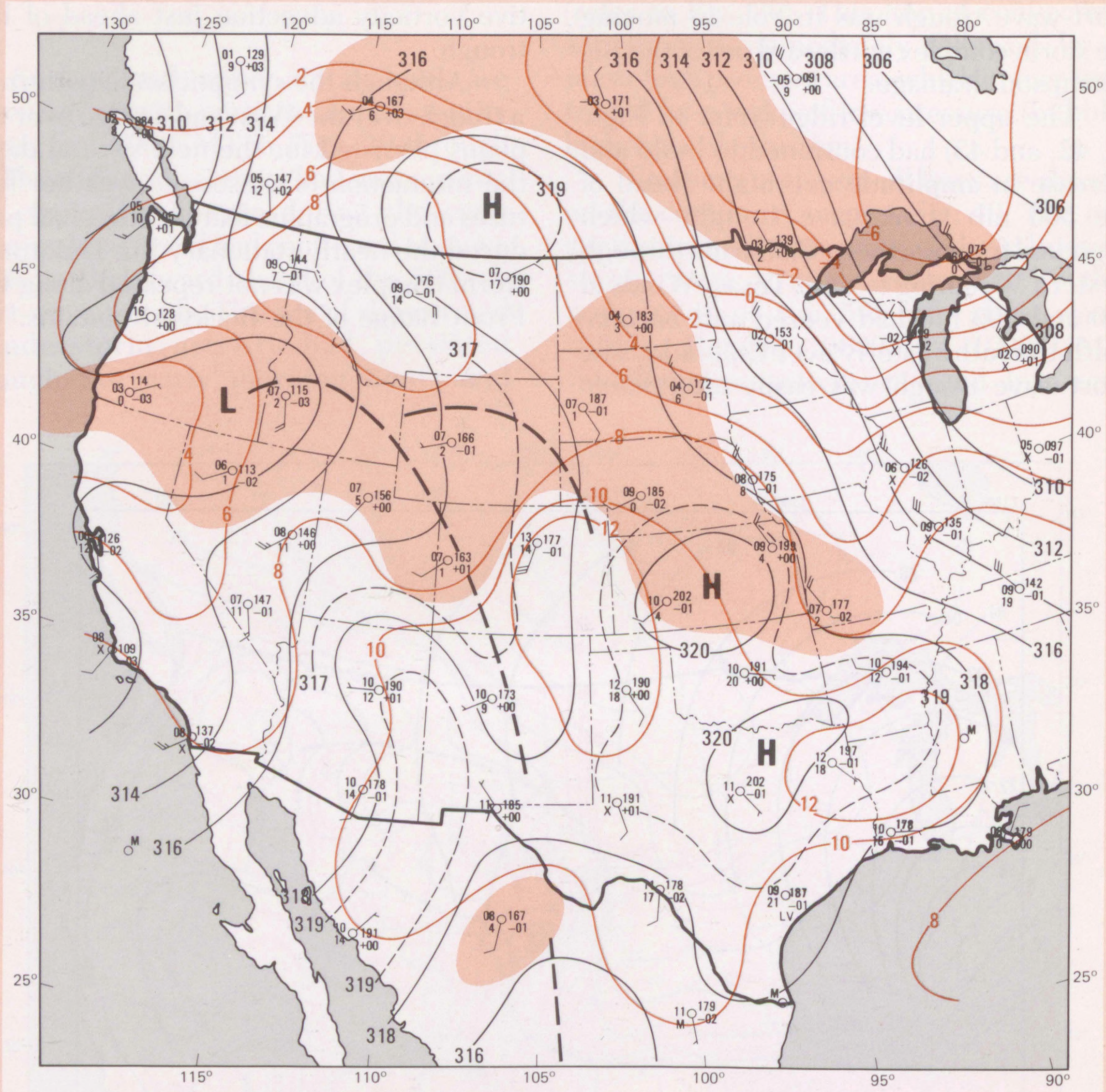

Figure 41. 700 mb analysis for 1200 GMT, 1 August 1976. Refer to legend of Fig. 5 for details.

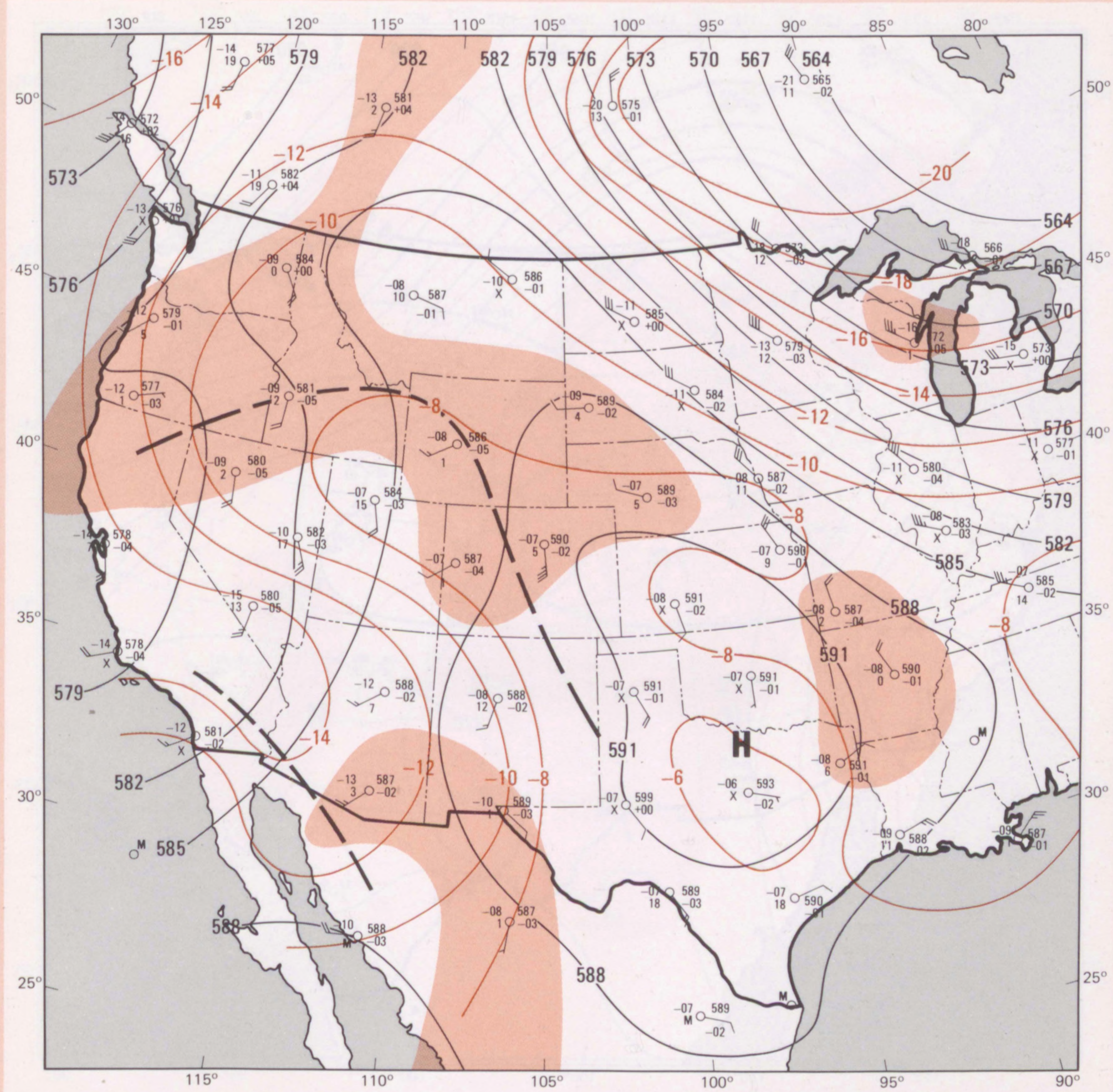

Figure 42. 500 mb analysis for 1200 GMT, 1 August 1976. Refer to legend of Fig. 6 for details.

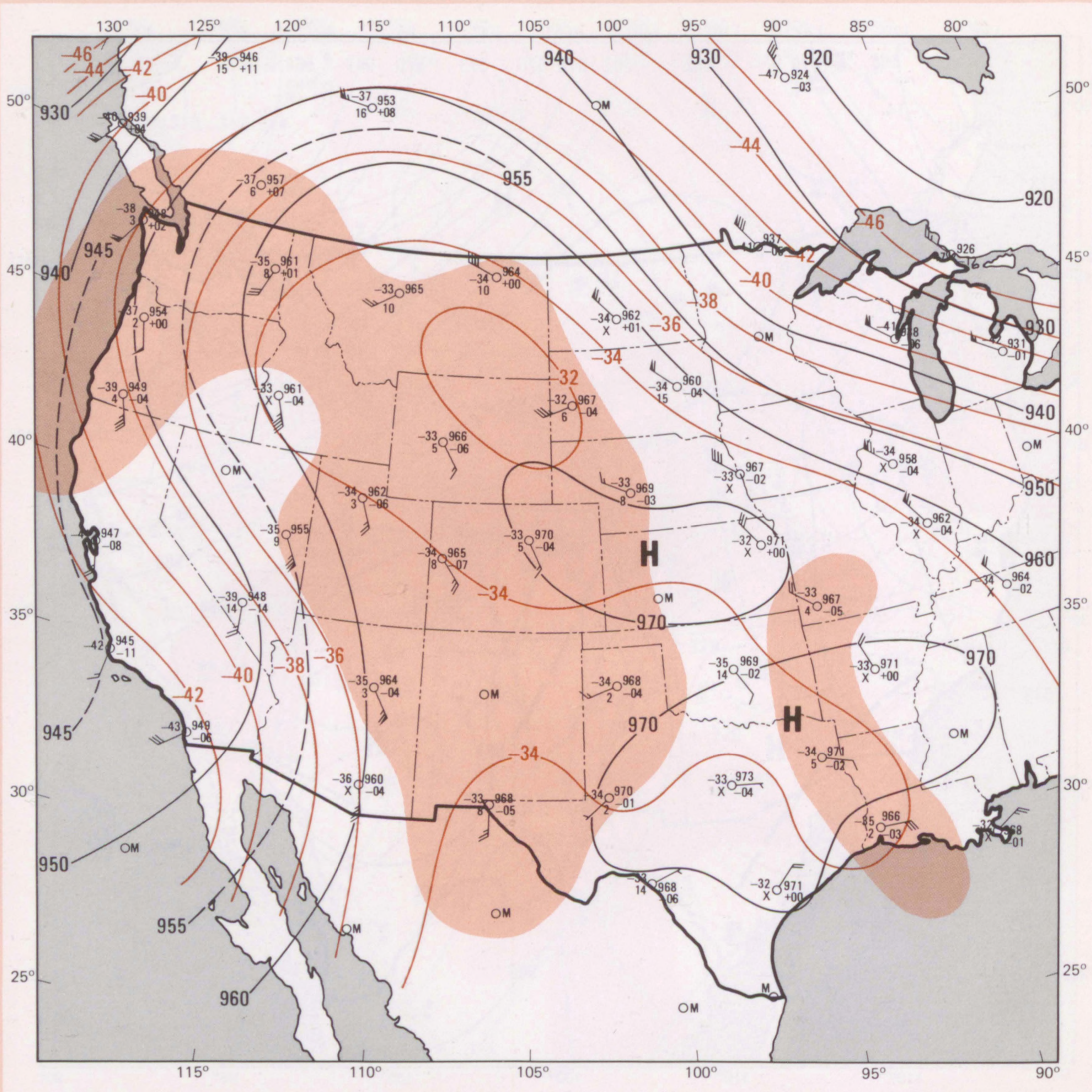

Figure 43. 300 mb analysis for 1200 GMT, 1 August 1976. Refer to legend of Fig. 7 for details.

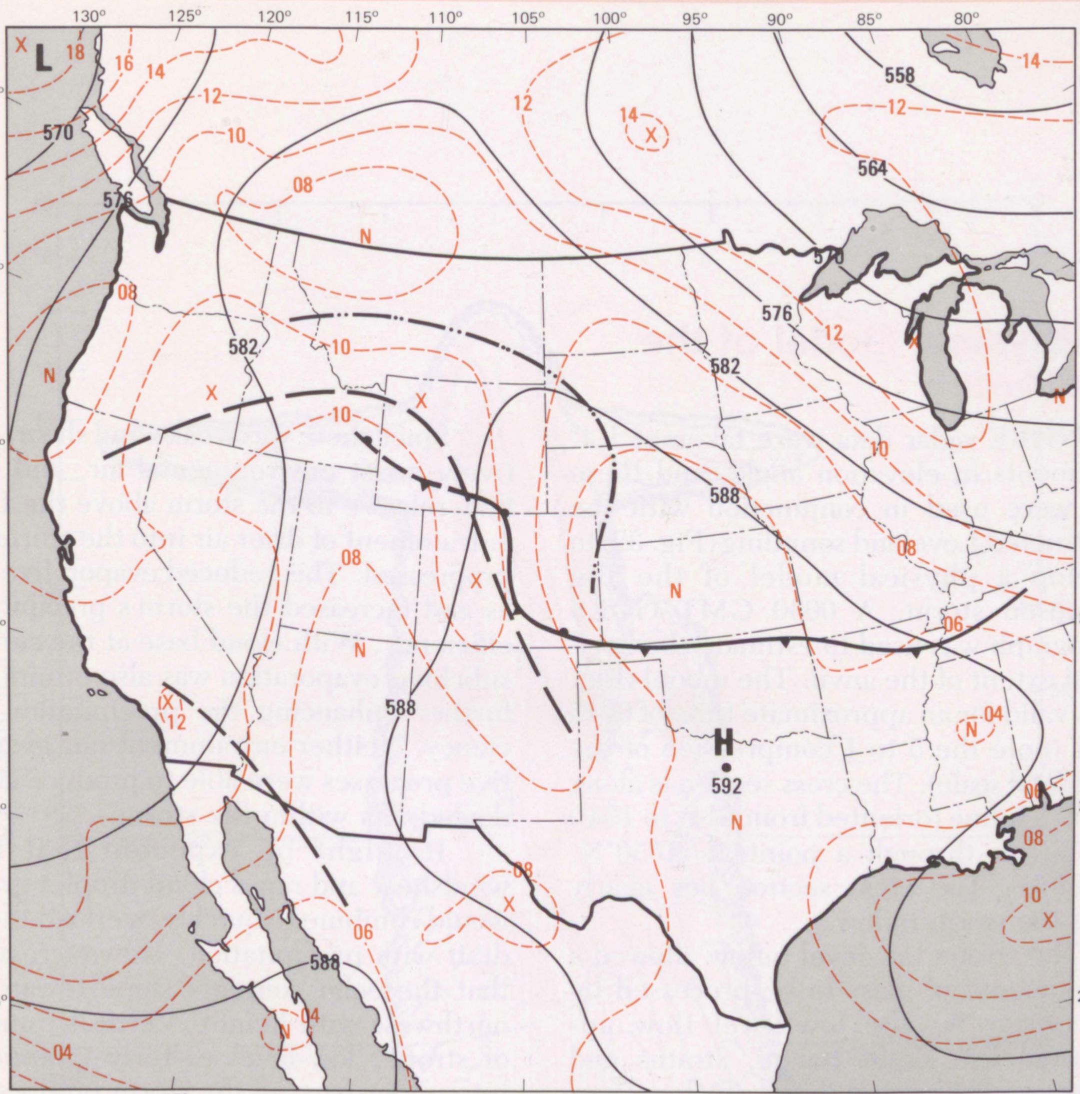

Figure 44. NMC-LFM vorticity analysis for 1200 GMT, 1 August 1976. Refer to legend of Fig. 25 for details.

5. Physical Model of the Storm

NHRE radar data were taken at 1.4° increments in elevation angle, and these data were used in conjunction with the constructed Loveland sounding (Fig. 32) to develop a physical model of the Big Thompson storm. A 0030 GMT GOES photograph was used to estimate the horizontal extent of the anvil. The model (Fig. 45) is valid for an approximate time of 0045 GMT (note the 5 to 1 compression of the horizontal scale). The cross section is along a NW–SE line (oriented from 314° to 134°) that passes through a point at 40°30′N, 105°21′W. The cross section lies nearly along the storm inflow.

The strong low-level inflow allowed a large amount of mass to be processed by the storm. As the low-level flow approached the Front Range, stratus and stratocumulus formed in the shallow layer between the LCL and the LFC. The 0000 GMT Ft. Collins surface observation indicated a thin, broken deck of cloud based at 4,000 ft AGL (1.2 km). When this low-level air was forced above the LFC, explosive convective growth occurred. Radar data indicated that new cells formed in the inflow and moved north-northwestward into the storm complex. Cloud base was effectively on the ground in the storm area. This, combined with the high incloud freezing level (5.8 km MSL) and height of the −25°C isotherm (9.6 km MSL), indicated an unusually deep (for Colorado storms) layer for warm cloud coalescence processes to act.

Since there was weak wind shear, relatively moist environmental air, and little flow relative to the storm above the LFC, entrainment of drier air into the storm was suppressed. This reduced evaporative losses and increased the storm's precipitation efficiency. With cloud base at the surface, subcloud evaporation was also minimized, further enhancing the precipitation efficiency. Neither entrainment nor evaporative processes were able to produce strong downdrafts within the storm.

It might be expected that light windshear and rapid cloud droplet growth would combine to quickly overload the updraft with precipitation. However, notice that the echo contours slope toward the northwest with height. Vertical transport of strong, low-level easterly momentum into upper parts of the storm produced an updraft structure that sloped with height toward the northwest. The tilted updraft allowed large precipitation droplets to fall out of the rear of the updraft, enabling the system to exist in a nearly steady state.

This model of the Big Thompson storm is considerably different from that developed by St. Amand et al. (1972) for the Rapid City, South Dakota, storm complex. Their model cloud sloped strongly to the east above 450 mb and invoked a recycling of water substance to help explain the high precipitation efficiency of the system. Deep convection that develops within a negatively sheared air mass (characterized

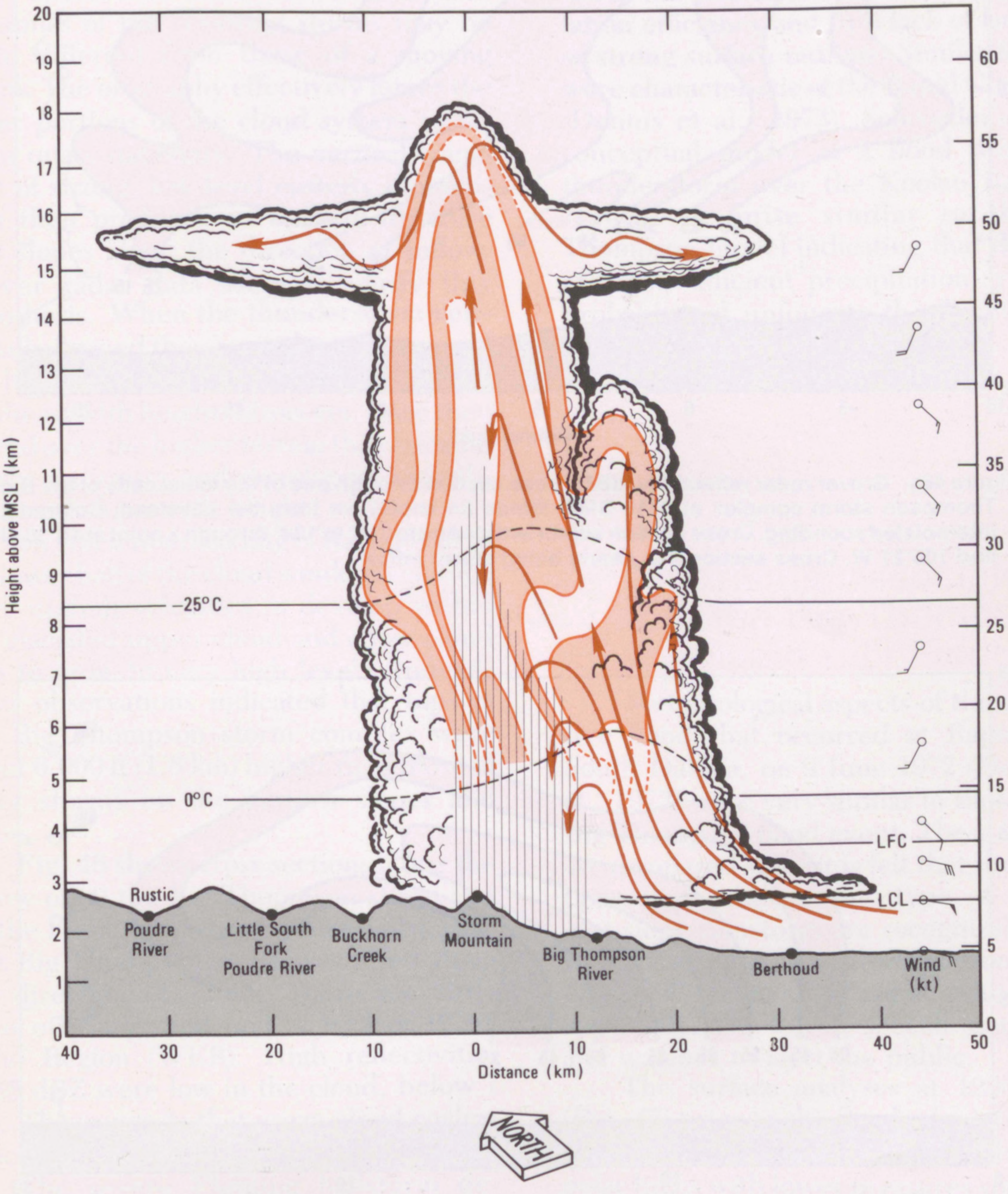

Figure 45. Physical model of one of the initial cells of the Big Thompson storm complex. LCL, LFC, winds, and levels of 0°C and −25°C isotherms are from interpolated Loveland, Colorado, sounding. Grover 0045 GMT radar reflectivities are shown with 10 dBZ contours beginning with 15 dBZ level.

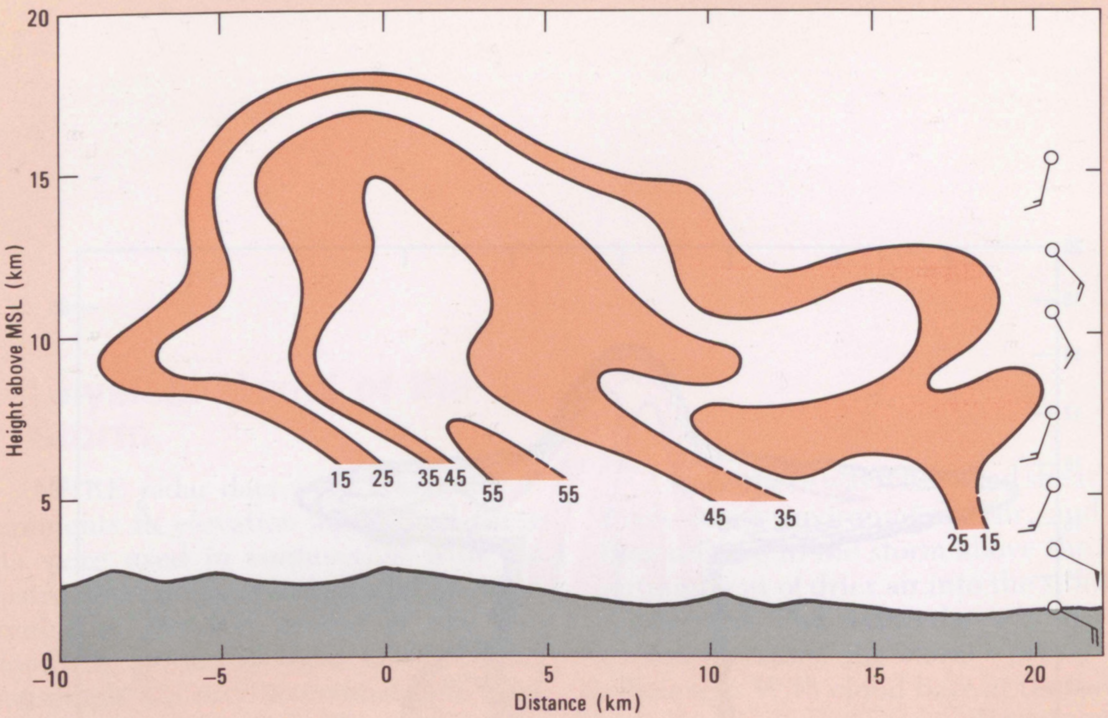

Figure 46a. Grover radar reflectivity (dBZ) cross section through one of the initial cells of the Big Thompson storm complex at 0045 GMT. Winds (in knots) are from the Loveland, Colorado, interpolated sounding. Cross section was orientated from 314° to 134° through a point at 40°30′N and 105°21′W. Cross section lies nearly along storm inflow.

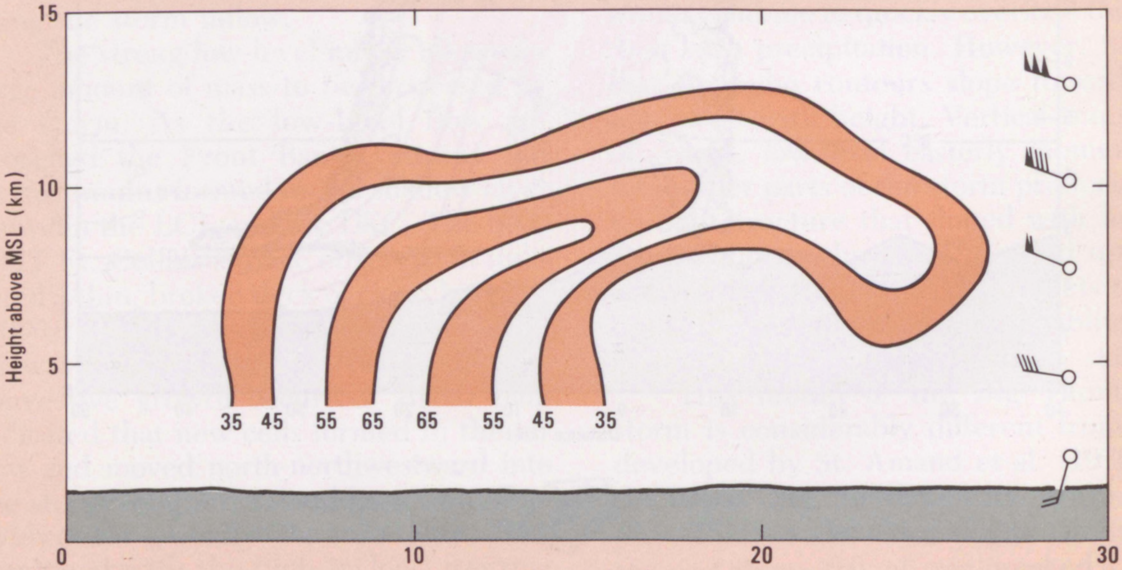

Figure 46b. Grover radar reflectivity (dBZ) cross section through the severe Fleming, Colorado, hailstorm (after Browning and Foote, 1975). Winds (in knots) are from a nearby upper-air sounding. Cross section lies nearly along storm inflow.

by strong easterly flow in low levels decreasing with height) will normally tend to slope toward the east with height. Westward movement is greater near cloud base than at middle and upper levels and produces the slope. However, if terrain lifting triggers intense convection within a negatively sheared air mass, the structure and dynamics of the resulting storms may be quite different from those of a moving storm. The orography effectively forces the lower portions of the cloud system to remain quasi-stationary. The vertical transport of strong, low-level easterly momentum then produces an updraft structure that slopes along the direction of inflow. Grover radar data seem to verify this hypothesis. When the thunderstorm cells initially formed they moved rapidly toward the higher terrain and sloped toward the southeast with height. However, once they moved over the higher terrain they became nearly stationary and developed a northwestward slope with height.

An efficient unloading of the updraft in the lower half of the cloud would encourage large updraft velocities to develop within the glaciated upper cloud and allow cloud tops to grow to very high levels. Indeed, radar observations indicated that tops of the Big Thompson storm complex were about 6,000 ft (1.8 km) higher than those of other storms on the eastern slopes and plains.

Fig. 46 shows cross sections along the inflow of (a) the Big Thompson storm and (b) the Fleming storm (a severe hailstorm). The Big Thompson storm was tilted along the direction of inflow. There was little echo overhang and only a hint of Weak Echo Region (WER). High reflectivities $\geq$55 dBZ were low in the cloud, below 7 km. This suggests that warm cloud coalescence processes were highly efficient.

The severe Fleming hailstorm developed in a strongly sheared environment and bore little resemblance to the Big Thompson storm. (For details on the Fleming storm refer to Browning and Foote, 1975.) It displayed a large WER with a massive overhang of high reflectivity particles. High reflectivities $\geq$ 55 dBZ extended upward within the storm to over 10 km. Severely sheared storms are highly inefficient precipitation producers (Browning and Foote, 1975; Marwitz, 1972).

The negatively sheared Big Thompson storm was characterized by a high precipitation efficiency and by a lack of large hail or strong surface outflow. Similar features were characteristic of the Rapid City storm (Dennis et al., 1973). Schroeder's (1977) conceptual model of a flood producing thunderstorm over the Koolau Range in Hawaii is quite similar to the Big Thompson model indicating that this type of highly efficient precipitation system is probably not unique to the Front Range area.

6. Comparison of Conditions Associated With the Big Thompson and Rapid City Floods

Meteorological aspects of the destructive flood that occurred at Rapid City, South Dakota, on 9 June 1972 (Dennis et al., 1973) were very similar to those of the Big Thompson flood event. These features are compared since it is felt that the conditions that produce this type of intense east-slope rainstorm are recognizable 3 to 12 h in advance. Early recognition of this type of flash flood potential would allow more effective use of special statements and watches to alert the public.

The surface analyses at 1200 GMT (Fig. 47) prior to the floods show that surface conditions were dominated by large polar highs with lower pressures south and west of the threat areas. The dashed line on the Rapid City map (Fig. 47a) represents a weak wind shift line. Both cases were characterized by a zone of unusually moist air with high dewpoints north of the polar front and by hotter, drier air west and south of the front.

Figs. 48 and 49 are the 700 and 500 mb analyses at 1200 GMT. The common features of importance are the following:

1. The large, negatively tilted ridge over the plains with a trough over the west.
2. A short-wave trough south and west of the threat areas. This short wave was moving northward up the back of the ridge.
3. Light south to southeasterly winds over the threat areas.
4. Abundant moisture over much of the western United States.

Fig. 50 presents the 1200 GMT upper-air soundings taken at Rapid City and Huron, South Dakota, and also shows the 1200 GMT Denver sounding and the 1920 GMT Sterling sounding. In both cases, the soundings taken east-northeast of the threat areas were more representative of the air mass in which intense thunderstorms were triggered later in the day. Both the Huron and Sterling soundings were conditionally very unstable but with temperature inversions capping the unstable, moist boundary layer. Both soundings were taken near the upper ridgeline and showed easterly winds below the inversions.

The surface analyses at 0000 GMT (Fig. 51), just prior to the floods, showed that strong easterly winds were pushing moist, conditionally unstable, boundary layer air westward onto higher terrain. A zone of moist air north of the polar front fed the storms, while drier air lay south and west of the front. Pressures were lower south and west of the front helping to maximize the easterly, upslope flow.

Figs. 52 and 53 depict the 700 and 500 mb analyses at 0000 GMT. Notice that at 700 mb moist southeasterly flow exists in the threat areas ahead of the approaching short waves. The 500 mb short-wave troughs, which eventually moved the flood producing storms away from the mountains, were approaching from the southwest. Winds over the threat area were light southerly, and the movement and orientation of the 500 mb short-wave troughs helped maintain lower pressures west of the threat area.

The 0000 GMT Rapid City and interpolated Loveland soundings are shown in Fig. 54. Both soundings were conditionally unstable with strong easterly winds and very high moisture contents within the lowest 1 to 1.5 km. Winds above 500 mb were light south to southeasterly. The Rapid City sonde sampled active convection (Dennis et al., 1973) and thus did not exhibit the temperature inversion.

Table 3.
Comparison of upper-air parameters for Rapid City, Loveland, and typical severe thunderstorm soundings

Location	Time (GMT)	Mean vapor mixing ratio (lowest 100 mb) (g kg^{-1})	Lifted Index (lowest 100 mb)	Planetary Boundary Layer (lowest km) (deg/kt)	Wind velocity (deg/kt)		
					700 mb	500 mb	300 mg
Rapid City	0000 GMT, 10 June 1972	14.0	−5	100/40	140/31	150/18	140/08
Loveland (interpolated)	0000 GMT, 1 Aug. 1976	14.8	−6	100/50	130/30	190/15	170/15
Typical plains severe storm *	——	12 to 14	−4 to −6	200/35	225/40	235/50	245/70

*Data from Maddox (1976).

Table 3 compares the Rapid City and Loveland soundings with conditions associated with severe Central Plains thunderstorms (storms producing large hail and/or damaging winds and/or tornadoes). L.I.'s and moisture contents are comparable; however, the wind fields are dramatically different. The wind veers with height in both types of soundings, but the heavy rain soundings are characterized by strong easterly winds near the surface and light southerly winds aloft. This "reverse" shear contrasts markedly with the strongly sheared severe storm environment.

The following list summarizes similar meteorological conditions associated with both the Rapid City and Big Thompson flash floods.

A. Common large scale features

1. A middle and upper tropospheric long-wave trough lies over the western United States with a negatively tilted ridge just east of the threat area.

2. A weak 500 mb short-wave trough rotates northward in the long-wave trough and approaches the threat area.

3. Light southeast to south-southeast winds (5 to 8 m s^{-1}) are present in the upper troposphere over the threat area.

4. A slow moving, or stationary, polar front lies just south of the threat area.

5. Unusually moist (vapor mixing ratio of 13 to 15 g kg^{-1}) and strong (15 to 25 m s^{-1}) easterly low-level flow moves into threat area.

6. High moisture content is present through a large depth of the troposphere (surface through 300 mb).

B. Common mesoscale features

1. Afternoon heating west of the threat area and cold advection east of storm area combine to intensify thickness and pressure gradients. Low-level wind flow maximizes about sunset.

2. A narrow band of conditionally unstable air (L.I. = −4 to −7) moves southward and westward behind the polar front. This air mass is capped by a temperature inversion.

3. Orographic lift provides the mechanism needed to release the instability, and heavy rains fall over middle elevations of the affected drainages. The moisture content of the low-level air is so great that the lifting needed to trigger storm development occurs east of the highest terrain.

4. Convective cells move slowly north-northwestward, and continued cell redevelopment on the southeast flank of the thunderstorm complex results in a quasi-stationary precipitation system.

C. Common microphysical characteristics

1. A high freezing level (5 to 6 km MSL) in the cloud and low cloud bases combine to produce a deep warm cloud layer in which precipitation particles may grow by coalescence processes.

2. Negligible vertical wind shear and light winds relative to the storm, at middle and upper levels, combined with moist environmental air and cloud bases at or near the surface, suppress evaporative losses and the formation of downdrafts. These conditions contribute to high precipitation efficiency.

Most of these important large scale and mesoscale features can be detected and monitored if National Meteorological Center analyses and forecasts are used in conjunction with aviation teletype data, radar reports, and satellite photographs. As recently emphasized by Mogil and Groper (1976), when the detection level shifts from the large scale down to actual storm reports, the forecaster should rely heavily upon mesoscale analyses and interpretations to delineate the potential for excessive rainfall.

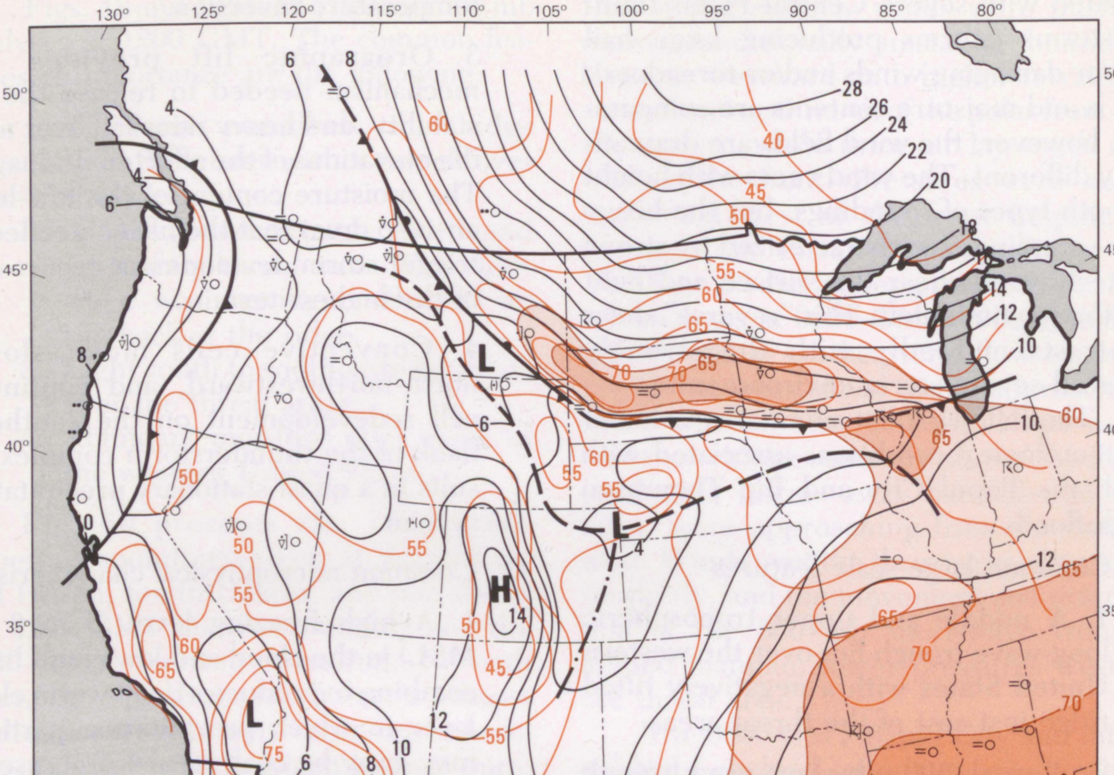

Figure 47a. Rapid City synoptic scale surface analysis for 1200 GMT, 9 June 1972. Refer to legend of Fig. 4 for details.

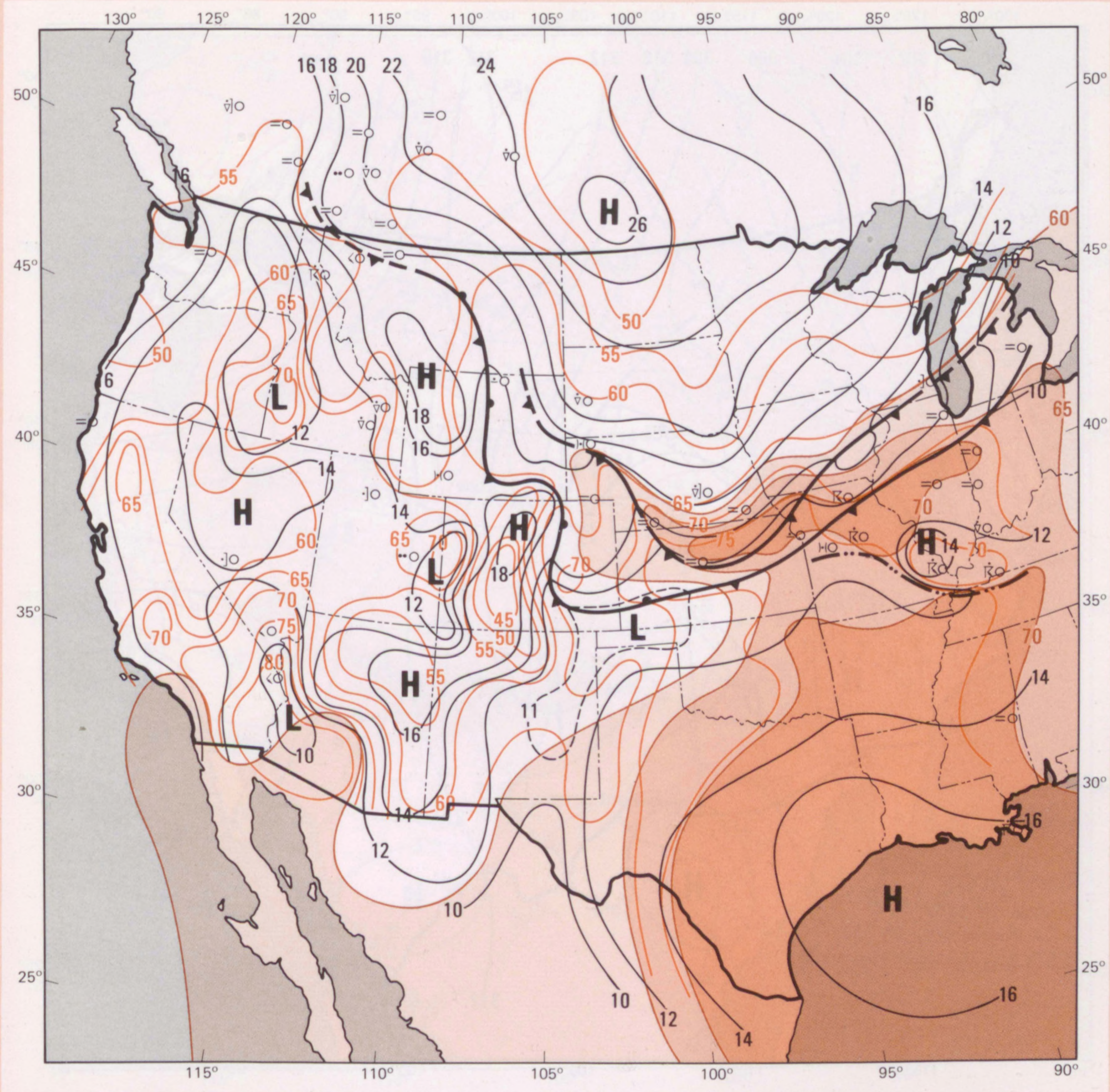

Figure 47b. Big Thompson synoptic scale surface analysis for 1200 GMT, 31 July 1976. (Same as Fig. 4.)

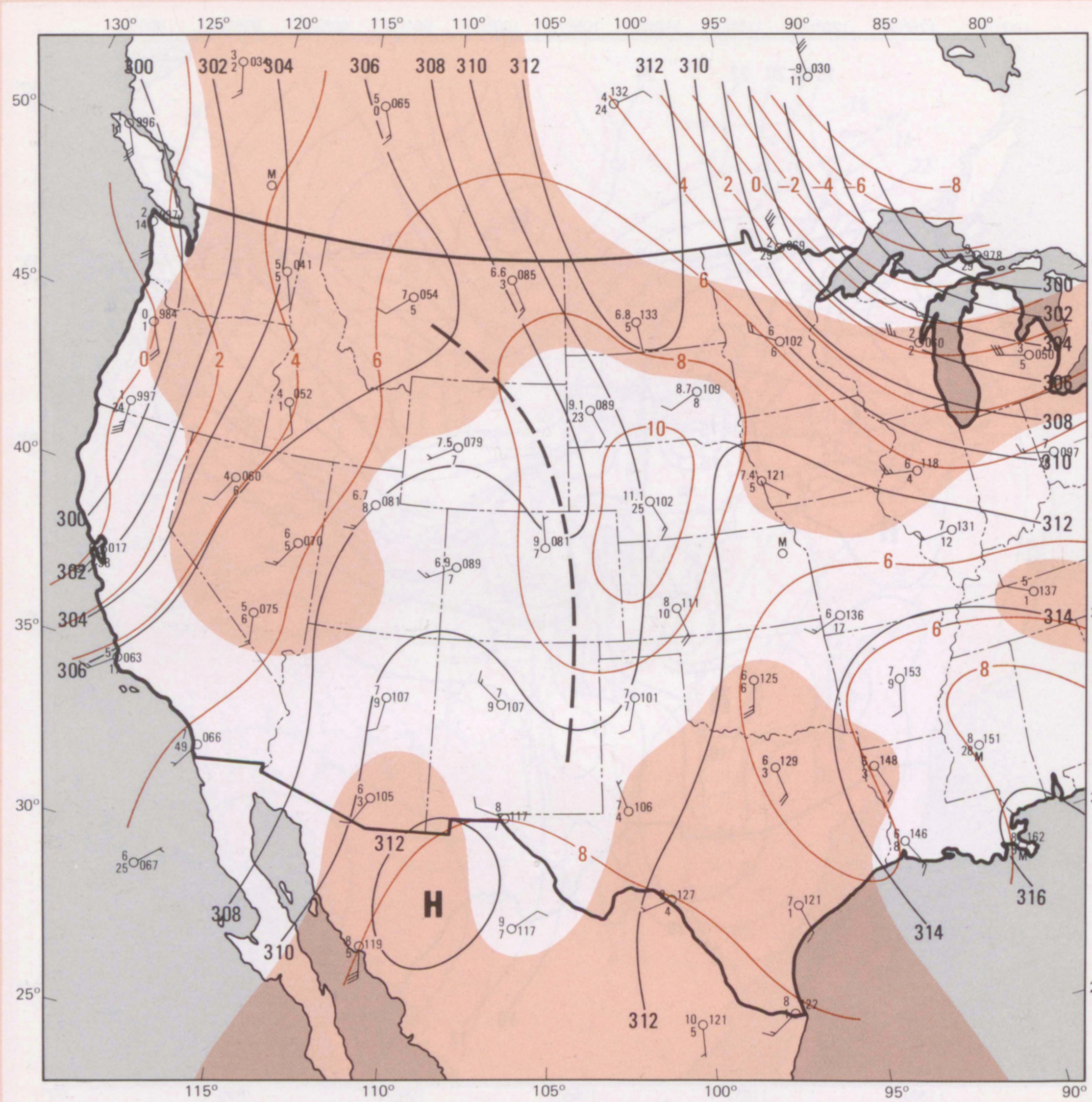

Figure 48a. Rapid City 700 mb analysis for 1200 GMT, 9 June 1972. Refer to legend of Fig. 5 for details.

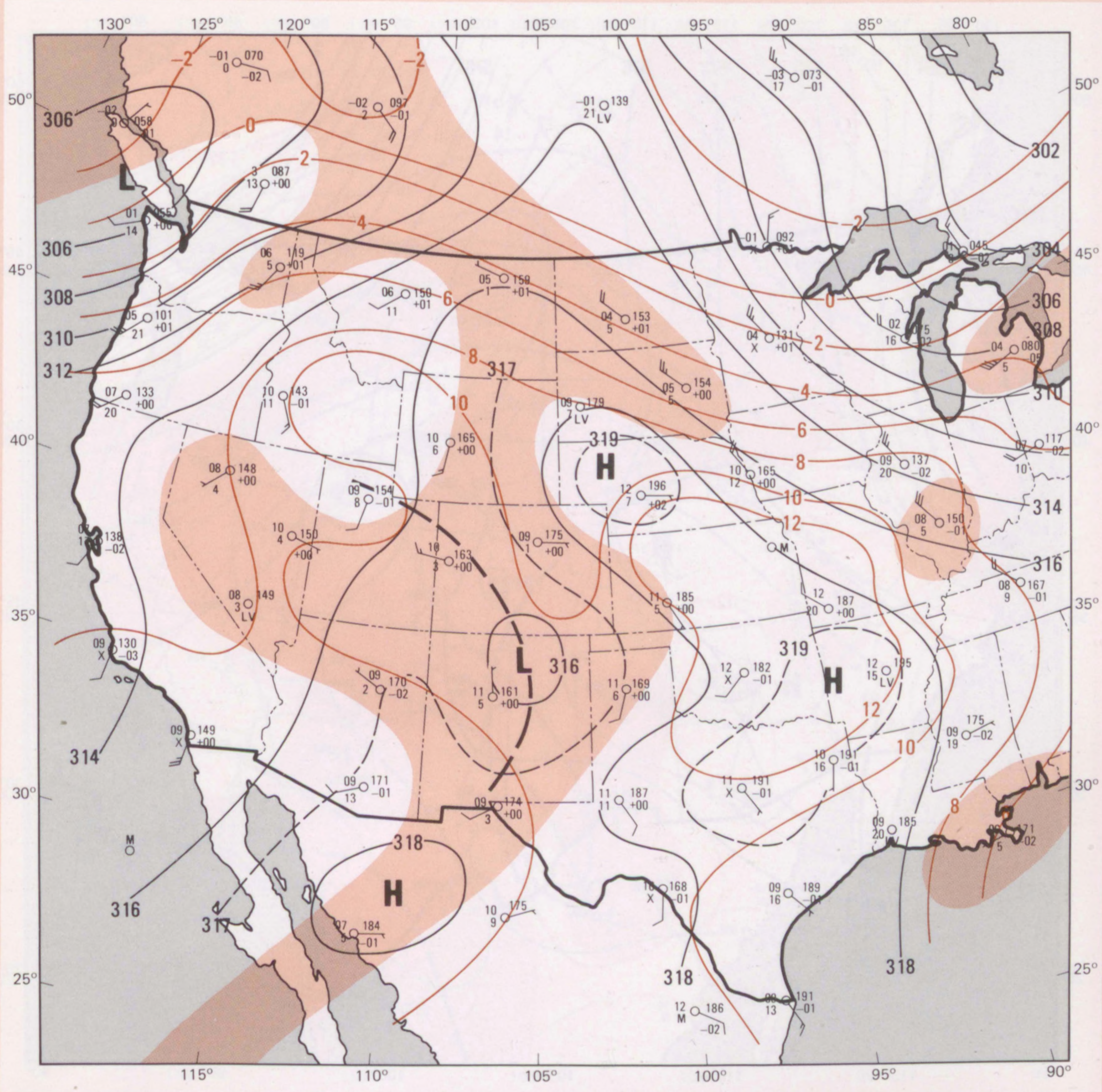

Figure 48b. Big Thompson 700 mb analysis for 1200 GMT, 31 July 1976. (Same as Fig. 5.)

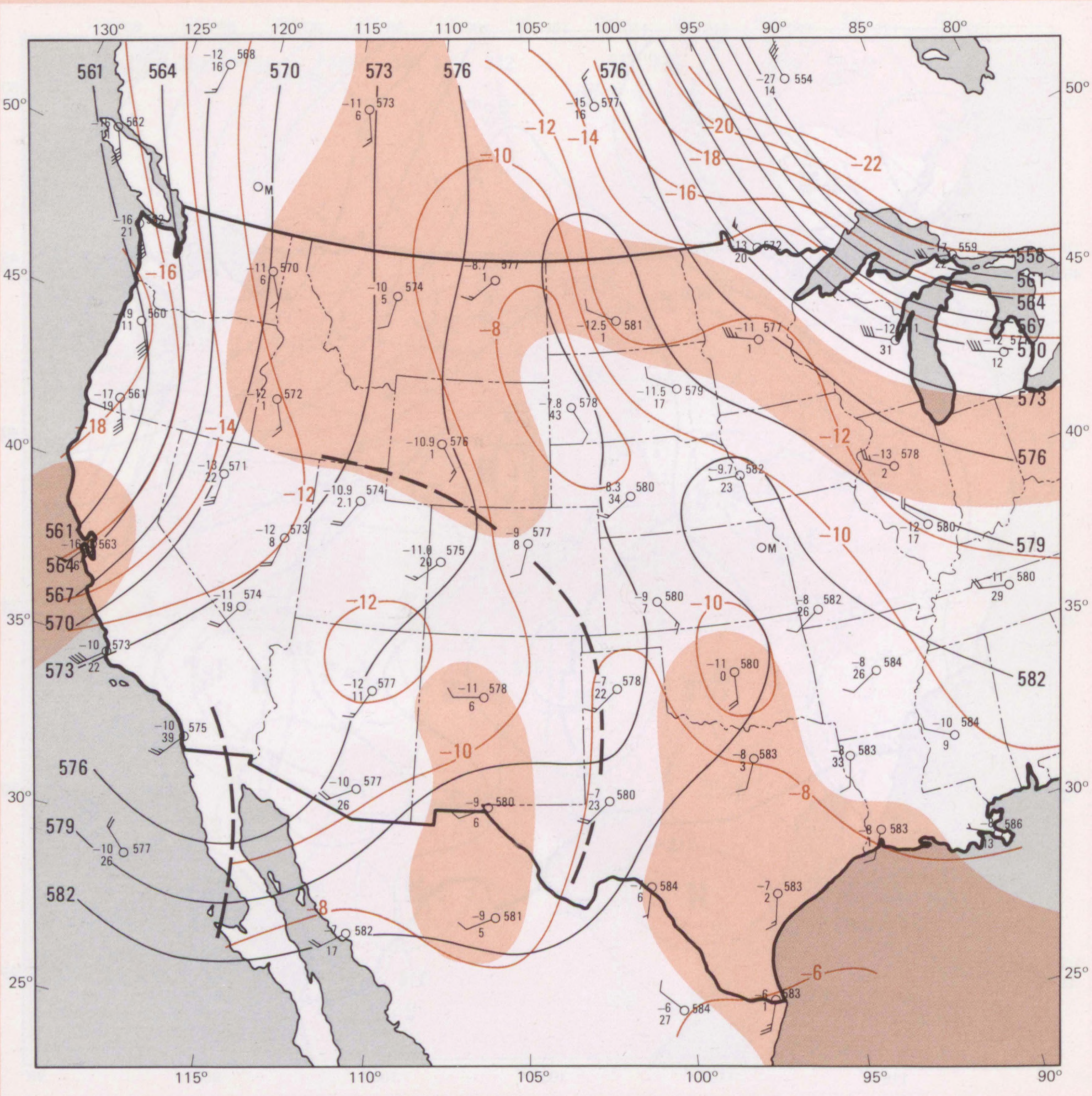

Figure 49a. Rapid City 500 mb analysis for 1200 GMT, 9 June 1972. Refer to legend of Fig. 6 for details.

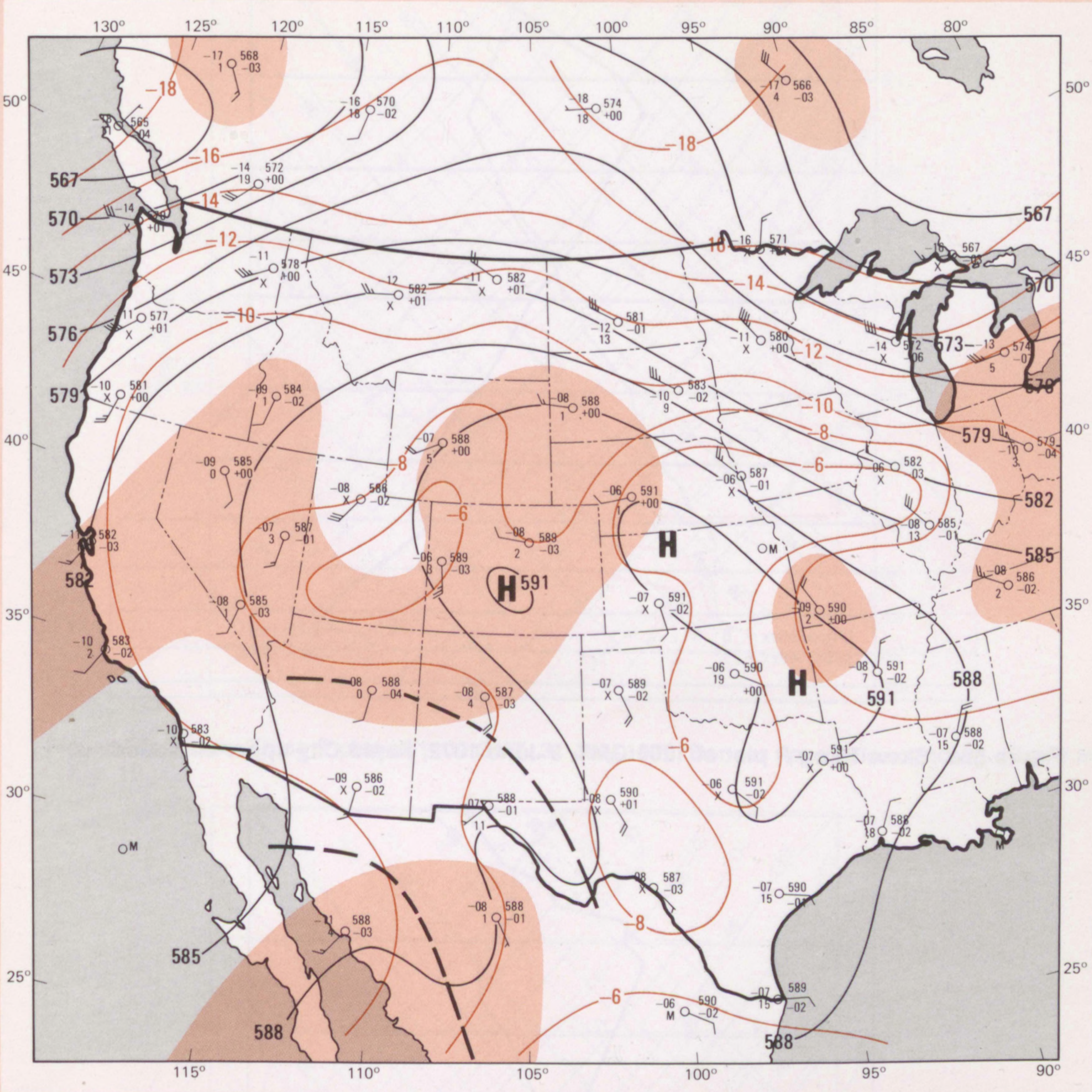

Figure 49b. Big Thompson 500 mb analysis for 1200 GMT, 31 July 1976. (Same as Fig. 6.)

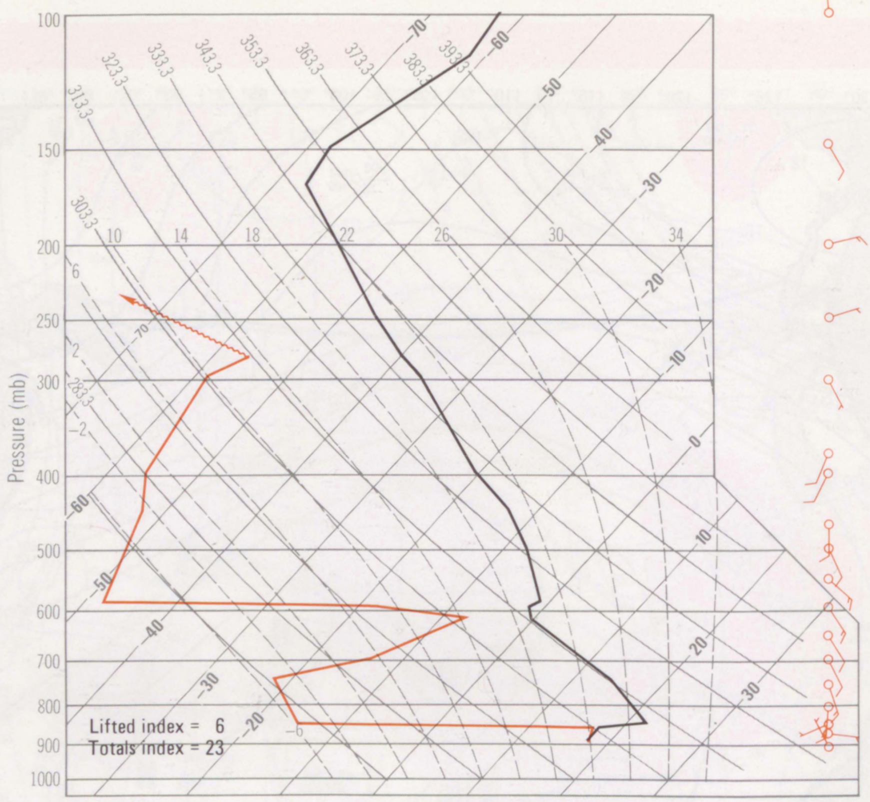

Figure 50a. Skew T/Log P plot of 1200 GMT, 9 June 1972, Rapid City upper-air sounding.

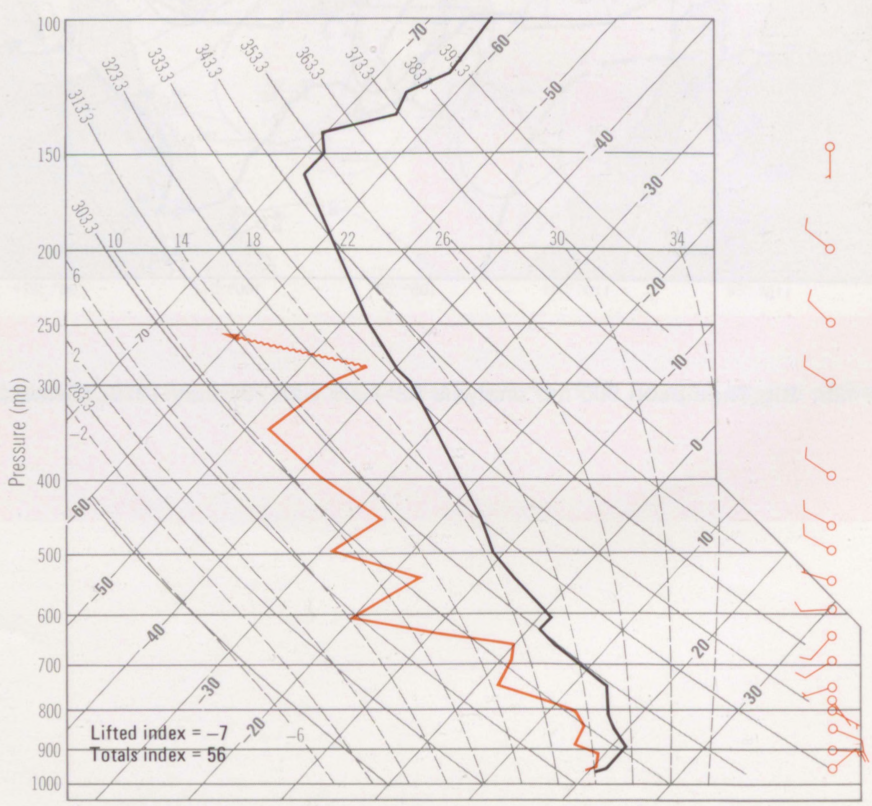

Figure 50b. Skew T/Log P plot of 1200 GMT, 9 June 1972, Huron, South Dakota, upper-air sounding.

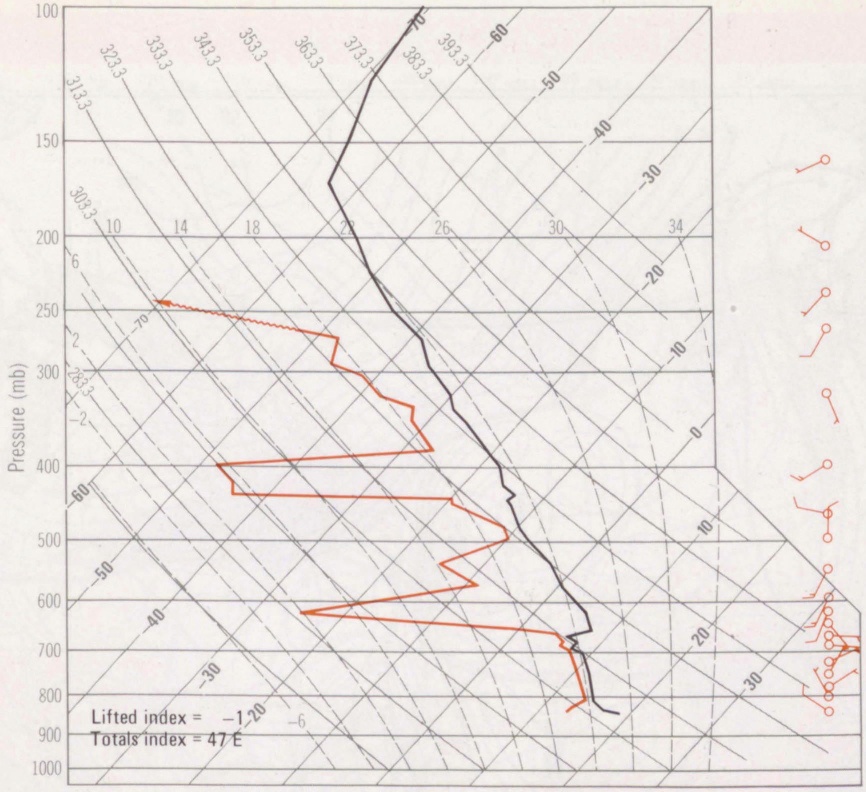

Figure 50c. Skew T/Log P plot of 1200 GMT, 31 July 1976, Denver upper-air sounding. (Same as Fig. 10.)

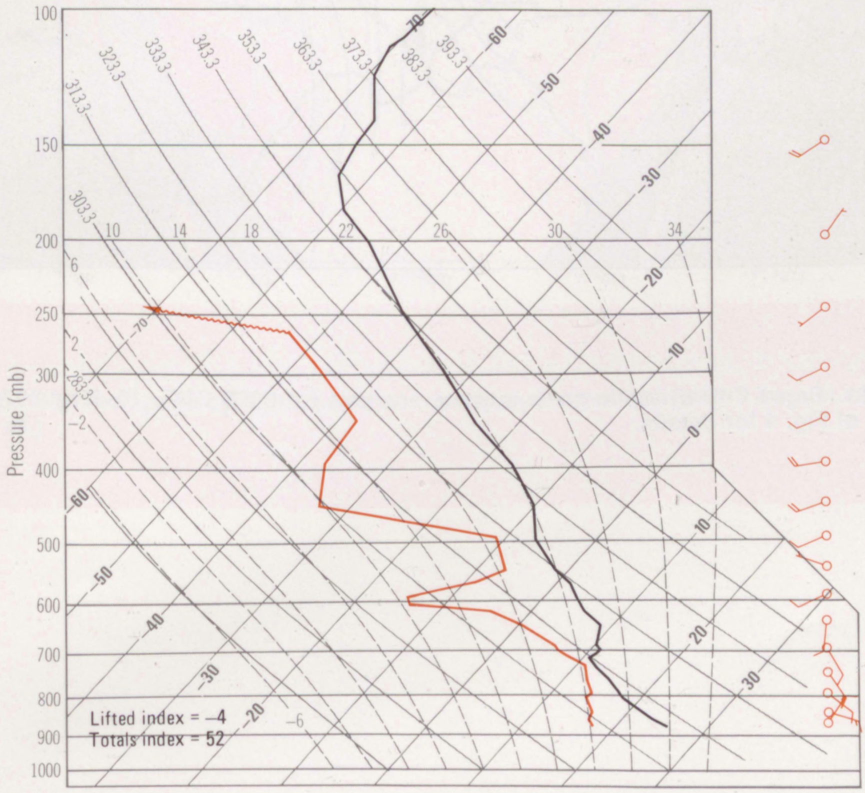

Figure 50d. Skew T/Log P plot of 1920 GMT, 31 July 1976, Sterling, Colorado, upper-air sounding. (Same as Fig. 13.)

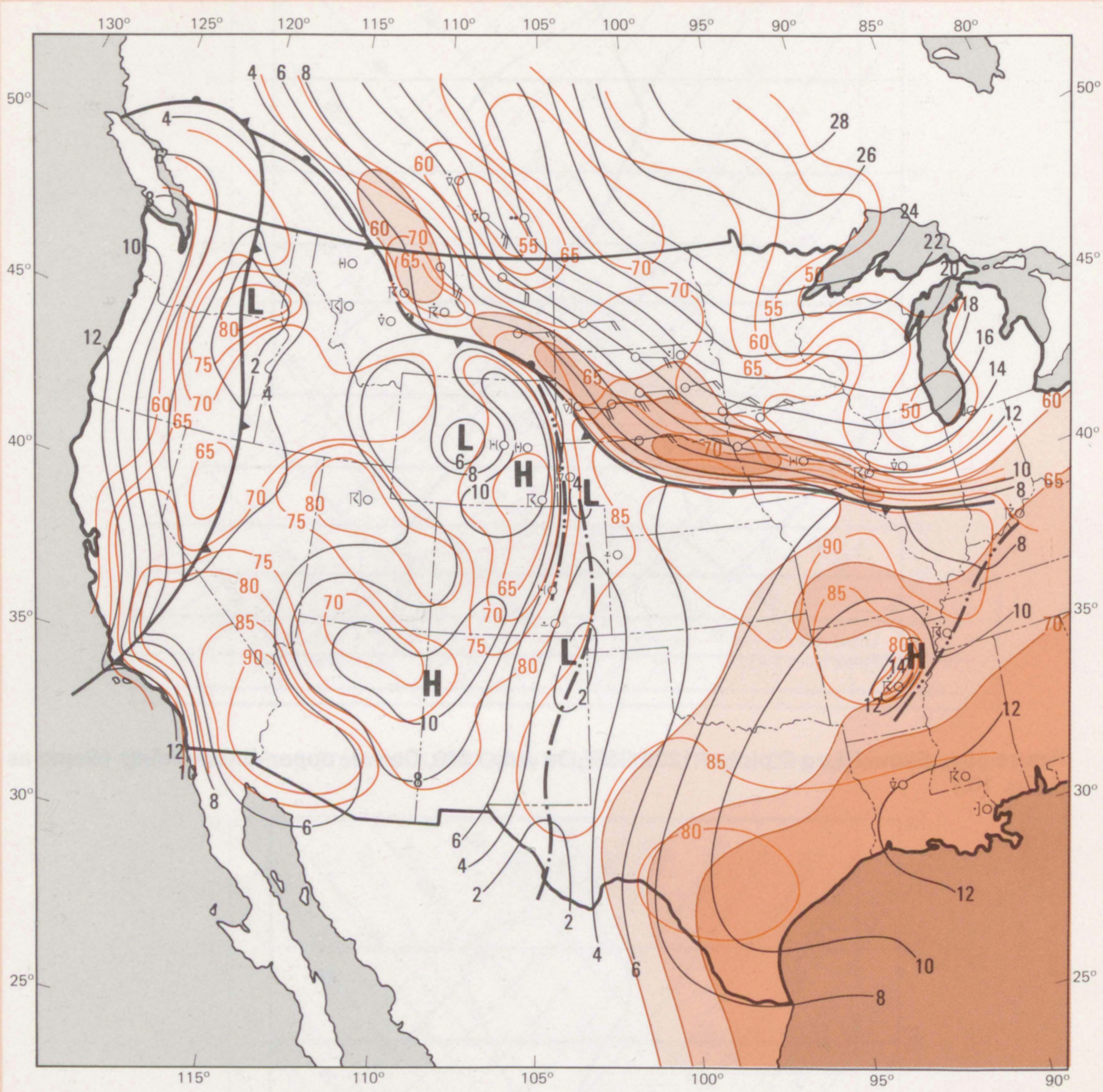

Figure 51a. Rapid City synoptic scale surface analysis for 0000 GMT, 10 June 1972. Refer to legend of Fig. 4 for details.

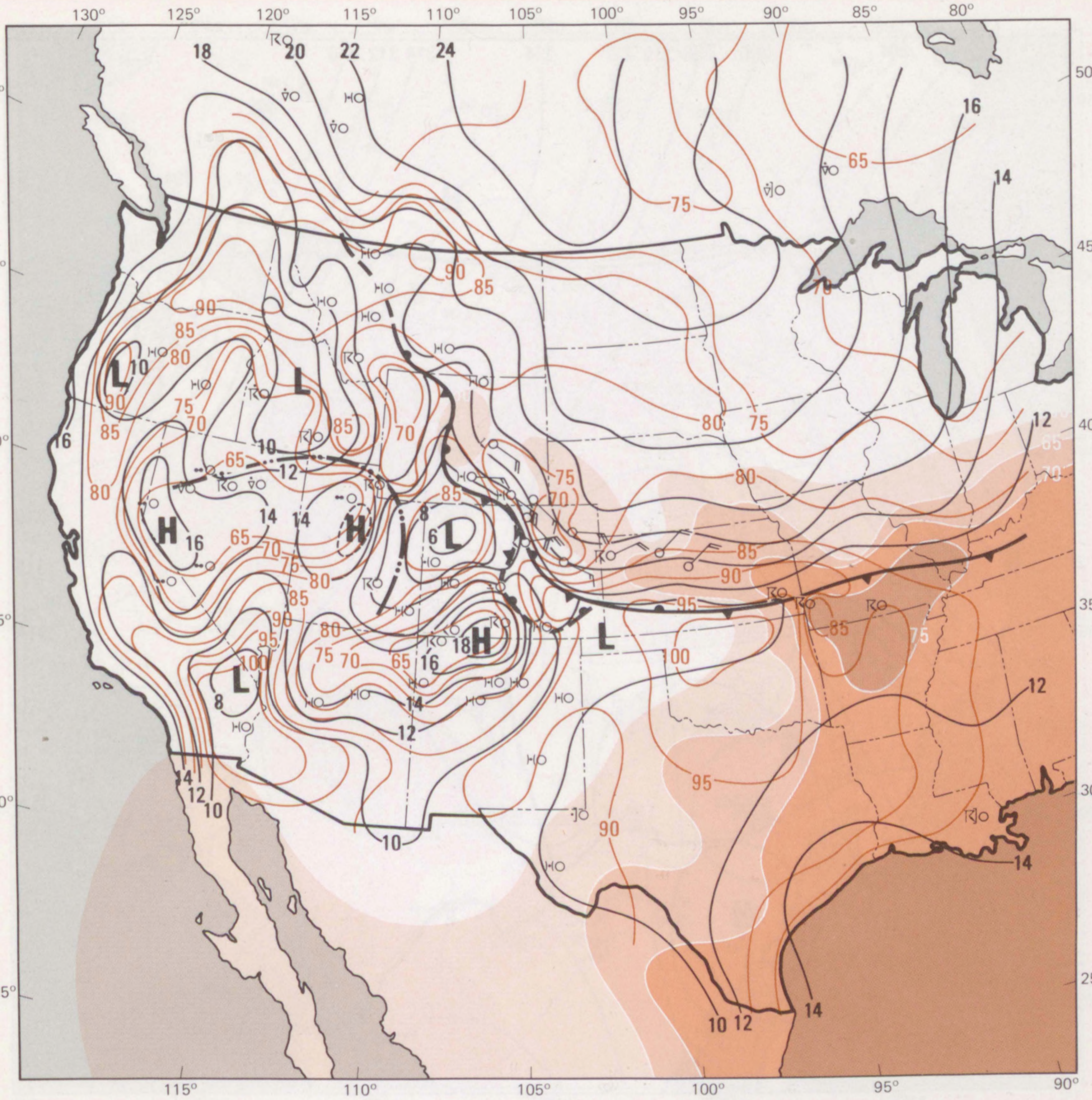

Figure 51b. Big Thompson synoptic scale surface analysis for 0000 GMT, 1 August 1976. (Same as Fig. 18.)

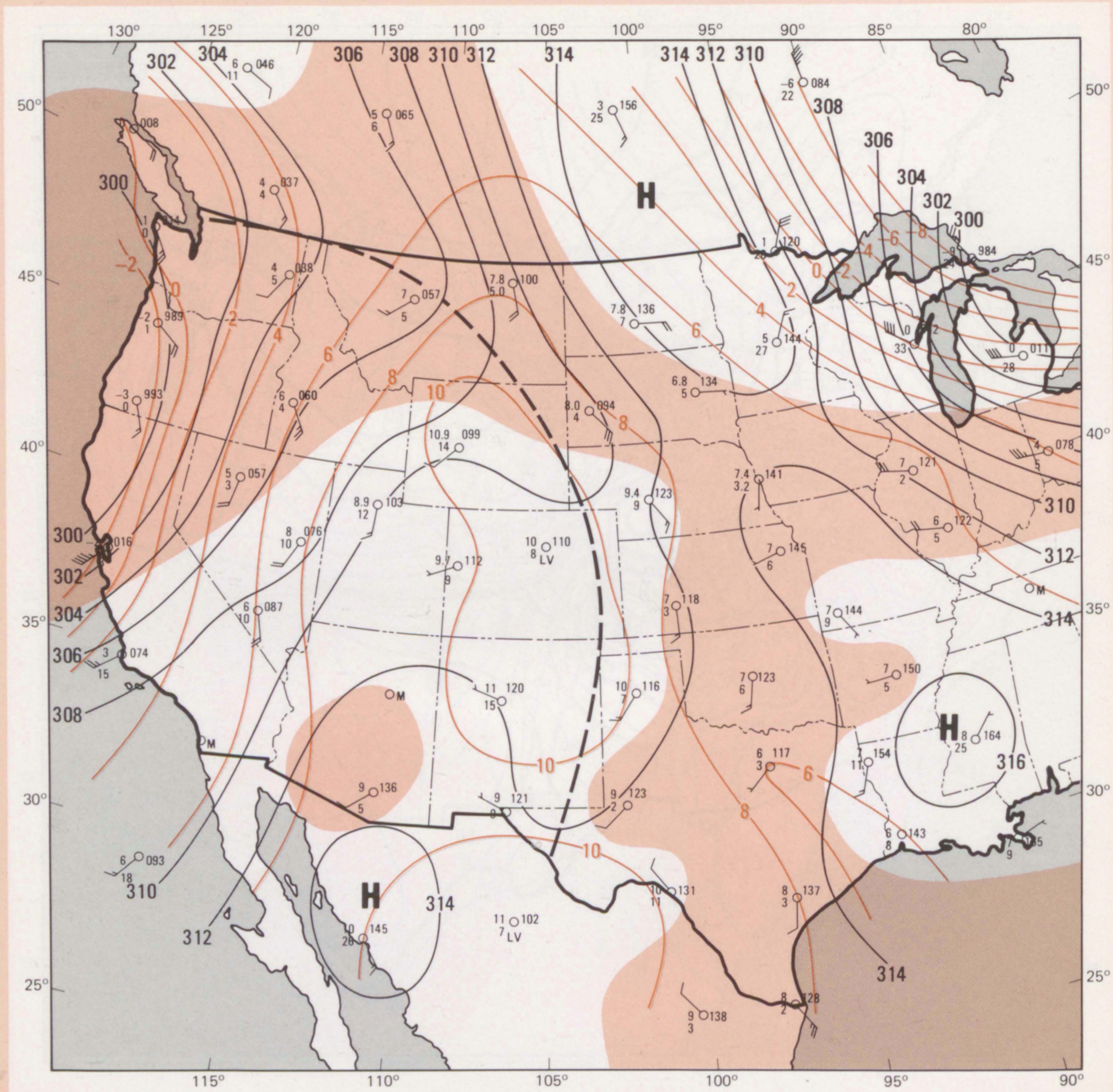

Figure 52a. Rapid City 700 mb analysis for 0000 GMT, 10 June 1972. Refer to legend of Fig. 5 for details.

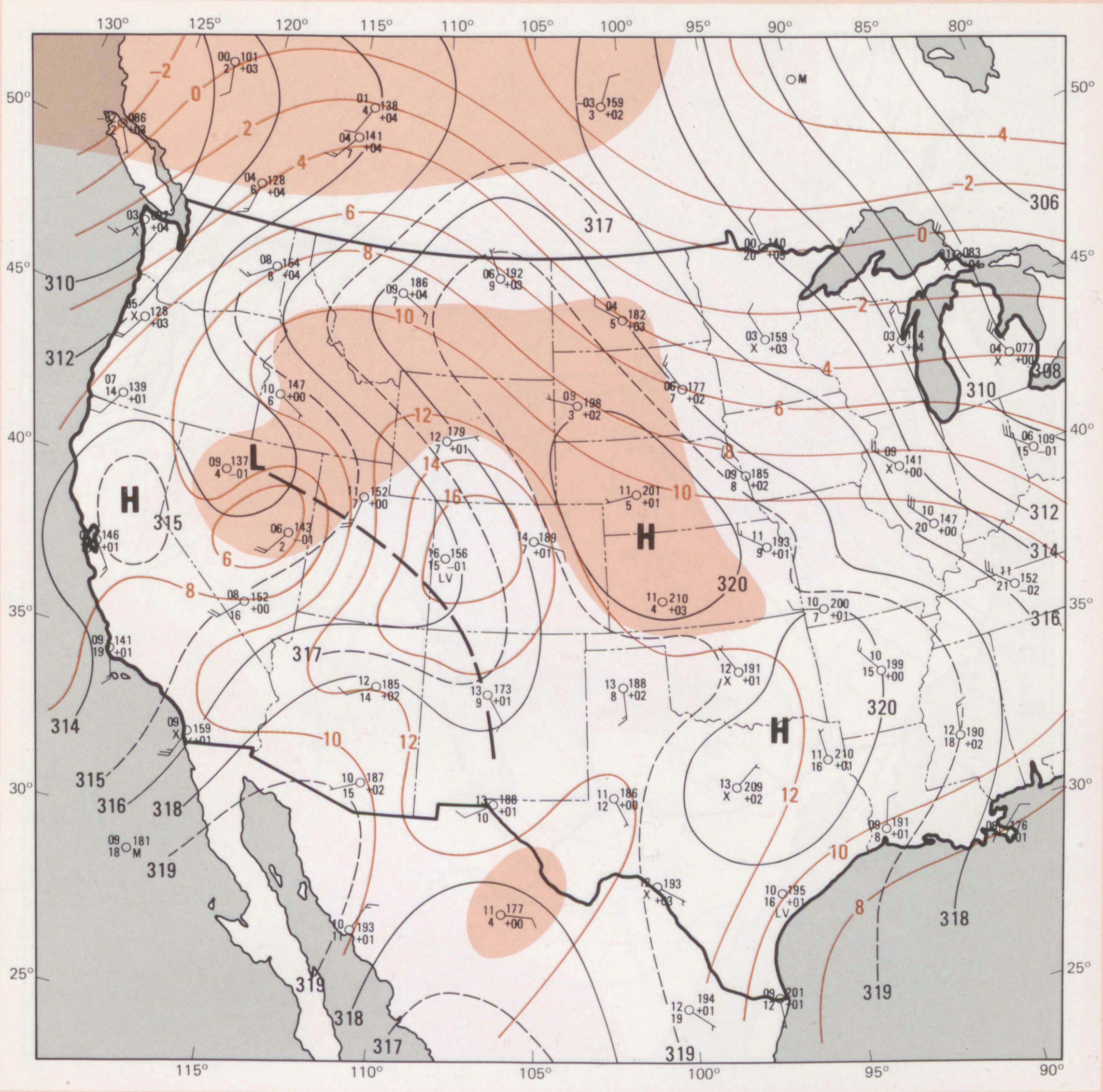

Figure 52b. Big Thompson 700 mb analysis for 0000 GMT, 1 August 1976. (Same as Fig. 21.)

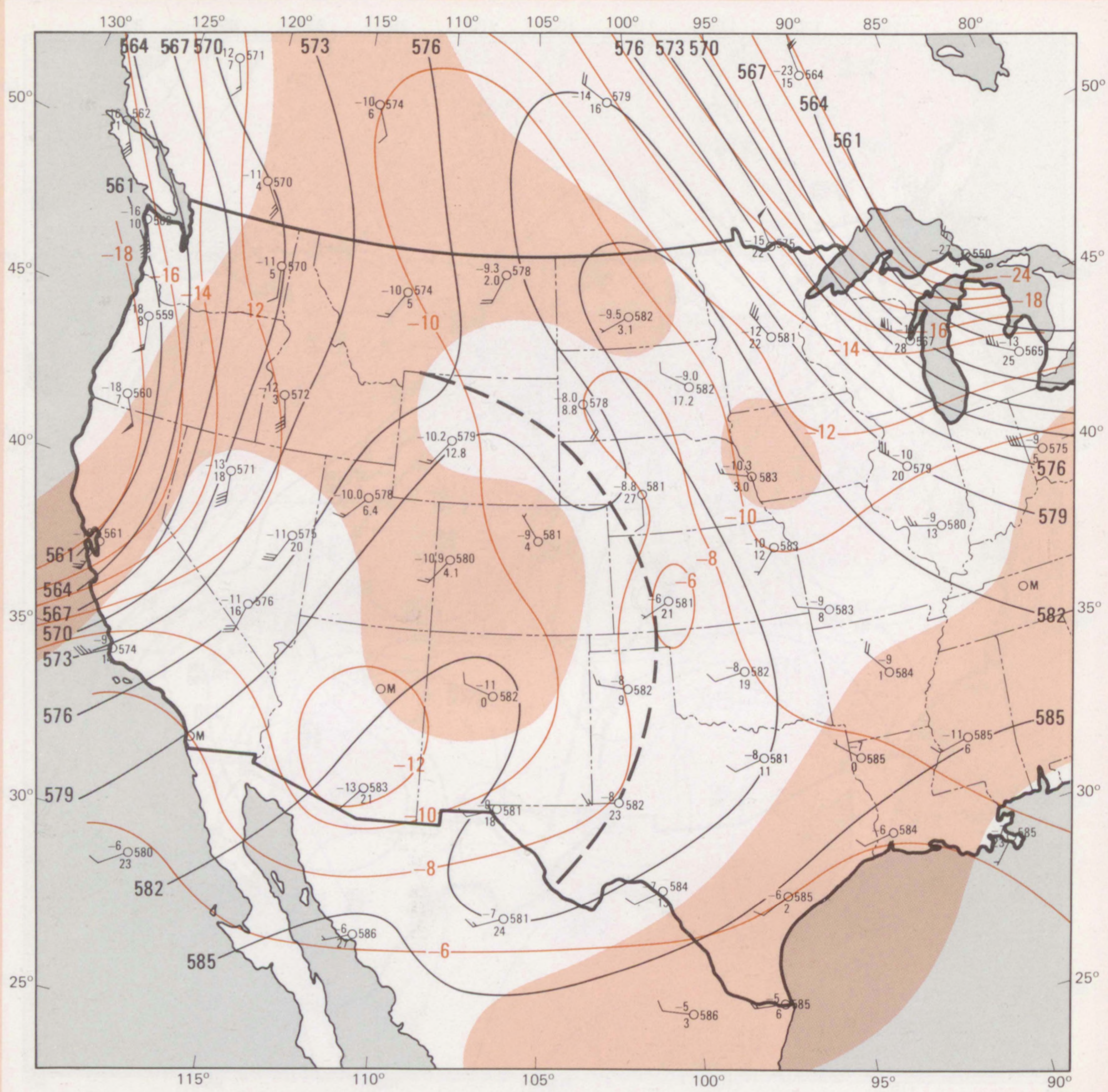

Figure 53a. Rapid City 500 mb analysis for 0000 GMT, 10 June 1972. Refer to legend of Fig. 6 for details.

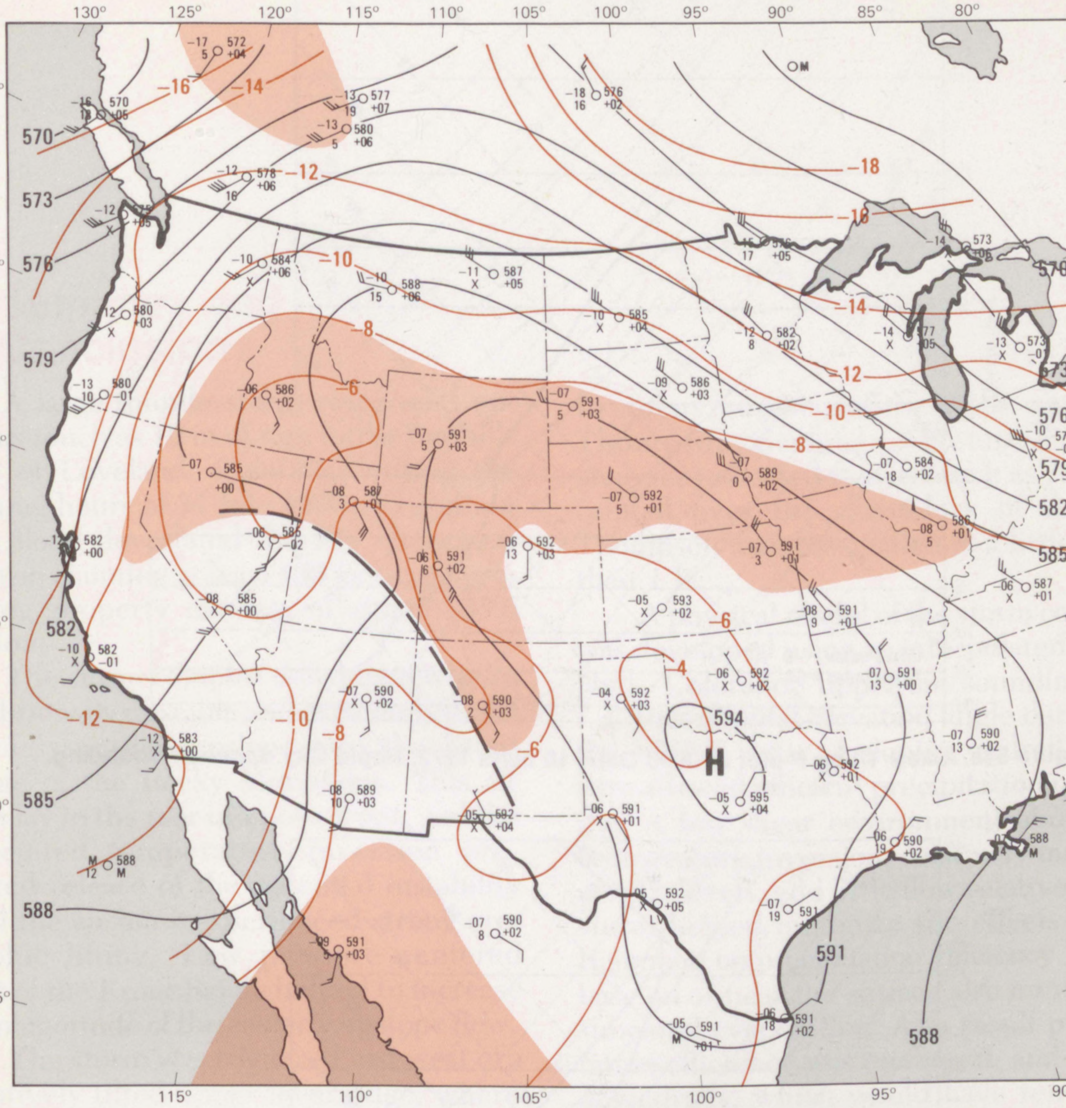

Figure 53b. Big Thompson 500 mb analysis for 0000 GMT, 1 August 1976. (Same as Fig. 22.)

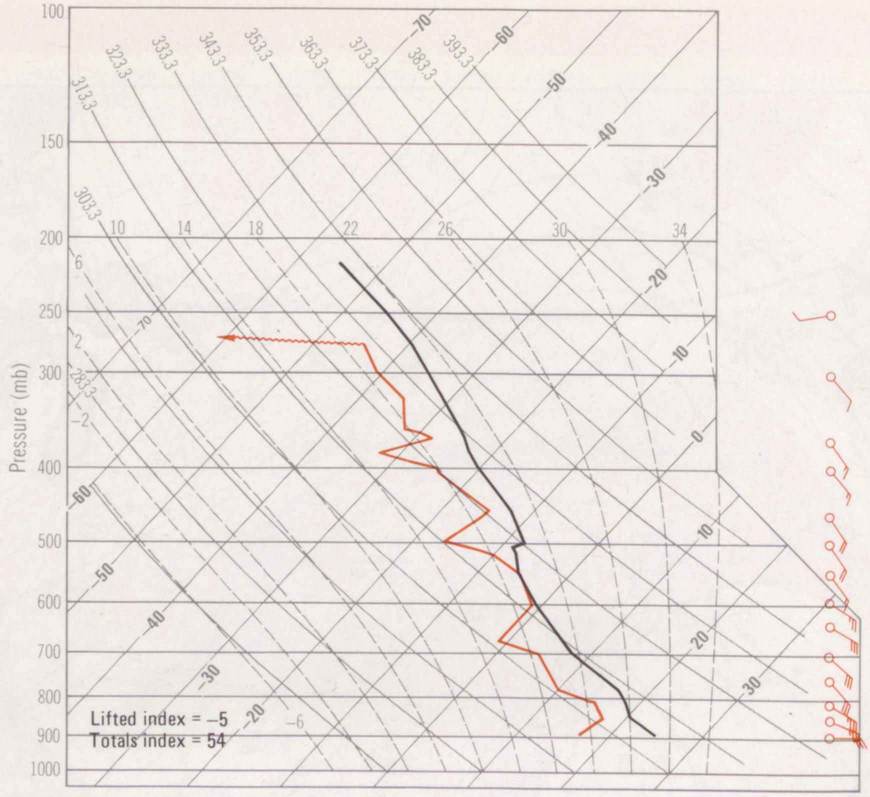

Figure 54a. Skew T/Log P plot of 0000 GMT, 10 June 1972, Rapid City upper-air sounding.

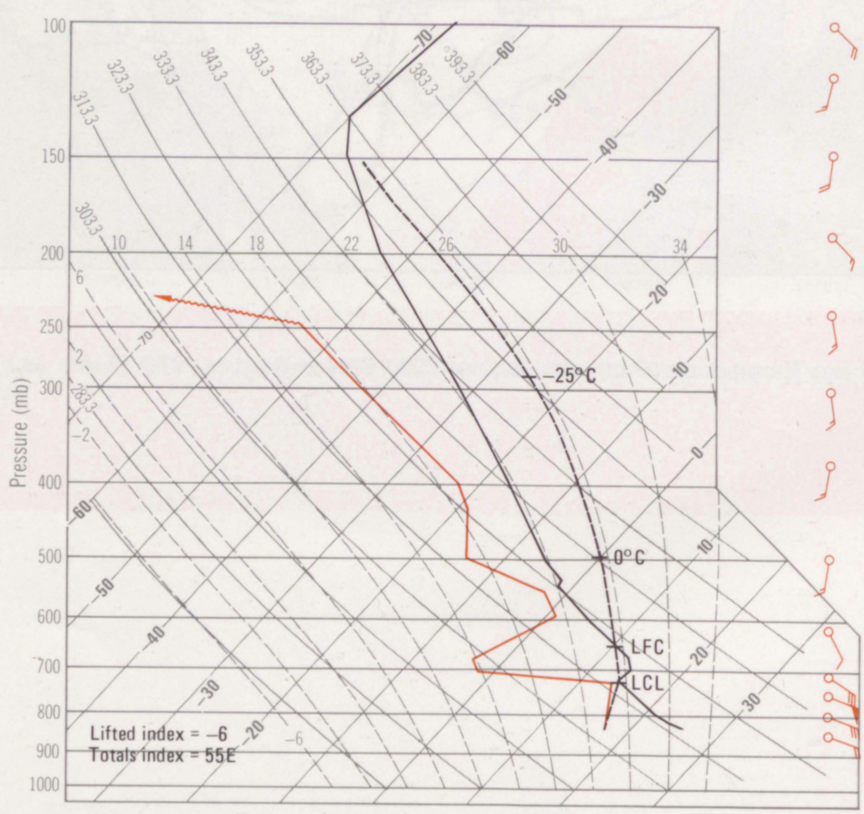

Figure 54b. Skew T/Log P plot of 0000 GMT, 1 August 1976, upper-air sounding constructed for Loveland, Colorado. (Same as Fig. 32.)

7. Summary and Conclusions

A large thunderstorm complex dropped as much as 10 in of rain in the foothills west of Loveland, Colorado, during the evening hours of 31 July 1976. A resultant flash flood devastated the Big Thompson Canyon claiming at least 139 lives and producing property damage of about $35.5 million.

The storm complex developed when a conditionally unstable and extremely moist air mass pushed upslope into the Front Range of the Rocky Mountains. This air mass lay to the rear of a polar front, and the associated temperature inversion prevented release of the potential instability until the air mass experienced strong orographic lifting. Low pressure centered west of the Front Range helped to increase the magnitude of the easterly upslope flow.

The storm was triggered just west of a negatively tilted upper level ridge, where winds above the temperature inversion were light southeasterly. These weak steering winds allowed the storm complex to remain nearly stationary over the Front Range for 2 to 3 h as new cells generated on the sourtheast flank and moved into the storm complex. A weak 500 mb short-wave trough, approaching the storm area from the south-southwest, moved the storm slowly northward into Wyoming and eventually out onto the plains.

Local area surface analyses indicated that prefrontal, high-based thunderstorms that moved over the Front Range west of Boulder may have limited the southward extension of the storm complex and helped to focus moist inflow into the Big Thompson drainage. Detailed radar analyses indicated that as much as 7.5 in of rainfall over the main fork of the Big Thompson may have fallen in a little more than 1 h.

A physical model of the storm complex was developed using an interpolated Loveland, Colorado, upper-air sounding and 1.4° incremental elevation angle data from the NHRE radar. A sloping updraft structure allowed efficient precipitation unloading. A low shear environment above the temperature inversion, relatively moist air at high levels, and little flow relative to the storm helped minimize the effects of entrainment on precipitation efficiency. Cloud base on or near the surface also minimized subcloud evaporation. As a result precipitation efficiency was increased, and strong downdrafts, which would have tended to force new cell development at other locations, were subdued.

Meteorological conditions associated with the Big Thompson and Rapid City flash floods have been compared. These events were very similar, and a set of important meteorological features associated with this type of convective cloudburst has been presented. Recognition of these features should be of use in predicting the potential and issuing watches for this type of severe storm with geographical areas and lead times similar to those currently issued for expected tornado activity.

8. Acknowledgments

The authors would like to thank the many persons and organizations who supplied data used in this study. The Department of Atmospheric Science, Colorado State Univ., provided data for Ft. Collins. Dr. C. Glenn Cobb supplied Greeley data measured at Ross Hall, Univ. of Northern Colorado. John M. West of Rockwell International Corp. supplied the Rocky Flats data, and Frank Pratte of Wave Propagation Laboratory (NOAA–ERL) provided the data from Table Mountain. James F. W. Purdom of NOAA–NESS Applications Group supplied copies of GOES imagery. The NHRE and the National Center for Atmospheric Research Field Observing Facility obtained and supplied the invaluable sounding, radar, and surface data from the NHRE site in northeastern Colorado. National Climatic Center (NOAA–EDS) personnel expeditiously filled several large data requests. John Asztalos of Waukesha, Wisconsin, provided copies of photographs that he had taken of the developing storm.

9. References

Browning, K. A., and G. B. Foote, 1975. Air flow and hail growth in supercell storms and some implications for hail suppression. National Hail Research Experiment Tech. Rept. No. 75/1, 77 pp.

Dennis, A. S., R. A. Schleusener, J. H. Hirsch, and A. Koscielski, 1973. Meteorology of the Black Hills flood of 1972. Institute of Atmos. Sci., Report 73-4, South Dakota School of Mines and Technology, Rapid City, 41 pp.

Grozier, R. U., J. F. McCain, L. F. Lang, and D. C. Merriman, 1976. The Big Thompson River Flood of July 31-1 August, 1976. Larimer County, Colorado, U.S.G.S. and Colorado Water Conservation Board Flood Information Report, Denver, 78 pp.

Lott, G. A., 1976. Precipitable water over the United States, Volume 1: Monthly means. NOAA Tech. Rept. NWS 20, 173 pp.

Maddox, R. A., 1976. An evaluation of tornado proximity wind and stability data. *Mon. Wea. Rev.*, **104**:133–142.

Marwitz, J. D., 1972. The structure and motion of severe hailstones. Part III: Severely sheared storms. *J. Appl. Meteor.*, **11**:189-201.

Miller, R. C., 1972. Notes on analysis and severe storm forecasting procedures of the Air Force Global Weather Central. Air Weather Service Tech. Rept. 200 (Rev.), 102 pp.

Mogil, H. M., and H. S. Groper, 1976. On the short range prediction of localized excessive convective rainfall. Preprints, Conf. on Hydro-Meteorology, Amer. Meteor. Soc., Ft. Worth, 9–12.

NOAA, 1976. Big Thompson Canyon flash flood of July 31–August 1, 1976. Natural Disaster Survey Report 76–1, U.S. Dept. of Commerce, Rockville, Md., 41 pp.

Randerson, D., 1976. Meteorological analysis for the Las Vegas, Nevada, flood of 3 July 1975. *Mon. Wea. Rev.*, **104**:719–727.

Schroeder, T. A., 1977. Meteorological analysis of an Oahu Flood. *Mon. Wea. Rev.*, **105**:458–468.

St. Amand, P., R. J. Davis, and R. D. Elliott, 1972. Report on Rapid City flood of 9 June 1972. Report to South Dakota Weather Control Commission, Pierre, South Dakota, 37 pp.

Williams, G., 1976. Application of the National Weather Service flash-flood program in the Western Region. NOAA Tech. Memo. NWS WR-103, 20 pp.

☆ U. S. GOVERNMENT PRINTING OFFICE: 1977 — 780-900

Environmental Research LABORATORIES

The mission of the Environmental Research Laboratories (ERL) is to conduct an integrated program of fundamental research, related technology development, and services to improve understanding and prediction of the geophysical environment comprising the oceans and inland waters, the lower and upper atmosphere, the space environment, and the Earth. The following participate in the ERL missions:

MESA *Marine EcoSystems Analysis Program.* Plans, directs, and coordinates the regional projects of NOAA and other federal agencies to assess the effect of ocean dumping, municipal and industrial waste discharge, deep ocean mining, and similar activities on marine ecosystems.

OCSEA *Outer Continental Shelf Environmental Assessment Program Office.* Plans and directs research studies supporting the assessment of the primary environmental impact of energy development along the outer continental shelf of Alaska; coordinates related research activities of federal, state, and private institutions.

WM *Weather Modification Program Office.* Plans, directs, and coordinates research within ERL relating to precipitation enhancement and mitigation of severe storms. Its National Hurricane and Experimental Meteorology Laboratory (NHEML) studies hurricane and tropical cumulus systems to experiment with methods for their beneficial modification and to develop techniques for better forecasting of tropical weather. The Research Facilities Center (RFC) maintains and operates aircraft and aircraft instrumentation for research programs of ERL and other government agencies.

AOML *Atlantic Oceanographic and Meteorological Laboratories.* Studies the physical, chemical, and geological characteristics and processes of the ocean waters, the sea floor, and the atmosphere above the ocean.

PMEL *Pacific Marine Environmental Laboratory.* Monitors and predicts the physical and biological effects of man's activities on Pacific Coast estuarine, coastal, deep-ocean, and near-shore marine environments.

GLERL *Great Lakes Environmental Research Laboratory.* Studies hydrology, waves, currents, lake levels, biological and chemical processes, and lake-air interaction in the Great Lakes and their watersheds; forecasts lake ice conditions.

GFDL *Geophysical Fluid Dynamics Laboratory.* Studies the dynamics of geophysical fluid systems (the atmosphere, the hydrosphere, and the cryosphere) through theoretical analysis and numerical simulation using powerful, high-speed digital computers.

APCL *Atmospheric Physics and Chemistry Laboratory.* Studies cloud and precipitation physics, chemical and particulate composition of the atmosphere, atmospheric electricity, and atmospheric heat transfer, with focus on developing methods of beneficial weather modification.

NSSL *National Severe Storms Laboratory.* Studies severe-storm circulation and dynamics, and develops techniques to detect and predict tornadoes, thunderstorms, and squall lines.

WPL *Wave Propagation Laboratory.* Studies the propagation of sound waves and electromagnetic waves at millimeter, infrared, and optical frequencies to develop new methods for remote measuring of the geophysical environment.

ARL *Air Resources Laboratories.* Studies the diffusion, transport, and dissipation of atmospheric pollutants; develops methods of predicting and controlling atmospheric pollution; monitors the global physical environment to detect climatic change.

AL *Aeronomy Laboratory.* Studies the physical and chemical processes of the stratosphere, ionosphere, and exosphere of the Earth and other planets, and their effect on high-altitude meteorological phenomena.

SEL *Space Environment Laboratory.* Studies solar-terrestrial physics (interplanetary, magnetospheric, and ionospheric); develops techniques for forecasting solar disturbances; provides real-time monitoring and forecasting of the space environment.

U.S. DEPARTMENT OF COMMERCE

National Oceanic and Atmospheric Administration

BOULDER, COLORADO 80302